Improving applicability of a parametric model for breakwater layout design

J.W. (Jelle) Teeling

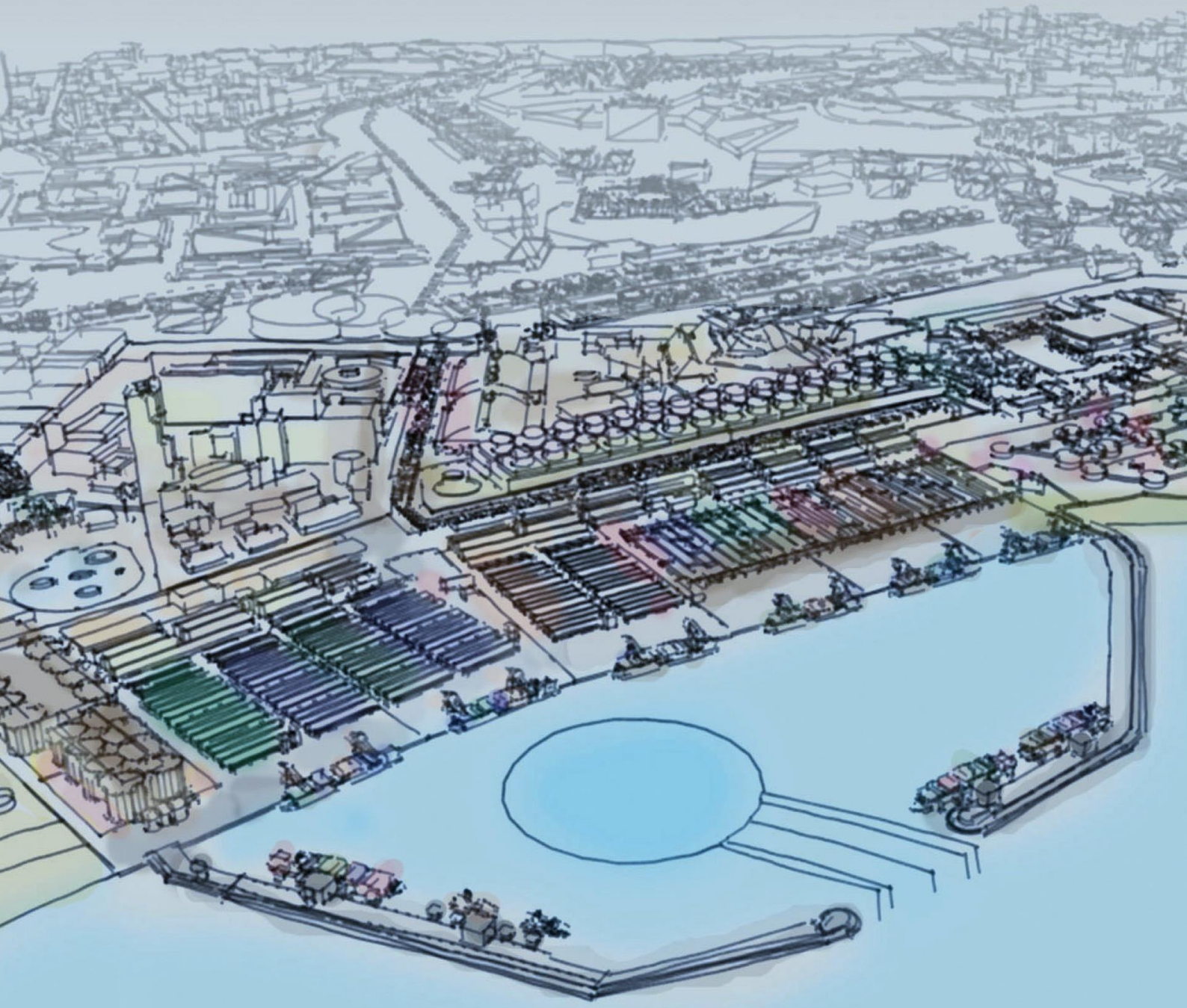

TU Delft

ARCADIS

Improving applicability of a parametric model for breakwater layout design

by

J.W. (Jelle) Teeling

in partial fulfillment to obtain the degree of

Master of Science
in Hydraulic Engineering

at the faculty of Civil Engineering and Geosciences
at Delft University of Technology.

to be defended publicly on Thursday July 23, 2020 at 2:00 PM.

Source cover image:
https://www.businesswire.com/news/home/20160208005531/en/Republic-Georgia-Selects-Anaklia-Development-Consortium-Build, ***Business Wire***

Student number:	42432099	
Project duration:	September 2, 2019 – July 23, 2020	
Thesis committee:	Prof. dr. ir. S.G.J. Aarninkhof,	TU Delft, chair
	Ir. C. Parkinson,	Arcadis
	Ir. J. van Overeem,	TU Delft - Arcadis
	Ir. A.J. Lansen	TU Delft

This thesis is confidential and cannot be made public until July 14, 2022.

An electronic version of this thesis is available at `http://repository.tudelft.nl/`.

TU Delft

ARCADIS

Acknowledgements

As I am writing this, my time as a student is coming to an end. After eleven months of research, programming, testing and reporting, my thesis is coming to an end. The end of my thesis will also conclude my Master of Science program ”Hydraulic Engineering” at the Delft University of Technology. Looking back at the past year, I can say that I really enjoyed my time working on this thesis. This thesis has allowed me to further develop myself in many different aspects. It has introduced me to the wonderful world of programming and the immense amount of possibilities to which it can be applied, in which I have steadily developed an interest in these past months. I also really enjoyed my time at Arcadis, where I carried out my thesis and where I have spent many days at the office this past year.

Conducting this research would not have been possible without the help and support that I have received from my committee. First off, I would like to thank Jan van Overeem, who introduced me to this topic and brought me in touch with Arcadis. No matter what type of issues I encountered, you were always willing to make time to discuss, to provide feedback, or to steer me back on track. I would like to thank Chris Parkinson, for his guidance and support during every step of the way. It did not matter if it was a port design related question or a question about my report, you always provided helpful insights and feedback. I would also like to thank Joost Lansen for his feedback and valuable additions. I really appreciate the fresh perspective you provided during our meetings, which have helped me a lot in shaping the report in the final stages of this thesis. Last but not least, I would like to thank Stefan Aarninkhof for his critical but constructive comments and enthusiasm during our committee meetings.

Apart from my committee, I would also like to thank my colleagues and the other graduate students at Arcadis. Our discussions, coffee moments and occasional after-work drinks made it that I really enjoyed my time at the office. Special thanks go out to Matthijs Benit, for his enthusiasm and advice concerning wave modelling. I really appreciate you taking the time to provide valuable advice to help me with the development of the model.

I especially want to thank the person who developed the original model, Sebastiaan Woerlee. Thank you for taking the time to teach me about the model concept and the optimisation, for helping me improve my Python skills and for your continuous interest during the project.
Finally, to my family and friends, thanks for the constant support during the year. I would have enjoyed this year a lot less without it!

Jelle Teeling
Rotterdam, July 2020

Summary

Digitization and automation of design processes are becoming increasingly important in the engineering practice. As a result, a research project was conducted to create a parametric model for the conceptual design of breakwater layouts. This research resulted in a functioning model (from now on referred to as the original model) that serves as a proof-of-concept. Within the original model, certain aspects of design have been simplified.
The presence of these simplifications impose limitations on the applicability and accuracy of the model. By further development of the original model, it is possible to improve upon simplifications and increase the applicability of the model.
In this research, possible subjects of improvement have been reviewed and several subjects have been selected for implementation. These implementations have been made to increase the applicability of the original model and to bring the model concept a step closer to its eventual purpose: a reliable support tool that can be used for breakwater layout design in the conceptual design phase.

The original model and the previous research were studied, to understand the original model and to determine which subjects can be improved upon. From these subjects, three have been selected for further improvement. Selection of these three subjects was based on their expected influence on the applicability of the model. In addition, their impact regarding breakwater design, the interaction between subjects and the available tools to implement each subject have been kept in mind. The selected subjects are the incorporation of bathymetry, modifying the modelling of wave transformation from deep water conditions toward the shoreline and the implementation of sedimentation processes.

In the original model, the bathymetry was assumed to be a homogeneous slope with a straight shoreline, with depth contours parallel to the shoreline. For the incorporation of bathymetry profiles, a grid has been implemented. The implementation of the grid allows for the incorporation of a complete 3D bathymetry.
In the original model, the transformation of waves travelling from deep water conditions towards the shoreline was modelled using basic shallow water equations that assumed parallel depth contours. This method is inaccurate for a 3D bathymetry. In the updated model, the modelling of the wave transformation uses a simple but adequate wave model. Three different wave models were reviewed and compared. Based on this comparison, the REFRAC model was chosen for the modelling of wave transformation for waves travelling from deep water conditions towards the shore. The REFRAC model allows for quick modelling of the wave transformation while being able to account for all variations in the bottom profile.
In the original model, sedimentation was accounted for in a highly simplified manner. For the implementation of more accurate sedimentation processes, a divide has been made between the following three processes: longshore sediment transport, channel sedimentation and harbour basin siltation. Longshore sediment transport is accounted for using equations (Van Rijn, 2015) to approximate the accretion over a certain time period. For downdrift accretion, a schematized method is used that is based on a method presented by Van Rijn (2015). Channel siltation is accounted for by calculating the filling rate per channel section using the Soulsby-Van Rijn equation (Soulsby, 1997). Harbour basin siltation (usually of minor importance) is accounted for by using a yearly siltation rate.

After the addition of the grid, the modification of the modelling of wave transformation and the implementation of sedimentation processes, their impact on the results generated by the model were assessed. This was done for each component separately, to assess whether the implementation of these components was executed well and led to expected results.
The generated results after addition of the grid and the modification of the wave transformation were assessed using a test case that can also be run for the original model. The added sedimentation processes were assessed using test cases to check whether the generated results by the updated

model are similar to that of the test case. In addition, the influence of varying parameter values was assessed to check whether the changes observed in the results are in line with expectation.
From these assessments, it has been observed that the addition of the grid and the integration of REFRAC was executed effectively, as the produced results are in line with expectation. In addition, it has been observed that the updated model is able to account for all depth variations. From the results of the sedimentation processes assessments, it has been observed that both processes produce results that are similar to the test cases and are in line with expectation.

Further assessment of the model results was performed with the use of a case study. An initial and a revised conceptual design of the Anaklia Deep Sea Port (which is currently in development) have been compared with the results generated by the updated model and the original model. It has been observed that the breakwater layout generated by the updated model coincides better with the conceptual designs than the breakwater layout generated by the original model. In addition, the method used for the determination of channel sedimentation was further assessed. This assessment has been done by comparing the sedimentation volume for the initial conceptual design calculated by the updated model with the results provided in project reports of the initial conceptual design. The sedimentation volume found in the updated model is within the range of estimated sedimentation described in the project reports.

Based on the case study results, several differences between the conceptual designs and the design produced by the updated model were recognized and reviewed. Based on these differences, several valuable points of improvement were recognized. These points of improvement show directions in which further development of the model would improve the model.

From this research, it is shown that the model concept for parametric breakwater layout design that has been developed has a lot of potential. The updated model has a larger applicability than the original model, and can be applied to all types of bathymetries and produce results that are more reliable than the results of the original model. The additions and modifications that have been made are demonstrated to be valuable for the further development of the model. The model performance of the updated model is similar to the original model concerning its consistency. Because the updated model is more detailed, the run-time has increased significantly from 1 - 2.5 hours to 2.5 - 4 hours per run. This run-time is still acceptable for its intended purpose, as traditional methods used for conceptual port design usually take much longer.
There are still some limitations, uncertainties and recommended points of improvement. However, the updated model that has been produced in this research is seen as a substantial step closer towards the eventual objective: a reliable support tool for the design of the breakwater configuration during the conceptual design stage.

Contents

List of Figures

List of Tables

1 Introduction

Maritime transport has, since its inception, always been essential for the world economy. These days it covers over 90% of the worlds trade (Cerdeiro et al., 2020). Ports are an essential node in this network, as they form the connection with land-based transport.
The main function of commercial ports is to unload and/or load vessels, with as high an occupancy and productivity as possible. The design of ports is focused on making this possible, while also keeping the required investments to a minimum.
Port design can be split into the design of multiple components. An important component is the design of the breakwaters. Their main function is to assure moderate conditions within the harbour, minimizing the amount of downtime. These conditions depend on the layout of the breakwaters. Due to breakwater construction being expensive, the design objective is to find the ideal trade-off between capital expenditure, operational expenditure and downtime costs.
The general layout of the breakwaters is determined in the conceptual design phase and is refined later in the design process. Determining the breakwater layouts during the conceptual design phase is an iterative process and lot of man-hours go into determining the starting point for the eventual design.

Recently, a study has been done to assess the possibility to partly automate this process (Woerlee, 2019). A parametric model has been created for the design of breakwater layouts for an idealized situation. This model is from now on referred to as the original model.
The original model creates different layouts from scratch, compares them and optimises them, to eventually determine a layout that approximates the optimal breakwater configuration. The optimisation is performed using genetic algorithms.
The model concept should eventually be able to serve as a support tool to be used during breakwater design. By further developing the original model, this objective can be reached.

1.1. The original model

The original model uses genetic algorithms to develop the optimal layout for a port with one long quay, parallel to the shoreline, at which all the berths are situated. If the reader is not familiar with the original model or optimisation using genetic algorithms, it is highly recommended to the reader to first read Section 2.1. In this section, a more detailed description of the model is presented.

The port components that are accounted for in the original model are visualised in Figure 1.1. The model currently focuses on container cargo. Therefore, limiting factors concerning the downtime (such as the limiting wave height at the berth) are set by default to those for container vessels.

The optimal layouts of both the primary and the secondary breakwaters are determined by the model. During this process, the need for a secondary breakwater is also assessed. If addition of a secondary breakwater proves to be unnecessary, the optimal layout will show this.
The primary breakwater is constructed using three breakwater segments (denoted by [A] in Figure 1.1b). The secondary breakwater is constructed using two breakwater segment (denoted by [B] in

Figure 1.1b). The distance between the shore-end of the breakwaters is determined by the required number of berths. If expansion is desired in the future, this can be given as input by the user in the form of the eventual number of berths desired. In this case, the distance between the shore-end of the breakwaters is determined by the total number of berths that are planned to be installed in the future. In this manner, room for expansion is provided. To ensure that the breakwaters are not placed too far apart, land costs per unit length are accounted for.

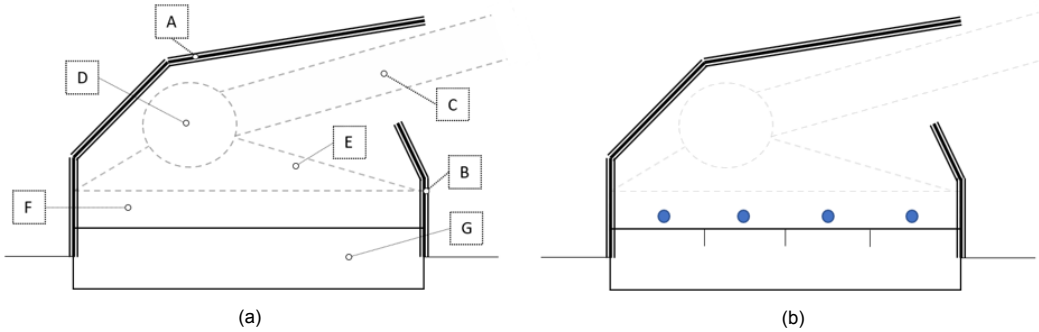

Figure 1.1: (a) A schematization of a port and its components, in which [A] is the primary breakwater, [B] is the secondary breakwater, [C] is the approach channel, [D] is the turning basin, [E] is the manoeuvring basin, [F] is the berthing basin and [G] is the quay (b) A schematization of a port, in which the berth locations are marked by the blue dots

Next to the layout of the breakwaters, the original model also has to take into account the wet infrastructure, which includes:

- The approach channel (denoted by C in Figure 1.1a)
- The turning basin (denoted by D in Figure 1.1a)
- The berthing basin (denoted by F in Figure 1.1a)
- The manoeuvring basin (denoted by E in Figure 1.1a)

These components are incorporated in the following manner. The approach channel is straight, with a distinction being made between the distance required for the vessel to slow down for the tugs to hook up and the stopping distance. This distinction leads to the possibility to choose between an entirely shielded channel or the channel being shielded only for the distance needed for eventual stopping.
The breakwater configuration must also provide space for the turning basin, the berthing basin and the manoeuvring area. The turning basis diameter is determined based on the guidelines of PIANC (1995), as are the other port design components. The turning basin is placed at the end of the approach channel, with the centre of the channel aligning with the centre of the basin. The berthing basin is placed in front of the quay. The manoeuvring area is the area between the turning basin and the berthing basin.

The bathymetry is schematized as a homogeneous slope, of which the bed slope is determined by the corresponding input value given by user. The wave processes that are incorporated are shoaling, refraction and diffraction (inside the harbour basin). Siltation of the harbour basins and the navigation channel are incorporated with a yearly siltation rate, which is used to determine the maintenance dredging volumes.
Both maintenance and capital dredging are taken into consideration, as is possible re-use of the dredged material. The required capital dredging is determined by the volumes that have to be dredged to construct the navigation channel, the berthing basin, the manoeuvring basin and the turning basin. The percentage of the dredged material that can be re-used depends on the corresponding percentage that is given as input value by the user. The re-usable soil volumes are used in the cost calculation for the needed infill for construction of the quay.
The model requires input regarding design specifications (such as the number of berths, the design vessel dimensions and the limiting wave height at the berth) and environmental conditions (such as wave height, incoming wave direction and wind speeds). Based on this input, initial layouts are generated, after which an optimisation occurs using a NSGA-II algorithm (Deb et al., 2002). The optimisation

is based on a fitness score that is given to each layout individual. This leads to a optimized breakwater layout solution.
This fitness score is based on three aspects:

- Capital Expenditure (from here on referred to as CAPEX)
- Operational Expenditure (from here on referred to as OPEX)
- Downtime Costs

These values are determined for each generated layout.

The study was done as a proof of concept and the model that was created demonstrated that the concept is viable with a lot of potential. The model framework has been made with the optimisation method using genetic algorithms as its core. It is now possible to further expand the model to make it applicable to more realistic situations. Further development of the original model will lead to a step closer to automating this part of the design process, improving the model results and therefore reducing the required time and manpower. In turn, the port development process will be sped up, which will result in a reduction of design costs.

1.2. Problem statement

In the original model, certain aspects that can influence breakwater design are simplified or left out of scope. These simplifications were sufficient for a proof of concept. However, the eventual goal is for the model concept to be applicable as a support tool for actual design projects. To reach this objective, some of the current simplifications have to be improved and certain additions have to be made, such that the updated model is a sufficient representation of reality for the concept design phase. It is impossible to fit all possible improvements into the scope of a single MSc dissertation. Therefore, it is essential to focus on improving subjects that have a definite impact on the model output, whilst the interaction between the different aspects and run-time of the model also has to be taken into account.

1.3. Objective

Taking into account what is mentioned in the problem statement, the objective of the research is formulated as follows:

To improve overall applicability of the model; important aspects for the improvement of the applicability of the model have to be recognized and integrated, while staying true to the concept design nature of the model and preventing it from requiring too much computation time.

An important statement that should not go unnoticed is the fact that it should conform to the concept design nature of the model. To provide a indication of the required accuracy, the AACE classes for cost estimates are consulted (AACE International, 2019). The original and the updated model belong to either class 4 or 5. For these classes, an accuracy of -30% to +50% is seen as fairly accurate.
The model is meant to serve as a support tool for this stage of design, which is an important aspect that has to be kept in mind during all research and with all modifications that are made to the model.

1.3.1. Research question

To reach the main objective of this research, the research is aimed at answering the main research question, which comes forth from the objective:

How can the original model be improved to increase the applicability of the model and produce results that are sufficient for conceptual design?

To be able to answer the main research question, several sub-questions have to be formulated to answer the main question. These are as follows:

- *What are the most important factors to consider/improve in the original model in order to increase the applicability of the original model?*

- *What are the relevant processes regarding these factors concerning breakwater layouts for ports?*
- *Which tools are currently available for quantifying these processes and which are most suited for implementation regarding the current framework of the model?*
- *How can these tools be added to the original model, taking into consideration the possible interaction between certain processes?*
- *How can the need for and required length of the second breakwater be defined?*
- *How can the required modifications and additions be made without requiring excessive computation time?*
- *What are the effects of the added processes on the performance of the model compared to the original model?*

1.3.2. Scope

The original model was built within a certain framework. The scope was kept narrow (Woerlee, 2019) for the initial development of the model. In this research, this framework and the scope will be expanded upon. From the original model, the following assumptions and constraints will remain valid for the updated model:

- The site on which the breakwater will be constructed is pre-selected. This means that the model is not used to find the most ideal position for a port along the coastline. Its function is to be a support tool for breakwater layout design, not for site selection.
- The type of port considered is that of a cargo port focused on container cargo. This assumption is made to reduce the amount of variables that have to be taken into consideration while further developing the model.
- The soil is assumed homogeneous, meaning that there is no difference in soil type in the area where the port is constructed and that the soil type also does not differ in depth. Possible re-use of soil after dredging is assumed as a percentage of the total dredged soil, given by the user.
- Water density differences are not taken into account.
- The port design features one long, straight quay, at which all berths are situated. This quay is constructed parallel to the shoreline.
- The costs (on which the layout alternatives are assessed) consist of CAPEX, OPEX and downtime costs. Other costs (such as the construction of land based port infrastructure or hinterland connections) are not taken into consideration.
- Social and environmental aspects (such as public opinion, environmental assessments and soil contamination) are not taken into account, as they are considered more relevant to site selection than breakwater design.
- Extreme conditions, like ice, hurricanes or other rare extreme natural phenomenon are not taken into account.
- The estimated downtime due to waves is based on wave height. Wave period is not used in the calculation.

These assumptions and constraints form the basis framework upon which this research is constructed. The expansion of the framework and the scope depends on the processes that will be improved upon. The analysis and selection of these subjects is presented in Section 2.2. The framework and the scope are adjusted accordingly.

1.4. Thesis outline

In this introductory chapter (Chapter 1), a brief description of the previous research has been given. Thereafter, the research objective is presented, along with the research question. To meet the research objective, the research is conducted in several steps.

First, the original model is analysed. Thereafter, the recommended points of improvement are reviewed. Based on this review, subjects are selected that are seen as essential for the improvement of

the model. These subjects will be studied using literature, to determine the tools that will be used to implement the subjects into the model. The analysis of the original model, the selection of the essential subjects and the literature study of these subjects will be described in Chapter 2.

The selected subjects have to be implemented in the model. A methodology is developed to accomplish this implementation, and is presented in Chapter 3. This methodology is based on the tools that will be used for this implementation.

An assessment is made of which additions and modifications have to be made to follow the methodology. After the additions and modifications have been made, a updated model will have been developed. The performance of this updated model and the added components have to be assessed. This assessment is presented in Chapter 4.
To validate the results produced by the updated model, a case study is performed. In this case study, actual conceptual designs of a port project are compared with the design produced by the model. A description of the case study and the results will be presented in Chapter 5. In Chapter 6, the original model and the updated model are compared. The advantages and disadvantage are described and recommendations are given regarding the use of both models.

In Chapter 7, the research results are discussed. The uncertainties and limitations of the updated model are presented, along with a reflection on the choices that have been made during the research. Last of all, the conclusions of the dissertation and recommendations for further study and development are presented in Chapter 8.

2

Original model analysis and subject selection

To increase the applicability of the model, it is of importance to have a good understanding of the original model. Important aspects to understand are:

- The optimisation
- The limitations
- The computation time and which modules take most time to run
- The incorporated processes

Therefore, the original model has been analysed (see Section 2.1) based on the report by Woerlee (2019). The subjects that can be improved are presented in Section 2.2. Of these subjects, three subjects have been selected for further study and implementation. These subjects are: bathymetry, wave transformation and sedimentation. To improve the original model regarding these subjects, it is essential to understand the processes that are relevant. Therefore, relevant wave processes are presented in Section 2.3, followed by relevant sedimentation processes in Section 2.4.
The implementation of the correct bathymetry mainly depends on finding the best method to implement this in the model. Finding the best method to implement the correct bathymetry depends on choices that allow for efficient programming and not specifically on literature. Therefore, it will not be treated in this chapter, but in the Methodology (Chapter 3).

2.1. Original model description

The original model, developed by Sebastiaan Woerlee (2019), is a parametric model for breakwater layout configuration to be used in the conceptual design phase as described in Chapter 1. The model output is an optimised breakwater layout, based on input values given by the user. This optimisation is performed with the use of genetic algorithms.

2.1.1. Input

The input values are given by the user via a separate input file, in which the user can define values for the design parameters (such as the limiting wave height at the berth and the design vessel specifications), as well as the environmental conditions for the location that is considered. The total list of input parameters can be found in Appendix A.
The design parameters and environmental conditions are used to compute the port infrastructure and breakwater components. The design of the port infrastructure and breakwater components is based on the guidelines given by PIANC for approach channels (PIANC, 1995), harbour basins (PIANC, 2014) and breakwater design (PIANC, 2016). For the design of the breakwater cross-section, a standard cross-section is used (Woerlee, 2019).

The environmental conditions provided by the user are used to determine the environmental conditions within the port and the navigation channel. Based on the environmental conditions within the port and navigation channel, the occurring operational and navigational downtime are estimated for each layout alternative.

2.1.2. Optimisation

The core of the model is the optimisation. The optimisation is performed using genetic algorithms. Genetic algorithms perform an optimisation based on the same principles as natural selection. The best alternatives are selected for the next generation and from these alternatives, new alternatives are created using cross-over and mutation. The worst alternatives are removed. In this manner, an optimum can be approached after a certain number of generations.
Genetic algorithms were chosen because they are best suited for the required optimisation. They reach an optimum within reasonable computation time and do not require data apart from the input parameters. There are different types of genetic algorithms. These types are each suited for specific optimisation problems. The type of genetic algorithm that is used in the model is a Non Dominant Sorting Algorithm, NSGA-II (Deb et al., 2002).
The choice for NSGA-II is due to the type of optimisation that has to be performed. For the generated breakwater layouts, there is a constant trade-off between CAPEX/OPEX costs and the downtime costs. The objective of the optimisation is to find the optimum between the downtime costs and CAPEX/OPEX costs, as is portrayed in figure 2.2a. Optimisation regarding this type of problem is called a multi-objective optimisation (Woerlee, 2019). The NSGA-II algorithm performs well regarding this type of optimisation. The convergence and consistency of the optimisation depend on the optimisation parameters. These parameters are (Woerlee, 2019):

- The population size (the number of layout alternatives in a generation, set to 120)
- The mutation rate (the probability that a mutation will occur for a variable component of the breakwater (such as the outer node of the primary breakwater), set to 0.19)
- The mutation size (the standard deviation of the disturbance due to a mutation, set to 0.25)
- The convergence rate (the required convergence for the model to stop running, set to 0.001)

2.1.3. Model run

When running the model, an initial generation of 120 breakwater layout alternatives is created. Each layout is constructed with the following components (shown in Figure 2.1):

- A primary breakwater, consisting of 3 segments and 4 nodes:
  1. Node 0 is located on $(0, 0)$.
  2. Node 1 is located at $(0, y1)$. The x-coordinate is 0. The y-coordinate is variable.
  3. Node 2 is located at $(x2, y2)$. Both coordinates are variable.
  4. Node 3 is located at $(x3, y3)$. Both coordinates are variable.
- A secondary breakwater, consisting of 2 segments and 3 nodes. If a the secondary breakwater is constructed depends on the SEC value (either 0 or 1). This value is decided randomly for each alternative. The secondary breakwater is constructed if the layout alternative has a SEC value of 1 and is not constructed when the value of SEC is 0.
  1. Node 4 is located at $(x4, 0)$. The y-coordinate is 0. The x-coordinate is variable.
  2. Node 5 is located at $(x5, y5)$. The x-coordinate is the same as $x4$. The y-coordinate is variable.
  3. Node 6 is located at $(x6, y6)$. Both coordinates are variable.
- The turning basin center (xtb, ytb), of which the coordinates are both variable.
- The navigation channel, of which the orientation (denoted by θ_{ch}) is variable.
- The manoeuvring basin, of which the location depends on the location of the turning basin.
- The berthing basin and the quay, which depend on the design requirements provided by the user.

The direction in which the layout is constructed depends on the value of RHS. This value is either 0 (which means that the layout alternative is constructed in negative x-direction) or 1 (which means the

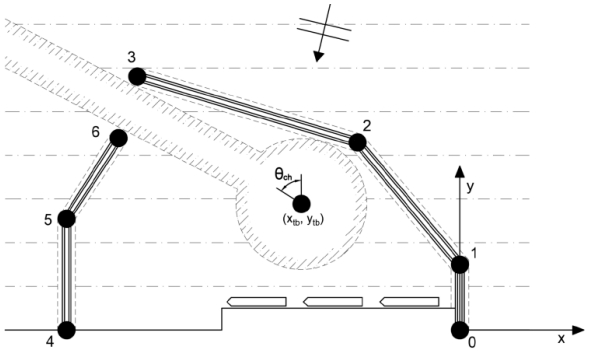

Figure 2.1: A visual representation of a layout alternative and its decision variables, with $RHS = 0$ and $SEC = 1$ (Woerlee, 2019).

layout alternative is constructed in positive x-direction). The value of RHS is randomly determined for each layout individual.
The variable aspects of a layout alternative are called the decision variables. These are:

$$(RHS,\ y1,\ x2,\ y2,\ x3,\ y3,\ SEC,\ x4,\ y5,\ x6,\ y6,\ xtb,\ ytb,\ \theta_{ch})$$

The layout configurations are created at random, with random values being generated for the decision variables. These random values are within defined bounds. The locations of the breakwater nodes have to be selected within these bounds, as the generated layout alternatives have to meet certain design criteria (such as the breakwater not interfering with the navigation channel or the berthing basin). The location of the turning basin is also selected randomly within defined bounds. The navigation channel location depends on the turning basin, as it aligns with the turning basin center. The possible angle and position of the navigation channel depend on the location of the turning basin and the breakwater gap, since the navigation channel has to align with both. The berthing basin is located directly at the berth and the manoeuvring area is situated between the berthing basin and the turning basin. An example of a generated layout is given in Figure 2.2b.

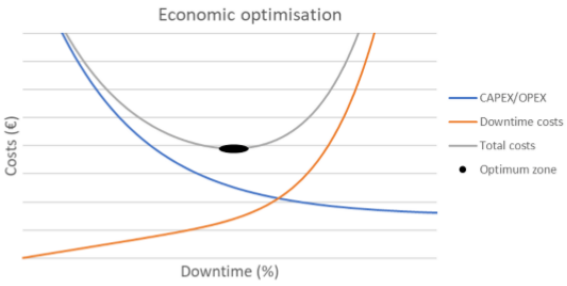

(a)

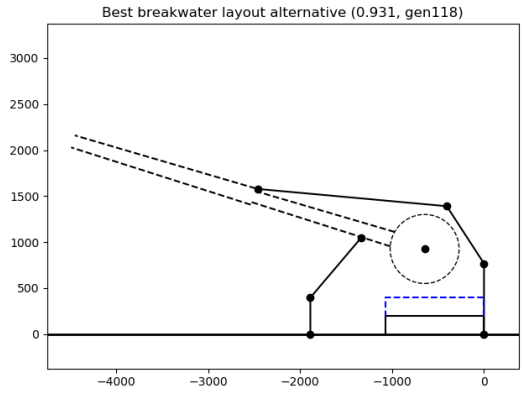

(b)

Figure 2.2: (a) Economic optimum between downtime and CAPEX/OPEX (Woerlee, 2019) (b) An example of a layout generated by the original model (Woerlee, 2019)

After the initial group of 120 layouts is generated (denoted in the model as generation 0), a fitness score is assigned to each layout alternative. This fitness score is based on the CAPEX, OPEX and downtime costs that accompany a layout alternative. Equation 2.1 is used to determine the fitness score.

$$f_f\,(X_i) = \frac{PC}{f_c\,(X_i) + f_d\,(X_i)} \tag{2.1}$$

in which:

PC	=	Predicted sum of the CAPEX/OPEX and downtime costs, given by the user	[€]
f_f	=	Fitness score	[-]
f_c	=	CAPEX/OPEX costs	[€]
f_d	=	Downtime costs	[€]
X_i	=	Layout alternative	[-]

For the determination of the fitness score, the CAPEX/OPEX costs and downtime costs have to be determined. Equation 2.2 is used to calculate the CAPEX/OPEX costs, while Equation 2.3 is used for the calculation of downtime costs.

$$f_c\,(X_i) = C_{bw}\,(X_i) + C_{dr}\,(X_i) + \sum_{t=1}^{T_L} \frac{C_{dr,o}\,(X_i) + \Phi_{bw,m} \cdot C_{bw}\,(X_i)}{(1+r)^t} \tag{2.2}$$

in which:

$f_c\,(X_i)$	=	CAPEX/OPEX costs	[€]
C_{bw}	=	Costs for breakwater construction	[€]
C_{dr}	=	Capital dredging/filling and land costs	[€]
$C_{dr,o}$	=	Maintenance dredging costs	[€/yr]
$\Phi_{bw,m} * C_{bw}$	=	Breakwater maintenance costs	[€/yr]
r	=	Discount rate	[–]
T_L	=	Lifetime	[yr]

The construction costs of the breakwaters are determined based on the breakwater volume and the configuration of both breakwaters. These components depend on the environmental conditions, the user-defined design parameters, the depth profile and the length of the breakwater segments. Capital dredging costs for the channel and basins are included, based on the volumes that have to be dredged. Possible re-use of the dredged material is also taken into account in the input values, as a percentage of the dredged volume given by the user.
The maintenance dredging costs are based on a pre-defined sedimentation rate (given in m/yr). The breakwater maintenance costs are determined as a pre-defined percentage $\Phi_{bw,m}$ of the costs for the breakwater construction.

$$f_d\,(X_i) = \sum_{t=1}^{T_L} \frac{C_{w,o}\,(X_i)}{(1+r)^t} \tag{2.3}$$

in which:

$f_d\,(X_i)$	=	Downtime costs	[€]
C_{wo}	=	Yearly downtime cost	[€/yr]
r	=	Discount rate	[–]
T_L	=	Lifetime	[yr]

Downtime costs are influenced by the operation time during which downtime occurs. Downtime can be divided into navigational downtime (reaching the quay) and operational downtime (production at the berth). It takes into account the time period during which reaching the berth is not possible, as well as the time period during which berthing or execution of berth operations are not possible. In the model, it is assumed that operational downtime occurs when navigational downtime occurs.
In the model, downtime due to environmental conditions is taken into account. Other factors are not accounted for.
Since the OPEX and downtime costs are calculated per year, they have to be capitalised. This capitalisation is done by discounting them with a discount rate (denoted by r) over the design lifetime (denoted by T_L). In this manner, the net present value is found, making comparison and addition of CAPEX, OPEX and downtime costs possible.

Based on the fitness score, layout alternatives are selected to serve as ”parents” for the mating pool, through which a new population will be created through cross-over and mutation. Cross-over results in

a new layout being created using the decision variables of the layouts that serve as ”parents”. Using mutation, values of decision variables can be changed, which ”mutates” the existing layout alternative into a new layout alternative.
This new population is added to the original population. From the new and the original population, the layout alternatives are selected that will form the new generation.
This loop will be repeated until the convergence criteria for the fitness score of the best individual is met, after which the loop will break and the optimal breakwater layout is found.

2.2. Possible subjects for improvement

In the research by Woerlee (2019), recommendations concerning further research and points of improvement have been described. The main subjects in need of further research or improvement are the following:

1. Bathymetry
2. Sediment transport and siltation
3. Wave processes
4. Downtime cost estimation
5. Integration with cross section tool
6. Increased layout complexity
7. Variation in vessel and tugboat types
8. Navigation channel alignment
9. Client preference and constraints
10. Model tuning

Each subject has been described and their expected added value to improving the applicability is presented in Section 2.2.1. From these subjects, a selection has been made. Further research is conducted concerning these selected subjects, after which they are implemented in the model. These subjects have been selected based on the main objective of the research: to improve the applicability of the original model. Apart from the main objective, the following aspects have been kept in mind during the selection of the subjects:

- The expected influence of the subject on the breakwater layout design
- The interaction between the subject and other subjects
- The available tools for implementation of the subject into the model

2.2.1. Subject assessment

Bathymetry

The addition of bathymetry is essential for the model to become more applicable as a design support tool for realistic situations. The original model currently assumes a constant bed slope, with depth contours oriented parallel to the coastline. In reality, bathymetry profiles are more complex. The bathymetry influences the volume of the breakwater segments, the required capital dredging volumes, the required operational dredging as well as the wave transformation towards the shore. The fitness score of the layouts is influenced by these aspects. Therefore, its influence on the configuration of the most optimal breakwater is significant.

Incorporated wave processes

The inclusion of realistic bathymetry profiles will have an effect on the wave transformation towards the shore. The wave processes that influence the wave transformation from deep water conditions towards a point nearshore are partially dependent on the water depth (Holthuisen, 2007). The equations that are used in the original model assume a constant bed slope with parallel depth contours. These equations will not lead to accurate results when the bathymetric profiles can not be modelled as a constant bed slope with parallel depth contours.
The local wave conditions are essential in the prediction of occurring downtime, as the wave conditions within the harbour basin partially depend on these local wave conditions. As the wave conditions within

the harbour basin determine the downtime at the berths, it is of importance that these conditions are also determined in an accurate manner.

Sediment transport & harbour siltation

Currently, the implementation of sediment transport and siltation in the model is highly simplified. Siltation of the navigation channel and the harbour basin is taken into account with a yearly siltation rate. This siltation rate depends on the width gap of the breakwater gap, the gap orientation and the soil type (which is provided by the user).
Sedimentation processes are of importance when designing a breakwater layout (Van Rijn, 2013). Longshore sediment transport can lead to accretion along the breakwaters. The accretion is an important factor in the design of the breakwater layouts, as a function of the breakwaters is to prevent the inflow of sediment into the harbour basin. The length of the breakwaters has to be chosen accordingly. Therefore, the inclusion of longshore sediment transport will lead to a more accurate breakwater layout design.
The siltation rate of the channel and the harbour basin is used in determining the maintenance dredging volumes (PIANC, 2008). The maintenance dredging costs are determined based on the maintenance dredging volumes. As the maintenance dredging costs form a significant part of the OPEX, these costs also have an influence on the fitness score. Therefore, a more accurate calculation of the maintenance dredging costs will increase the accuracy of the optimal breakwater layout.

Downtime cost estimation

The downtime costs are determined based on navigational downtime and operational downtime. The assumption is made that when navigational downtime occurs, operational downtime occurs.
In reality, this assumption is not necessarily true. For example, it can occur that a ship is berthed while conditions outside the port do are too rough, causing navigational downtime. During this period a ship may still be able to unload/load, which means that the downtime at the berth is smaller than the navigational downtime. It can be the same the other way around, having conditions inside the harbour that lead to downtime at the berth, while navigation is still possible.
A better understanding of the correlation between the two types of downtime will lead to a better prediction of the downtime costs (Woerlee, 2019). As the downtime costs are of significant influence on the fitness score, an increase in the accuracy of the downtime costs will lead to an increase in the accuracy of the optimal breakwater layout.

Integration with cross section tool

A parametric design tool for cross-sectional breakwater design is currently in development. With this tool, it is possible to determine the cross-section of the breakwater at any specific location. Integration of this tool with the original model will lead to a more accurate determination of the breakwater volumes. Currently, this volume is calculated based on a standardized cross-sectional design. A more accurate estimation of the breakwater construction costs will lead to a more accurate estimation of the CAPEX. As the CAPEX is of significant influence on the fitness score, a more accurate determination of the CAPEX will also lead to a more accurate optimal breakwater layout. Integration with this tool is not possible at the moment, as the tool is still in development. However, integration of the cross-sectional tool is recommended when the tool is finished.

Increased layout complexity

Currently, a single port layout is incorporated in the original model. This port layout features one long, straight quay at which all the berths are located. The quay is constructed parallel to the shoreline.
The incorporation of one port layout option reduces the applicability of the model. Applying the original model to port designs with a different layout is likely to produce inaccurate results. By increasing the port layout complexity that is incorporated in the model, the applicability of the model with regard to different port designs can be increased.

Variation in cargo vessel types

In the original model, the cargo vessel types that are considered are container vessels. It is not uncommon for ports to provide berthing spaces to different cargo vessel types. The type of cargo vessel that is considered will influence certain factors, like limiting wave heights at the berth, limiting values concerning other environmental conditions, the unloading speed and the size of the vessels.

By incorporation of different vessel types, the model will become applicable to different ports that handle different cargo types. As a result, the applicability of the model will be increased.

Navigation channel alignment

In the original model, the navigation channel is designed as one long channel, in which stopping length is included. In reality, the design of the navigation channel is not necessarily a one-size-fits-all approach. For example, the position of stopping can vary per site. Sometimes, the choice is made to include a bend in the navigation channel (ROM 3.1-99, 2007).
The addition of more options concerning navigation channel design gives the user more control and will lead to better results in port design projects with specific demands or boundaries.

Client preference and constraints

In the original model, specific client preference (such as budget constraints or allowed downtime) is not incorporated. The inclusion of these aspects will lead to a model that provides the user with more control over the model output. The addition of this feature will lead to the model producing better results for design projects with specific demands or limitations that have been set by the client.

Model tuning

In the original model, a set of optimisation parameters is used that results in convergence and sufficient consistency. Further research regarding the optimal set of optimisation parameters can lead to increased consistency of the model. The consistency, convergence and the ability of the model to escape local optima depends on the set of optimisation parameters that is used. These optimisation parameters are the population size (the number of layout alternatives per generation), the mutation rate (the probability that a decision variable is mutated), the mutation size (the size of the mutation if it occurs) and the convergence rate (an indicator for the convergence that needs to occur for the model to stop running). The current optimisation parameters lead to sufficient consistency for the model, as the optimum layout is found most of the time (Woerlee, 2019). By conducting additional research, it is possible to determine the optimal set of optimisation parameters. With the optimal set of optimisation parameters, the consistency of the model will increase.
It is important to keep in mind that additions or modifications to the model that lead to an increase or a decrease in the number of decision variables, can lead to the need for tuning of the optimisation parameters.

2.2.2. Subject selection

The subjects that will be improved upon and implemented in the model are selected based on the main objective of this research. The main objective is to improve the applicability of the original model. As applicability can relate to both project locations and port types, the choice is made to focus on increasing the applicability with regard to project locations. To improve its applicability, it is important that the updated model will produce accurate results at locations with complex depth profiles and locations where the morphological response of the shoreline has to be taken into account.
Based on the subject assessments presented in Section 2.2, the following three subjects are selected:

- Bathymetry
- Incorporation of wave processes
- Sediment transport and harbour siltation

The implementation of bathymetry is essential for increasing the applicability of the model. This applicability is currently limited as the original model is only applicable to locations that can be modelled with a constant bed slope and parallel depth contours. Implementation of bathymetry profiles will allow the model to also be applied to locations that have complex bathymetry profiles that can not be modelled as a constant slope with parallel depth contours.

The modelling of the wave transformation in the original model assumes a constant bed slope with parallel depth contours. The implementation of bathymetry profiles results in the need to modify the modelling of the wave transformation, as the assumption of a constant bed slope is not valid anymore. The local wave parameters have a significant impact on the downtime calculation, which in turn has a

significant influence on the fitness scores. Therefore, it is essential that the local wave parameters are determined using a method that can account for complex bathymetry profiles.
In the original model, the wave conditions within the harbour are modelled using the Goda diagrams. This method provides an estimate of the wave conditions within the harbour (Woerlee, 2019). With this method, diffraction is accounted for. Other processes such as shoaling, refraction and reflection can also influence the wave conditions within the harbour basin (Helm-Petersen, 1998). By accounting for these processes, a higher level of accuracy can be achieved.
However, incorporating these processes in the determination of the wave conditions within the harbour basin requires numerical modelling for each layout alternative. This does not fit the current framework of the original model and it is expected to be computationally expensive.
Therefore, it is chosen to solely focus on the improvement of the wave transformation from deep water conditions towards the shoreline in this research.

The implementation of sedimentation processes is selected as it will allow the updated model to be applied to locations where morphological coastline response will impact the design.
Accretion at the breakwaters is an important factor in the design of the breakwaters. Allowing the model to account for this accretion will lead to an optimal breakwater design that is more reliable considering the location of interest.
In addition, the calculation of the sedimentation volumes will be improved where possible, to allow for a more accurate calculation of the maintenance dredging volume. This modification will lead to a more accurate determination of the OPEX. As a result, the fitness score will be more accurate for each layout, which leads to a more accurate determination of the optimal layout.

After the implementation of these three subjects, the applicability of the updated model is expected to increase. The physical processes and theoretical background that is required for the implementation of the relevant processes is provided in the sections below.

2.3. Wave processes

Water depth has a dominant influence on wave transformations nearshore. The inclusion of bathymetry can create the need to alter the methods used for the modelling of the wave transformation. Therefore, understanding the effect of a more complex bathymetry on wave transformation is essential.
It is of importance that the local wave parameters are approximated accurately. The navigational downtime depends on the wave height in the navigation channel. The wave height and wave direction at the breakwater tips will serve as input for the calculation of diffraction effects. Based on these diffraction effects, the wave conditions in the harbour are determined.

2.3.1. Shoaling

Shoaling is an important process that has to be accounted for. It describes wave transformation due to changes in water depth. With the inclusion of bathymetry, it is essential to understand what the effects of changing water depth are on the wave height. Therefore, this process is described in detail below. For illustrative purposes, a wave is considered that travels perpendicular towards a coast with a straight shoreline and a homogeneous, smooth slope.

For offshore waves, deep water wave conditions are valid. This means the water depth is large enough to consider the influence of the seabed on waves negligible. If waves travel towards the shore, the water depth will reduce. At a certain point, the seabed will influence wave propagation and the wave will start to ”feel” the bottom. This point is reached when the wave water depth is smaller than half of the wavelength (Holthuisen, 2007). At this point, the following criterion is met:

$$\frac{h}{L} < 0.5$$

in which:
h = Water depth [m]
L = Wavelength [m]

From this point, the deep water wave conditions are not valid anymore. The wave height will start to increase when the water depth decreases, which will proceed until the wave breaks. This occurs when the breaker height is reached. The increase in wave height can be explained using an energy balance (Holthuisen, 2007), which is visualised in Figure 2.3.

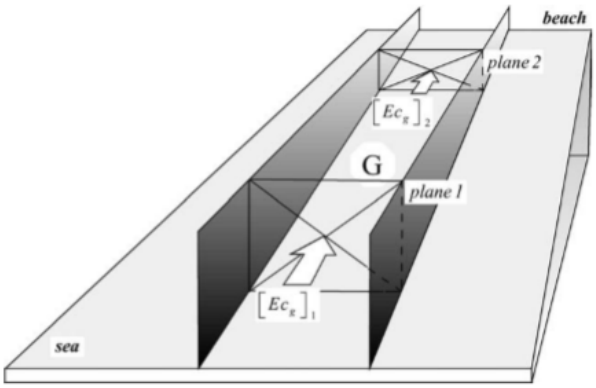

Figure 2.3: Visual representation of shoaling based on the wave energy balance (Holthuisen, 2007)

As shown in Figure 2.3, wave energy (denoted by $[Ec_g]_1$) travels through *plane 1* into volume G. Closer toward the shore, where the water depth is smaller, the wave energy leaves the volume through *plane 2*. When assuming that:

1. No energy is dissipated or generated
2. No energy leaves or enters through the lateral sides, the bottom or the surface
3. There is only energy transport in the wave direction

the following equation can be composed (Holthuisen, 2007):

$$P_2 b = P_1 b \rightarrow [Ec_g]_2 = [Ec_g]_1 \tag{2.4}$$

in which:

P	=	Wave energy flux	$[J/ms]$
b	=	Distance between adjacent wave rays	$[m]$
E	=	Wave energy	$[J/m^2]$
c_g	=	Wave group celerity	$[m/s]$

The influence of a change in water depth on the wave height can be determined using this energy balance. The wave energy E depends on the water density, the wave amplitude and the gravitational acceleration coefficient. It can be rewritten as:

$$E = \frac{1}{8}\rho g H^2 \tag{2.5}$$

in which:

E	=	Wave Energy	$[J/m^2]$
ρ	=	Water density	$[kg/m^3]$
g	=	Gravitational acceleration coefficient	$[m/s^2]$
H	=	Wave height	$[m]$

When substituting the equation for wave energy into equation 2.4, the energy balance is rewritten as:

$$\frac{1}{8}\rho g H_2^2 c_{g,2} = \frac{1}{8}\rho g H_1^2 c_{g,1} \tag{2.6}$$

in which:

ρ	=	Water density	$[kg/m^3]$
g	=	Gravitational acceleration coefficient	$[m/s^2]$
H	=	Wave height	$[m]$
c_g	=	Wave group celerity	$[m/s]$

Assuming the water density is constant, the balance shows that the change of amplitude is dependent on the change in wave group celerity. This dependency can be expressed as follows:

$$H_2 = \sqrt{\frac{c_{g,1}}{c_{g,2}}} H_1$$

The wave group celerity depends on the wave celerity (denoted by c) and the ratio between wave celerity and wave group celerity (denoted by n), which both depend on:

- The wavenumber k ($= \frac{2\pi}{L}$)
- The water depth h

Consequently, the wave group celerity also depends on the wavenumber and the water depth. Based on these relations, it is derived that the change in wave amplitude (and therefore wave height), partially depends on the change in water depth.
The square root of the initial group celerity divided by the group celerity at the location of interest shown in Equation 2.3.1, can be seen as a coefficient that can be used to determine the wave amplitude at the desired location. This coefficient is also known as the shoaling coefficient, K_s. The shoaling coefficient is expressed as:

$$K_s = \sqrt{\frac{c_{g,1}}{c_{g,2}}}$$

The shoaling coefficient can be used to determine the change in wave height due to the change in water depth.

2.3.2. Refraction

The illustrative case in Section 2.3.1 describes wave rays (i.e. a line normal to the wave crest) coming in at an angle perpendicular to the coastline. As a result, no depth variations along the wavefront occurs. When incoming wave rays approach the shoreline at an angle that is not perpendicular, depth variation along the wavefront does occur. This variation in depth leads to change in wave direction, which is called refraction.
The change in direction is due to a change in wave celerity. Wave celerity in intermediate and shallow water conditions is partly dependent on the water depth, as described in Section 2.3.1. The depth variation along the wavefront results in a variation in wave celerity along the wavefront. The wave crest will have a larger wave celerity where larger water depth is present. Consequently, the wave crest will cover a larger distance in deeper water. This results in a change in direction, as the wave turns towards shallower water (Holthuisen, 2007). This is illustrated in Figure 2.4.

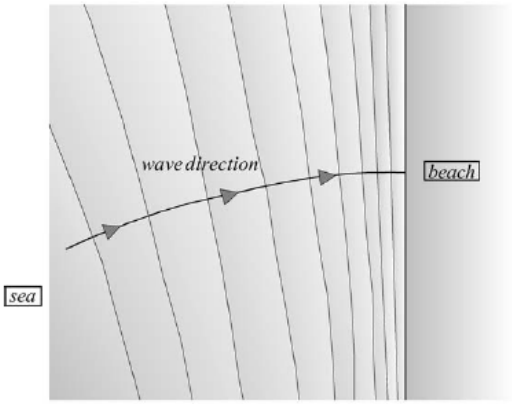

Figure 2.4: Wave refraction at a straight coastline with parallel depth contours (Holthuisen, 2007)

Refraction can result in wave rays converging or diverging. The divergence or convergence of wave rays affects the wave height. This can be derived from the energy balance in Equation 2.4. The difference with respect to shoaling is the variability of the width of the planes (denoted by b), which are not constant anymore due to convergence/divergence of the wave rays. This is illustrated Figure 2.5.

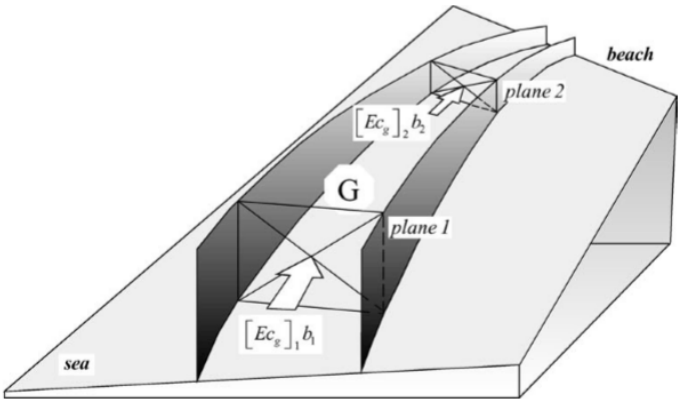

Figure 2.5: Refraction of waves on a slope, in which a visualisation is given of the planes that the energy will pass through (Holthuisen, 2007)

Assuming the same conditions as in Section 2.3.1, the following energy balance can now be composed:

$$P_2 b_2 = P_1 b_1 \rightarrow \left[Ec_g\right]_2 b_2 = \left[Ec_g\right]_1 b_1 \tag{2.7}$$

in which:

P	=	Wave energy flux	$[J/ms]$
b	=	Distance between adjacent wave rays	$[m]$
E	=	Wave energy	$[J/m2]$
c_g	=	Wave group celerity	$[m/s]$

The wave energy E can again be substituted by $\frac{1}{8}\rho g H^2$ and the energy balance can now be written as (Holthuisen, 2007):

$$\frac{1}{8}\rho g H_2^2 c_{g,2} b_2 = \frac{1}{8}\rho g H_1^2 c_{g,1} b_1 \tag{2.8}$$

When the water density is assumed to be constant, Equation 2.8 shows that the change in amplitude is now dependent on both the change in the wave group celerity and the change in distance between the wave rays. This can be expressed as:

$$H_2 = \sqrt{\frac{c_{g,1}}{c_{g,2}}}\sqrt{\frac{b_1}{b_2}} H_1 = K_s \sqrt{\frac{b_1}{b_2}} a_1 \tag{2.9}$$

Similar to the derivation of the shoaling coefficient K_s, it is also possible to derive a coefficient for refraction (denoted by K_r) using Equation 2.9. This coefficient can be expressed as:

$$K_r = \sqrt{\frac{b_1}{b_2}}$$

It can be seen that convergence ($b_1 > b_2$) of the wave rays leads to an increase in the refraction coefficient and therefore the wave height, while divergence ($b_1 < b_2$) will lead to a decrease.
Sufficiently accurate representation of wave refraction is therefore important, concerning both the wave height and wave direction. Both are detrimental in the determination of breakwater height and the determination of navigational and operational downtime.

When depth profiles become non-uniform and more complex, it can occur that wave rays converge extremely or even cross each other, as shown in Figure 2.6b. The wave direction is given with respect to shore-normal. The distance between the wave rays will approach zero, in which case ($b_1 >>> b_2$). As a result, the refraction coefficient would approach infinity. This would result in the wave height also approaching infinity, as it is linearly proportional to the increase of the refraction coefficient. At these points, the theory breaks. Infinitely large wave height can not occur, due to high wave steepness, non-linear effects and wave breaking.

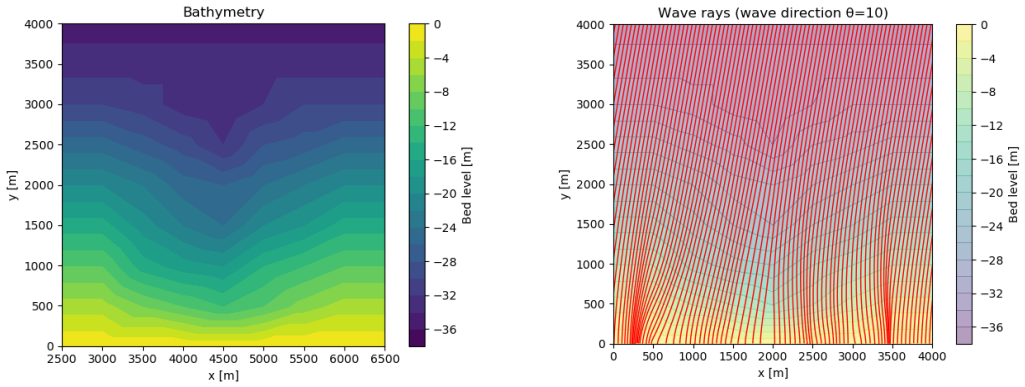

(a) (b)

Figure 2.6: (a) Depth contours of a complex depth profile (b) Visualisations of the crossing of incoming wave rays (portrayed as the red lines) for the complex depth profile

In these cases, the Eulerian approach offers a solution (Holthuisen, 2007). The geographic space is discretized in cells, leading to an average wave condition per cell. This way, the crossing of wave rays is avoided. Using this approach, wave models are able to give correct values for the refraction coefficient and wave heights accordingly. It should be noted that such a wave ray model is best applicable to monochromatic waves, with equal frequency and no directional spreading.

2.3.3. Diffraction

Incoming wave trains will be interrupted by the breakwaters. This will cause diffraction. Assuming constant depth and thereby the absence of shoaling and refraction, the waves will travel into the shadow zone of the structure in a circular pattern, with rapidly decreasing wave amplitudes (Holthuisen, 2007). This can be explained as follows. If, hypothetically, the wave train would stay uninterrupted by an obstacle (e.g. a breakwater), the wave train would continue its current path. This would mean no waves penetrate into the shadow region, leading to a perfectly calm environment, shown in Figure 2.7. In reality, energy will flow into the shadow region, leading to the diffraction phenomenon, shown in Figure 2.7.

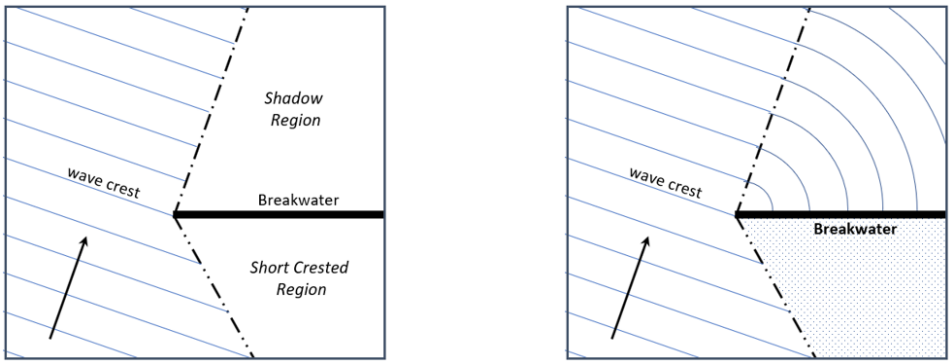

Figure 2.7: Left: Diffraction effects neglected - Right: Diffraction effects at an obstacle

In the short crested region (shown in Figure 2.7), a partially standing wave develops, due to the super-

position of incident and reflected waves.

The influence of diffraction on the environmental conditions in the harbour basin has to be taken into account. Methods to predict the influence of diffraction have been developed. These methods are valid when the following assumptions are made (Woerlee, 2019):

- Water is an ideal fluid, i.e. inviscid and incompressible
- Waves are of small amplitude and can be described by linear wave theory
- Flow is irrotational and conforms to a potential function satisfying the Laplace equation
- Depth shoreward of the breakwater is constant

These assumptions are compatible with concept design and the boundaries mentioned in Section 1.3.2.

One of these methods is the use of the Goda diffraction diagrams (Goda, Takayama, and Suzuki, 1978). These diagrams have been presented as tables (Rijksinstituut voor Kust en Zee, 2004). These tables can be used to determine the wave height at a certain location behind the point of diffraction, using a diffraction coefficient (denoted by K_d). This method is used in the original model to determine the wave conditions within the harbour basin.
To determine the diffraction effects within a harbour basin in a more accurate manner, numerical modelling has to be used. With the use of numerical models, processes such as shoaling, refraction and reflection are also accounted for. As a result, wave heights inside the harbour can be determined with a higher level of accuracy.

Diffraction effects do not solely occur inside the harbour basin, but also in the external environment outside the area shielded by the breakwaters. Therefore, diffraction influences the wave conditions nearshore and therefore also has an effect on longshore currents. This is further explored in Section 2.4.1.

2.4. Sediment transport

Sedimentation is an important aspect that has to be taken into account during port design. Siltation of the basins or the navigation channel leads to a need for dredging and/or a decrease in navigability. A function of breakwaters is to reduce possible negative effects due to sediment transport. Therefore, a sufficient representation of sedimentation processes is desired in the updated model.
Since sediment transport is a complex issue, it is of importance to review and understand the processes that lead to sediment transport. Based on this knowledge, available empirical and analytical equations to adequately quantify transport rates and sedimentation volumes are reviewed.
When considering sedimentation processes, a division is made between:

- Longshore transport of sediment
- Channel sedimentation
- Harbour basin siltation

The theory and equations that can be used to incorporate these sedimentation processes are presented below.

2.4.1. Longshore sediment transport

Longshore sediment transport is the occurrence of sediment transport along the shoreline, parallel to the shore. There are two types of load transport that occur:

- Suspended sediment transport
- Bed transport

Longshore transport is mainly due to suspended load transport, which occurs when sediment is stirred up by the turbulence of incoming (breaking) waves.
When a longshore current is also present, the suspended sediment is transported along the shore

(Mil-Homens, 2016). This longshore current is mainly due to incoming waves, but can also be due to the tide and/or due to wind. For longshore transport to occur, both sediment stirring and a longshore current have to be present.

Influence on port design

At a coastline where no morphological change occurs, it is assumed that an equilibrium is present (i.e. no gradients in the longshore sediment transport rates are present). The amount of sediment that enters a shore section is as large as the amount of sediment that leaves the section over a period of time. This means there is a constant flow of sediment.

When shore-normal hard structures are constructed, this will impact the shoreline development over time. The interruption of the longshore sediment transport by the structure will cause a disturbance in the (assumed) equilibrium.

Sediment transport is halted at the updrift side of the structure, which leads to accretion. At the downdrift side of the structure, the inflow of sediment is reduced to zero. However, the demand of sediment further downdrift of the structure remains the same. This demand of sediment causes the occurrence of downdrift erosion, as shown in Figure 2.8.

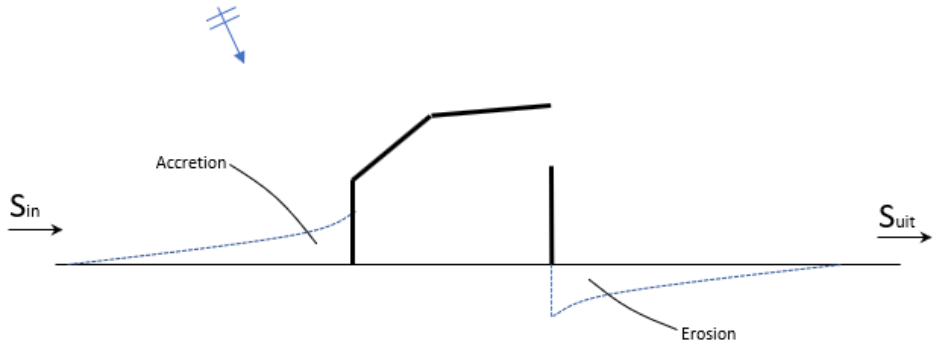

Figure 2.8: Morphological response at a hard structure without accounting for diffraction effects

Due to diffraction effects on the downdrift side of the structure, the wave heights and incident angles in the diffraction zone are reduced, leading to a change in sediment transport. This difference in wave height leads to a difference in wave setup. The difference in wave setup results in circular nearshore currents in the diffraction zone (Van Rijn, 2015).

These circular currents have to be taken into account. The circular current velocity can be larger than the velocity of the wave-induced currents in the diffraction zone. As a result, it can occur that a current is directed towards the structure. Consequently, this current can transport sediment towards the structure, leading to local accretion between the breakwater and the erosion zone, as shown in Figure 2.9.

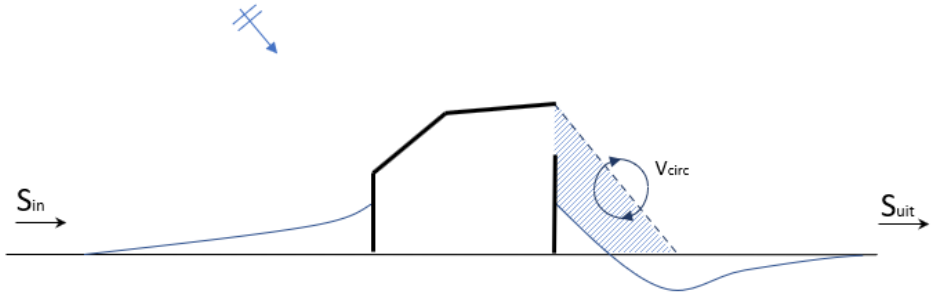

Figure 2.9: Circular currents (denoted by V_{circ}) appear in the diffraction zone due to breakwater diffraction and the expected morphological response. The diffraction zone is marked with a striped pattern

During the design of breakwater layouts, accretion on the updrift side and accretion and erosion on the

downdrift side should be taken into account. By approximating the accretion in the shore-normal direction along the breakwaters, a prediction can be made concerning the minimum length of the primary and secondary breakwater to prevent bypassing or siltation inside the harbour basin for a certain time period.

Bulk transport formula's
To determine accretion and erosion due to obstruction of sediment transport, sediment transport rates have to be determined. Sediment transport rates can be approximated using bulk transport formula's. Four bulk transport formulas that are often used are:

- CERC
- Kamphuis
- Bayram
- Van Rijn

CERC *(Van Rijn, 2014)*

$$Q_{t,mass} = 0.023(1-p)\rho_s g^{0.5} (\gamma_{br})^{-0.52} \left(H_{s,b-r}\right)^{2.5} \sin(2\theta_{br}) \tag{2.10}$$

in which:

$Q_{t,mass}$	=	Longshore sand transport (dry mass)	$[kg/s]$
p	=	Porosity factor (≈ 0.4)	[-]
ρ_s	=	Sediment density	$[kg/m^3]$
g	=	Gravitational acceleration coefficient	$[m/s^2]$
γ_{br}	=	Breaker depth index	[-]
$H_{s,br}$	=	Significant wave height (at breaker line)	$[m]$
θ_{br}	=	Incoming wave angle (at breaker line)	$[^o]$

Kamphuis *(Van Rijn, 2014)*

$$Q_{t,mass} = 2.33 \frac{\rho_s}{\rho_s - \rho} \left(T_p\right)^{1.5} (\tan\beta)^{0.75} (d_{50})^{-0.25} \left(H_{s,br}\right)^2 [\sin(2\theta_{br})]^{0.6} \tag{2.11}$$

in which:

$Q_{t,mass}$	=	Longshore transport (dry mass)	$[kg/s]$
ρ	=	Water density	$[kg/m^3]$
ρ_s	=	Sediment density	$[kg/m^3]$
T_p	=	Wave period	$[s]$
$tan\beta$	=	Slope surf zone	[-]
d_{50}	=	Median particle size	$[m]$
$H_{s,br}$	=	Significant wave height (at breaker line)	$[m]$
θ_{br}	=	Incoming wave angle (at breaker line)	$[^o]$

Bayram *(Bayram, Larson, and Hanson, 2007)*

$$Q_l = \frac{\epsilon}{(\rho_s - \rho)(1-p)g w_s} F \frac{5}{32} \frac{\pi \gamma_b \sqrt{g}}{c_f} A^{3/2} \sin\alpha_b \tag{2.12}$$

in which:

Q_l	=	Longshore transport rate	$[m^3/s]$
ϵ	=	Transport coefficient	[-]
ρ_s	=	Sediment density	$[kg/m^3]$
p	=	Porosity	[-]
g	=	Gravitational acceleration	$[m/s^2$
w_s	=	Fall speed	$[m/s]$
c_f	=	Friction coefficient	[-]
γ_b	=	Breaker depth index	[-]
A	=	Shape parameter	$[m^{1/3}]$
θ_b	=	Wave direction (at the breaker line)	$[^o]$

Van Rijn *(Van Rijn, 2014)*

$$Q_{t,mass} = 0.0006 K_{swell} \rho_s (\tan\beta)^{0.4} (d_{50})^{-0.6} (H_{s,br})^{2.6} V_{Longshore} \quad (2.13)$$

$Q_{t,mass}$	=	Longshore transport (dry mass)	$[kg/s]$
K_{swell}	=	Swell factor (= 1)	[-]
ρ_s	=	Sediment density	$[kg/m^3]$
$tan\beta$	=	Slope surf zone	[-]
d_{50}	=	Median particle size	$[m]$
$H_{s,br}$	=	Significant wave height (at breaker line)	$[m]$
$V_{longshore}$	=	Longshore current velocity	$[m/s]$

The CERC, Kamphuis and Bayram bulk transport formulas have been reviewed by Mil-Homens (Mil-Homens, 2016). It is found that Kamphuis performed best, due to its better performance for higher longshore transport rates (Mil-Homens, 2016) and its implicit integration of bed slope, which both CERC and Bayram have not.
Based on the Kamphuis and CERC formulas, Van Rijn (Van Rijn, 2014) developed a new equation to approximate sediment transport rates for sand, gravel and shingle beaches. It also includes integration of slope, comparable to the Kamphuis formula. Testing has shown that its performance is comparable to that of Kamphuis (Van Rijn, 2014).
In the Van Rijn equation, the sediment transport rate is linearly dependent on the current velocity. This provides the possibility to determine the sediment transport rate at any point, if the current velocity is known at that location. Therefore, it is also possible to take the nearshore circular currents into account. Due to the above-mentioned features, the Van Rijn equation is seen as the best option. Hence the choice to incorporate the Van Rijn equation into the model.
It should be noted that these longshore transport rate formulas are meant for determining the constant S (m^3/s) along the shore, between the shoreline and the breakerline.

Estimating updrift and downdrift accretion
Using the sediment transport rates, it is possible to forecast morphological changes along the coastline. For the determination of accretion on the updrift side of a shore-normal structure, the Pelnard-Considère equation (Pelnard-Considère, 1956) can be used to give a good estimation of the accretion length after a certain period of time:

$$L(t) = 2\sqrt{\frac{\phi' S t}{\pi d}} \quad (2.14)$$

in which:

L	=	Accretion Length in shore-normal direction	$[m]$
ϕ'	=	Wave direction	$[rad]$
S	=	Sediment transport rate	$[m^3/s]$
t	=	Time period	$[yr]$
d	=	Profile height	$[m]$

For determination of the profile height (denoted by d), single line theory can be used (Bosboom and Stive, 2015). The profile height is equal to the depth of closure (the depth that marks the end of the active coastal zone, denoted by DoC) and the dune height (denoted by h) combined, as shown in Figure 2.10.

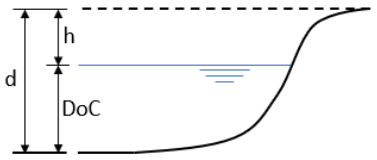

Figure 2.10: Visualisation of the profile height (denoted by d) and depth of closure (denoted by DoC)

For the morphological behavior on the downdrift side, the situation is complicated due to diffraction effects and the circular nearshore current. To make an approximation, a method determined by Van Rijn (2015) can be used. The bulk sediment transport formula is given in Equation 2.13.
Using the difference between the wave setup within the diffraction zone and the wave setup outside the diffraction zone, it is possible to approximate the circular current that occurs, using the following equation (Van Rijn, 2015):

$$V_{circ} = C\sqrt{hi} \tag{2.15}$$

in which:

V_{circ}	=	Circular current velocity	$[m/s]$
C	=	Chézy coefficient	$[m]$
h	=	water depth	$[m]$
i	=	slope of wave setup	[-]

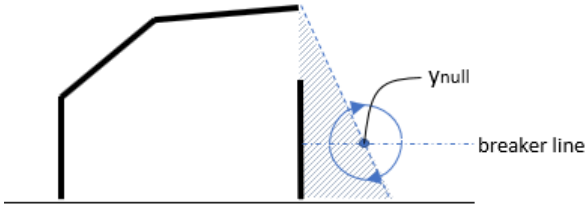

Figure 2.11: The location of the null point, denoted by y_{null}

The null point of the circular current is located on the intersection of the breaker line and the line of the shadow zone (see Figure 2.11). It should be kept in mind that, due to the current being circular, the longshore velocity component is dependent on the longshore location.
When V_{circ} is known, the total longshore currrent can be determined (Van Rijn, 2015). This can be done using the following equation:

$$V_{longshore} = rV_{wave} - V_{circ} \tag{2.16}$$

in which:

$V_{longshore}$	=	Longshore current velocity	$[m/s]$
V_{wave}	=	Longshore induced current velocity by waves	$[m/s]$
V_{circ}	=	Longshore component of circular current velocity	$[m/s]$
r	=	Adjustment factor	[-]

For a more detailed description, the user is referred to Appendix E.1.

When the total longshore current velocity is determined, it is possible to determine the sedimentation rates. Based on these sedimentation rates, a prediction for the minimum length of the primary and secondary breakwaters is made.

2.4.2. Channel sedimentation

Channel sedimentation has to be taken into account regarding the required maintenance dredging. Channel sedimentation occurs as a result of the decrease in flow velocity due to a sudden increase in water depth at the channel location (PIANC, 2008). This can be derived from:

$$\frac{u_{y,1}}{u_{y,0}} = \frac{h_0}{h_1} \tag{2.17}$$

in which:

$u_{y,0}$	=	Current flow velocity component perpendicular to the channel outside the channel	$[m/s]$
$u_{y,1}$	=	Current flow velocity component perpendicular to the channel inside the channel	$[m/s]$
h_0	=	Water depth outside the channel	$[m]$
h_1	=	Water depth inside the channel	$[m]$

The sudden increase in depth also leads to a change in flow direction. This is taken into account by the notation in equation 2.17. Next to change in the y-direction, there is also a component in the x-direction, the flow along the channel. The equation is given as follows:

$$\frac{u_{x,1}}{u_{x,0}} = \frac{C_1}{C_0}\sqrt{\frac{h_1}{h_0}} \tag{2.18}$$

in which:

$u_{x,0}$	=	Current flow velocity component parrallel to the channel outside the channel	$[m/s]$
$u_{x,1}$	=	Current flow velocity component parrallel to the channel inside the channel	$[m/s]$
h_0	=	Water depth outside the channel	$[m]$
h_1	=	Water depth inside the channel	$[m]$
C_0	=	Chézy coefficient outside the channel	$[m^{1/2}/s]$
C_1	=	Chézy coefficient inside the channel	$[m^{1/2}/s]$

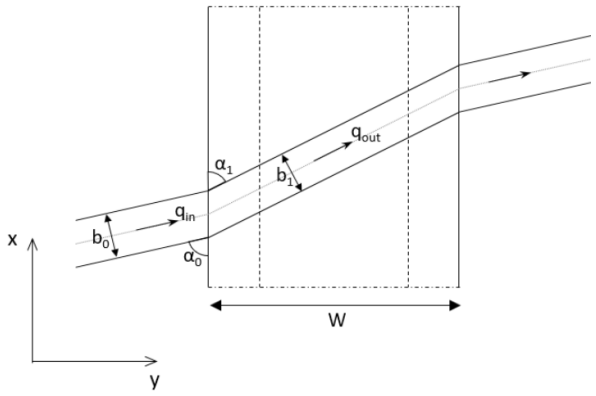

Figure 2.12: Visualisation of the approach used to determine channel sedimentation, including the channel width (denoted by W), the streamtube (denoted by b), the sediment transport (denoted by q) and the current flow angle w.r.t. the main channel axis (denoted by α)

From these equations, it is possible to derive that (assuming the Chézy-coefficient is constant) the incoming current flow velocity (denoted by $u_{x,0}$) can be larger than the current flow velocity inside the channel (denoted by $u_{x,1}$), depending on the difference in depth and the angle of approach of the current with regard to the channel (denoted by a_0). It should be noted that current flow does not accelerate within an instant and that a certain adaption length is needed for the equilibrium current flow velocity to be reached.
The angle of the current flow will also change due to the increase in depth. This change in direction can be determined using Equation 2.19 (PIANC, 2008).

$$tan(\alpha_0) = \sqrt{(h_0/h_1)^3 tan(\alpha_1)} \tag{2.19}$$

in which:

α_0	=	flow direction outside the channel	$[^o]$
α_1	=	flow direction inside the channel	$[^o]$
h_0	=	Water depth outside the channel	$[m]$
h_1	=	Water depth inside the channel	$[m]$

The current flow velocity in the channel can be determined if the change in flow direction is known. The equation to determine this current flow velocity is (Van Rijn, 2013):

$$u_1 = u_0(h_0/h_1)(sin\alpha_0/sin\alpha_1) \tag{2.20}$$

Current flow velocity, current direction and water depth are important parameters in the determination of sediment transport into the channel and the sediment transport out of the channel. The channel

sedimentation rate depends on the difference between the incoming sediment transport (denoted by q_{in}) and the outgoing sediment transport (denoted by q_{out}). For the calculation of the channel sedimentation rate, the sediment transport is defined per streamtube (denoted by b). Due to the difference in water depth, the flow direction will change in the channel. This change in flow direction results in a change in streamtube width (shown in Figure 2.12). This change in streamtube width has to be accounted for and can be calculated using Equation 2.21 (Van Rijn, 2013).

$$b_1 = v_0 h_0 b_0 / v_1 h_1 \tag{2.21}$$

Apart from currents, waves can also have an effect on the channel sedimentation rate. Waves approaching the channel will refract towards the channel direction, due to the deepening of the bed. The behavior of the wave can be determined using Snell's law. As the wave approaches the channel, the wave period will not alter. This will lead to an increase in wavelength, since the wave celerity will increase due to a larger depth. Assuming no loss of energy, the wave height will reduce. This leads to an overall reduction in the bed shear stresses that are induced by the waves, which in turn leads to settlement of sediment.
Due to the increase in water depth, flow is also attracted. Theoretically, this could even lead to a channel completely flushing itself. In reality, also due to wave activity and 3D-effects, this is generally not the case. Deepening a channel has larger sedimentation rates as a result and will almost always lead to an increase in required maintenance dredging. However, smart channel positioning might reduce the trapping efficiency and can therefore make a difference in possible costs.

Due to the importance of currents in the calculation of the sedimentation rate in channels, the types of currents that occur are reviewed. For currents in coastal waters, a distinction is made between tidal currents, residual currents. For the calculation of channel sedimentation rates, both the residual currents and the tidal currents have to be taken into account (Mangor et al., 2017).
The influence of waves should also be taken into account. The wave orbital velocity causes stirring of sediment, after which it can be transported by currents (Soulsby, 1997). The stirring of sediment can increase the transport of sediment and increase channel sedimentation rates.

Channel Sedimentation Equations
For the calculation of the sedimentation rates in a channel, several equations are available. The equations that are generally used are the Eysink-Vermaas equations (Van Rijn, 2013), the Van Rijn equations (Van Rijn, 2013) and the Soulsby-Van Rijn equations (Soulsby, 1997). For these equations, the channel is schematized as a rectangular cross-section, as shown in Figure 2.13.

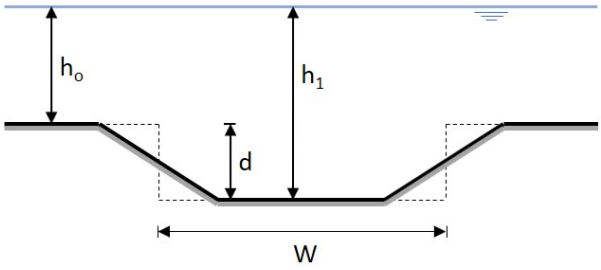

Figure 2.13: Channel schematization for determination of sediment trapping efficiencies for Eysink-Vermaas, Van Rijn and Soulsby-Van Rijn. The water depth outside the channel is denoted by h_0, the water depth inside the channel is denoted by h_1, the depth of the channel w.r.t. the seabed level is denoted by d and the schematized width is denoted by B

Both the Eysink-Vermaas and the Van Rijn equations determine a channel filling rate based on current flow velocity. Both equations do not account for wave orbital velocity. The Soulsby-Van Rijn equation is a modification of the Van Rijn equation. This equation determines the channel filling rate using current flow velocity and wave orbital velocity. The equation has been used by Michael Rustell (2016) for the determination of the channel filling rate in his model for LNG terminals.

The Soulsby-Van Rijn equation has been validated using the TRANSPOR model (Soulsby, 1997). TRANSPOR is a model that determines sediment transport due to waves and currents (Van Rijn, 2020). The results are shown in Figure 2.14.

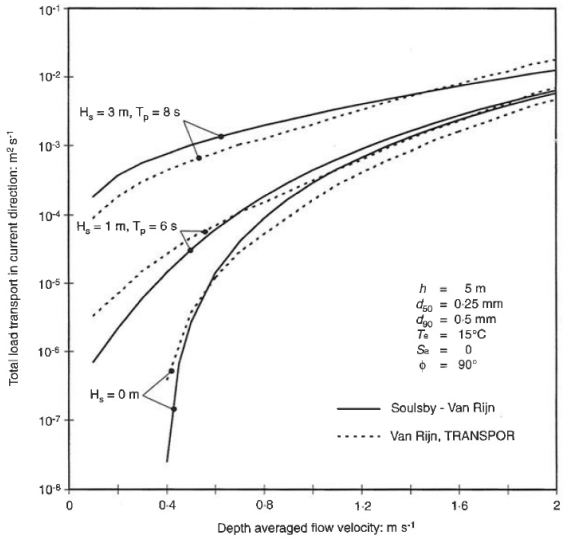

Figure 2.14: Performance comparison between Soulsby-Van Rijn and Van Rijn in combination with TRANSPOR (Soulsby, 1997)

The differences are smaller than factor 2, which is sufficiently accurate for equations that approximate sediment transport (Soulsby, 1997). The Soulsby-Van Rijn equation is chosen for implementation concerning the calculation of the channel filling rate. This equation is seen as most suited, due to its incorporation of both wave orbital velocity and current flow velocity.

Soulsby-Van Rijn

The Soulsby-Van Rijn equation is based on the following balance equation (Rustell, 2016):

$$q_t = q_{in} - q_{out} \tag{2.22}$$

in which:

q_t	=	Total flow of sediment per unit length	$[m^2/s]$
q_{in}	=	Sediment entering the channel per unit length	$[m^2/s]$
q_{out}	=	Sediment leaving the channel per unit length	$[m^2/s]$

The total flow of sediment (denote by q_t) is equal to the difference between the sediment entering and the sediment leaving the channel per unit time per unit length. This difference is used to determine the filling rate.

The transport of sediment into the channel (denoted by q_{in}) and the transport of sediment out of the channel (denoted by q_{out}) are determined with the following equation (Soulsby, 1997):

$$q = A_s \overline{u} \left(\left(\overline{u}^2 + \frac{0.018}{C_D} u_{rms}^2 \right)^{0.5} - \overline{u}_{cr} \right)^{2.4} (1 - 1.6 \tan\beta) \tag{2.23}$$

in which:

A_s	=	Coefficient for sediment transport	[-]
$\overline{u}$	=	Mean current flow velocity	$[m/s]$
C_D	=	Drag coefficient due to current	[-]
u_{rms}	=	RMS wave orbital velocity	$[m/s]$
$\overline{u}_{cr}$	=	Treshold current speed	$[m/s]$
$tan\beta$	=	Slope of the channel bank	[-]

The total flow of sediment is determined using the difference between the incoming and outgoing sediment transport. Thereafter, the total flow is used to determine the mean infill rate for a channel section. The equation for this infill rate (Soulsby, 1997):

$$\psi = \frac{q_t}{W(1-\varepsilon)} \sin(\alpha_1) \tag{2.24}$$

in which:

ψ	=	Mean infill rate	$[m/s]$
q_t	=	Total sediment transport per unit length	$[m^2/s]$
W	=	Width of the channel section	$[m]$
ϵ	=	Coefficient of settlement (= 0.4)	[-]
α_1	=	The angle of the current flow velocity inside the channel w.r.t. the main channel axis	$[^o]$

Using the infill rate, it is possible to determine the channel siltation volume over a period of time. A more detailed description of the parameters and the equations to calculate these parameters is given in Appendix E.2.

Calculation of the infill rate
For determination of the infill rate, the following environmental conditions are required locally:

- Wave height
- Tidal current flow velocity
- Tidal current flow direction
- Residual current flow velocity
- Residual current flow direction

Wave height and wave direction have to be locally determined. The residual current parameters have to be given as input by the user, as well as the tidal current parameters.
Tidal currents occur during both ebb and flood. Due to the use of mean current flow velocity in the Soulsby-Van Rijn equation, the tidal current flow velocity has to be added to the residual current flow velocity. Since the tidal currents can occur in opposite directions during ebb and flood, separate calculations have to be made for ebb and flood.

2.4.3. Siltation in basins

The sedimentation that occurs in the harbour basins influences maintenance dredging costs. To determine the yearly sedimentation volume in the harbour basin, a siltation rate is used. The siltation rates of harbour basins can be quantified with empirical equations that have been derived. These equations are described in a PIANC report on minimizing harbour siltation (PIANC, 2008). For these equations, the harbour basin is schematized as shown in Figure 2.15

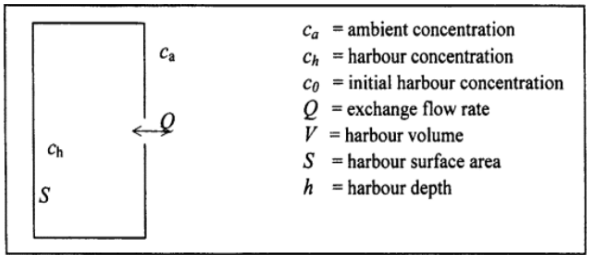

Figure 2.15: Simplified representation of a harbour basin and the important parameters (PIANC,2008)

The sedimentation rate inside the harbour can be calculated using the Equation 2.25 (PIANC, 2008). This equation is used to determine the filling rate during one tidal period.

$$F_{s,T} = SW_s \frac{Q}{Q + SW_s} c_a T \tag{2.25}$$

in which:

$F_{s,T}$	=	Sedimentation rate	$[m^3/s]$
S	=	Basin surface area	$[m]$
W_s	=	Effective sediment fall velocity	$[m/s]$
Q	=	Exchange flow rate	$[m^3/s]$
c_a	=	Ambient sediment concentration in the area	$[kg/m^3]$
T	=	Tidal period	$[s]$

The exchange flow rate is essential for the determination of the sedimentation rate. The total exchange flow rate is defined by the following equation (PIANC, 2008):

$$\langle Q \rangle = \langle Q_t \rangle + \langle Q_e \rangle + \langle Q_d \rangle + \langle Q_T \rangle \tag{2.26}$$

in which:

Q	=	Total exchange flow rate	$[m^3/s]$
Q_t	=	Exchange flow rate due to tidal filling	$[m^3/s]$
Q_e	=	Exchange flow rate due to horizontal entrainment	$[m^3/s]$
Q_d	=	Exchange flow rate due to density currents	$[m^3/s]$
Q_T	=	Exchange flow rate due to cooling water discharges	$[m^3/s]$

Of these parameters, the exchange flow rates due to density currents and cooling water discharges are not within the scope of this research project. These flow exchange rates are dependent on flow caused by differences in water density or water temperature, which are both not included in the boundaries set in Section 1.3.2.

The exchange rate due to tidal filling can be determined using the basin area and the tidal amplitude. The determination of the exchange flow rate due to horizontal entrainment depends partially on the basin area and the exchange flow rate due to tidal filling. Both of these parameters can be calculated without a problem if the breakwater configuration is known.

However, for the calculation of the exchange flow rate due to horizontal entrainment, two empirical coefficients are required. These empirical coefficients do not have a standard value, but have to be determined based on previous comparable port designs or hydraulic modelling (Eysink, 1989).
Also, for the calculation of the sedimentation rate, the effective falling velocity dependents on the retention time and the current flow velocity in the harbour are required. These two parameters that have to be based on a realistic and sound image of current patterns in the harbour (Eysink, 1989), which will have to be modelled. Regarding the type of model that is developed, this will not be executable. Therefore, using this method is not a viable option.

The theory behind the method does give helpful insight. From the reviewed literature, it can be derived that the siltation rate of the port basins is linearly proportional to the basin area and partly dependent on the entrance geometry (Eysink, 1989). An expected siltation rate of the basins is used, with corrected siltation rates based on the entrance geometry. The yearly siltation volume can be determined using the siltation rate and the basin area that corresponds to the model. This has already been included in the model, using a basin siltation rate in meters per year, of which the value depends on the entrance geometry.

3

Methodology

In Chapter 2, the bathymetry, the modelling of wave transformation and the sedimentation processes have been recognized as essential subjects for the improvement of the model applicability. Implementation of these subjects has to be performed in the correct order, as these subjects interact with each other.
Both wave transformation and sedimentation processes are influenced by depth. Therefore, implementation of the bathymetry has been performed first. Sedimentation processes are also influenced by wave height and wave angle. Therefore, the modification of the wave modelling has been performed after the implementation of the bathymetry profiles. Thereafter, the sedimentation processes have been implemented. As a result, the processes have been implemented in the order as shown in Figure 3.1.

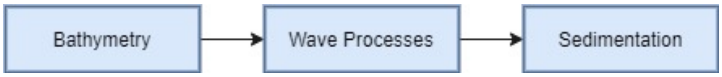

Figure 3.1: Order of process implementation

3.1. Bathymetry

In the original model, depth variation occurs only in the y-direction. The bathymetry is modelled as a homogeneous slope (see Figure 3.2). For the implementation of realistic bed profiles, a method had to be used that allows for non-homogeneous depth variations in both the x- and y-direction (see Figure 3.7).

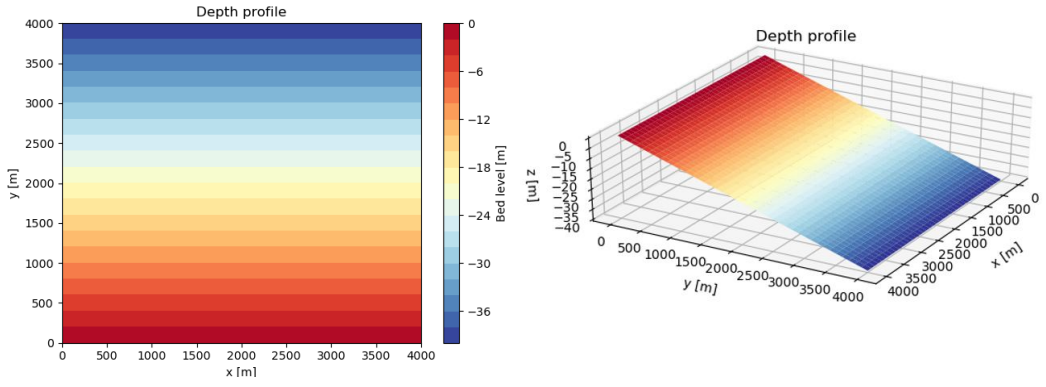

(a) (b)

Figure 3.2: (a) Contour lines for the depth profile in the original model (b) 3D visualisation of the depth profile in the original model

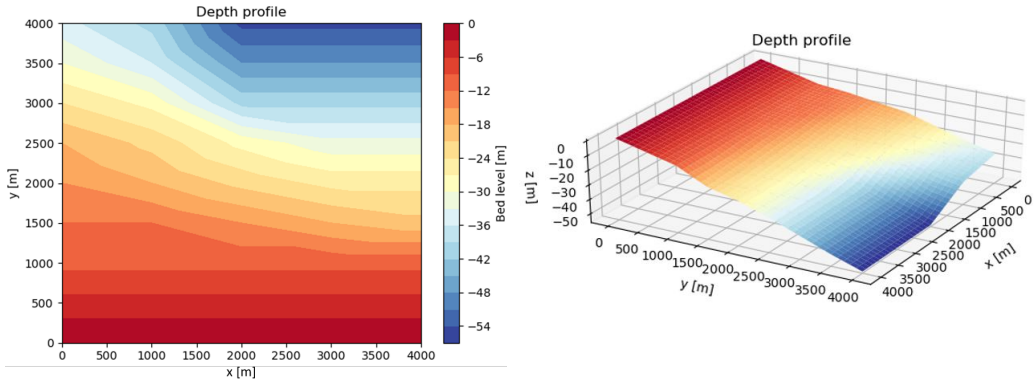

(a) (b)

Figure 3.3: (a) Contour lines of a depth profile with variation in both x- and y-direction (b) 3D visualisation of a depth profile with variation in both x- and y-direction

The method that is used for the implementation of the bathymetric profiles has to be accurate enough for conceptual design and fit the current model setup, while adding as little computation time as possible. Therefore, the following details have been kept in mind:

- In the original model, the locations of the breakwater nodes are defined in meters precise. As a result, the method used for the implementation of bathymetric profiles has to allow the model to determine the seabed level at these points. Determining these bed levels has to be performed without generating errors (such as grid boundary errors or points with undefined bed levels).
- The breakwater layouts can be constructed in both the negative and the positive x-direction. This feature has to work sufficiently after the implementation of bathymetry.
- Implementation of the wave processes and sediment transport processes should be kept in mind when selecting a method. A certain method might be a better match with the implementation of other processes.

3.1.1. Grid implementation

The inclusion of bathymetry can best be accomplished using a grid. Therefore, the inclusion of a grid is at the centre of integrating more realistic bed profiles into the model. In models, the type of grid that is used can vary in both shape and the type of grid cells. Commonly used grids are:

- Grids with triangular grid cells
- Grids with rectangular grid cells
- Grids using both triangular and rectangular grid cells (flexible mesh)

These grids are visualised in Figures 3.4a, 3.4b and 3.4c.

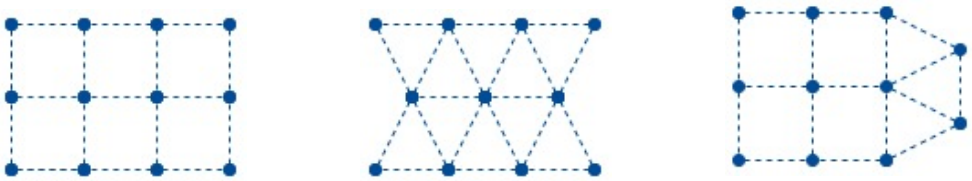

(a) Grid with rectangular grid cells (b) Grid with triangular grid cells (c) Grid with both triangular and rectangular grid cells

Next to different grid forms, the spatial step is also important. Depending on the size of the area of interest, the spatial step is usually adjusted accordingly. Variation of spatial step size within a grid is not uncommon, when certain area's within the entire grid area require more detail.
The grid form that has been chosen for the implementation of the bathymetry is a grid with rectangular grid cells and a constant spatial step. This type of grid is best suited for its intended purpose, which

is the assignment of depth values to x,y-coordinates. Variation of spatial size within the grid is unnecessary, as the areas that are covered are relatively small. An advantage of the rectangular grid with constant spatial step is that it can be applied in the wave model REFRAC (REFRAC Team, 1994)), which is used for the calculation of wave transformation (see Section 3.2).

The rectangular grid is created using bathymetry data in xyz-format. This is accomplished using Python, the same programming language that is used by the original model. The data is saved as a matrix, containing the depth values that correspond to x,y-coordinates. When creating the grid, the spatial step and the size of the grid can be determined by the user, based on user input. The default size of the grid is an area of $4 * 10^3$ m by $4 * 10^3$ m. This area has been chosen as the default area that is used in the original model. The default spatial step size is 10 m. This step size has been chosen as it will be accurate enough to account for bed level variations. In addition, a larger step size will reduce the size of the bed level data file that is used in the model compared to smaller step sizes like 5 m or 1 m. This reduction in the size of the bed level data file results in a smaller run-time of the updated model.

3.1.2. Direction of the layout

The generated layouts are constructed in both negative and positive x-direction. In the original model, this has been accomplished by assigning negative values to the x-coordinates. Since depth is determined solely by the y-coordinate in the original model, this method does not pose a problem.

With the implementation of the bathymetry profiles, the seabed level at a location now depends on both x- and y-coordinates. The seabed level that corresponds to these coordinates is drawn from a matrix containing the depth values. The x- and y-coordinates of a location correspond to indices in that matrix, which in turn corresponds to the seabed level at that location.

When the layout is constructed in the negative x-direction, the corresponding indices for the x-coordinates should also adjust to the negative direction. This can be done using negative indexing, visualised in Figure 3.5.

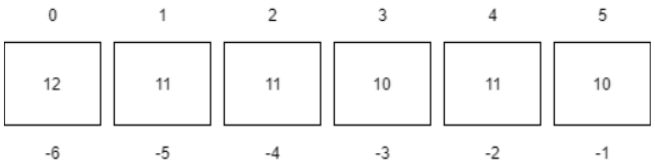

Figure 3.5: Negative indexing with an array

When regular indexing is used, an array is read from left to right. The first value in the array corresponds to the index 0, the second value corresponds to index 1 and so on. When negative indexing (i.e. reading an array from right to left) is used, the first index value is -1. This index value indicates to the model that negative indexing will be used.

The x-coordinate of the position of the primary breakwater at the shoreline is defined as x = 0. The resulting index value for that x-coordinate is also 0. When the breakwater is constructed in the negative x-direction, negative indexing will be used. The index 0 will then correspond to a bed level on the other boundary of the grid (located at the left side), instead of the actual bed level, which corresponds to index -1 (see Figure 3.5). Consequently, a correction is needed concerning the x-coordinates of the nodes and their corresponding index that is used for the determination of the seabed levels. Therefore, when negative indexing is used, the index corresponding to the x-coordinate is reduced by 1, to attain the correct seabed level.

The direction in which the layout is constructed, can be determined by the user in the input sheet. If the user is uncertain or wants to let the model assess both options, it is also possible to give "na" as input, which leaves the direction undefined. In this case, each generated individual can be constructed in positive or negative x-direction, comparable to the original model.

3.2. Wave processes

The addition of bathymetry profiles results in required modifications concerning the modelling of wave transformation. The method used in the original model is not able to accurately model the wave transformation for complex bathymetry profiles with depth variations in two dimensions, especially in relation to the process of refraction. To sufficiently model the wave transformation, a simple but adequate wave model is used. Three wave models have been reviewed:

- SWAN-One
- REFRAC
- APEX Wave Ray

To assess which of these models is adequate for implementation, attention has been given to the following aspects:

- Compatibility with the current model setup
- Wave direction accuracy
- Wave height accuracy
- Computation time

3.2.1. SWAN-One

SWAN-One is a one-dimensional wave modelling tool that uses the 1D-mode of the SWAN (Simulating WAves Nearshore) model. It is used to model wave transformation from offshore conditions to a requested point nearshore. It takes into account refraction, shoaling and influence of winds and currents. In SWAN-One, the depth contours of the bottom profile are assumed to be parallel to the shoreline (TU Delft, 2018). To run the model, the following input is required:

- The bottom profile, given as txt-file that contains the bed levels in shore-normal direction on locations between the offshore point and the shoreline, due to its one-dimensional nature.
- Current flow data (given in a txt-file), which should contain the location at which a current is imposed, as well as its parallel and perpendicular velocity with regard to the bottom profile.
- Boundary conditions (defined in the program interface), which includes wave parameters like wave height, wave period and wave direction. It is also possible to define a spectrum using a data file. When a deep water significant wave height is defined, it is internally converted to a 2D JONSWAP spectrum. Wind speed and wind direction can also be defined. The wind speed should be set in meters per second and direction in degrees with respect to north. The water level also has to be defined, being set at 0 meters by default.
- Output locations, which are defined at a distance with respect to the starting point ($x = 0$). It is possible to select multiple locations.

The number of steps during the computation is taken at 1000 by default. This can be changed by the user. The step size can also be defined by the user. After computation, the model generates the local wave parameters that are required for the downtime calculations in the breakwater model:

- Spectral significant wave height (H_{m0})
- Mean absolute wave periods ($T_{m-1.0}$)
- Mean wave direction (θ)

It also produces the following output:

- *Peak periods*
- *Directional spreading of waves*
- *Water depth*
- *Wave induced setup*
- *Wave height exceeded by 2%*
- *Mean wave height of highest 10%*

- *Mean wave height of highest 1/3rd of the Waves*

Wave transformation
An advantage of the SWAN models is its accurate calculation method for the wave transformation towards the shore. It takes into account the influence of other environmental aspects (winds and currents) on wave transformation, apart from refraction and shoaling.

Wave direction/wave development
A downside of the model is its one-dimensional nature. This leads to less accurate refraction computations for complex depth profiles, since seabed level variation can only be accounted for in one horizontal direction. As a result, the determined wave direction and the wave height are less accurate.

Compatibility
The compatibility between SWAN-One and the current model setup is far from ideal. For the integration of the SWAN-One model into the breakwater model, there are two possibilities.
The first option is to perform a calculation for each individual layout generated by the model. The coordinates of the point at which the wave parameters are desired need to be exported to the SWAN-One model, as well as the bottom profile perpendicular to those points. The environmental conditions have to be imported into SWAN-One from the input file. Then, the model is run, after which the output data has to be loaded into the breakwater model.
A second option is to do multiple runs beforehand. Each run has to be performed for a different section of the bathymetry. With this method, data containing wave height and wave direction can be created for each point on the grid. However, this method is less accurate than option one.

Computation time
Regarding computation time, it is expected that the use of this model will result in a significant addition to the run-time. Either the computations have to be executed for each individual layout (which will significantly increase computation time during the calculations) or the computations are done beforehand. Executing the computation beforehand will result in less computation time during the model run compared to the first option, but will take significant time to prepare and run beforehand.

3.2.2. REFRAC
REFRAC is a refraction model, following the geometrical optics approximation (Liu, 2009). It constructs the wave rays from an offshore starting point towards a given boundary of which the default is the coastline where the water depth is zero. The wave rays are computed using a 4th order Runga-Kutta scheme. Based on these rays, it is possible to approximate the wave direction at a desired location. These calculations are done using a data file containing depth values that correspond to x,y-coordinates. Apart from determining wave direction, REFRAC also provides the option to determine wave heights, using the Bouws-Battjes interpretation method (REFRAC Team, 1994).
For REFRAC, the following input is required:

- Bottom profile (given as .BOT file), containing depth values corresponding to x,y-coordinates.
- Offshore starting distance and offshore wave direction for the construction of one or multiple wave rays
- Incoming wave height at the offshore starting distance
- Wave period
- Water level

Apart from the above-mentioned input, there are also certain parameters that have a default value, but that can be modified by the user if preferred:

- Depth outside bottom grid (*Default = 1000 m*)
- Threshold depth (*Default = 0.05 m*)
- Maximum length of a ray in number of wavelengths (*Default = 1000*)
- Gravitational acceleration coefficient (*Default = 9.81* m^2/s)

- Numerical accuracy (integration step as fraction of the wavelength; *Default = 0.1*)
- Smoothing parameter (*Default = 0*)

As mentioned before, it is also possible to determine the wave heights, which are computed using the Bouws-Battjes interpretation method (Bouws and Battjes, 1982). In this method, the wave rays are used to approximate the amount of energy within a cell with a specified area, the size of which is determined by the user. Based on this energy, the wave height in that cell is determined.
The generated output is:

- Wave angle along the wave ray (θ), per unit wavelength
- Wavelength along the wave ray (L)
- Wave height at given coordinates (H_s)

Wave transformation
Computation of the wave height is done using the Bouws-Battjes method (Bouws and Battjes, 1982), taking into account shoaling and refraction. The computation is performed for an area of which the size is determined by the user. The grid cell sizes in this area can also be determined by the user. The grid cell size can be defined as small as the user wants, leading to the desired accuracy. It is also possible (and recommended) to average the amount of energy with neighbouring cells when unrealistic peaks would occur, leading to smoothing of the wave heights.

Wave direction
The wave direction is given as data along the wave rays that have been computed by the program, per unit wavelength. The distance between the wave rays is user-defined, which gives the possibility to adjust the density of the wave rays. It is possible to define them as close as the user prefers.

Compatibility
The bathymetry grid that is required as input for REFRAC has the same format as the one used for the breakwater model. The grid that is constructed in the breakwater module can therefore be used as input for the REFRAC model. This makes REFRAC very compatible with the breakwater model in its current and planned form.

Computation time
The model can be run beforehand, after definition of the bathymetry grid. The amount of computation time required for running REFRAC depends on the number of the wave conditions and the desired accuracy, but is still relatively small. The output data can be imported into the breakwater model, after which the wave data can be drawn from the data file for each point, leading to no increase in computation time while running the model.

3.2.3. APEX Wave Ray
The APEX Wave Ray model (sometimes referred to as the PROP model) is used to determine the wave transformation from offshore conditions to a point nearshore. It is possible to take shoaling, refraction and diffraction and the influence of the wind, bottom friction and currents into consideration. To determine the wave parameters at a desired point, the calculation has two be divided into two steps. First, an input wave field has to be defined. This can be done using one of the following operations:

1. Reverse Hindcasting (Operation name: *REVHCS12*)
2. Simple Spreading (Operation name: *SPREAD12*)
3. Hindcasting (Operation name: *HCAST12*)

The input required for Simple Spreading is a wave spectrum, in which different wave directions, periods and wave heights are defined. This can either be done in series (in the model referred to as *SER*), which means that the wave in spectrum input is given all at once. This method is preferred when working with a pre-established set of conditions. It is also possible to define the input as a matrix (in the wave model referred to as *MAT*), which provides the possibility to assess every wave height with every wave period in every defined direction.

For Hindcasting, the required input consists of wind speeds, main directions, wave periods, spreading index and storm duration.
For Reverse Hindcasting, the wave heights, wave periods, main directions, storm duration and wind speed for each wave height for each direction are required.
After the wave input field is defined, wave transformation that occurs when waves travel from offshore to a point nearshore can be calculated with the wave model. In APEX Wave Ray , this is done using transformation operations, each accounting for one or more processes (like refraction, diffraction or shoaling). These operations are listed below:

- Diffraction Coefficients (*CDIF*)
- Diffraction (*DIFFR12*)
- Refraction (*REFR12*)
- Corner Refraction (*CRFCR*)
- Refraction, Shoaling and Dissipation (*HIS1D*)

The output of these operations is either a wave spectrum or a coefficient, depending on which operation is performed. When deciding on which operation to use it is of importance to see that the input is the same as the output generated by the operation that is executed before. In addition, when multiple operations have to be performed, the order of the operations is of importance. A more detailed description of the APEX Wave Ray model can be found in Appendix D.
Most transformation operations need additional input apart from the wave spectrum defined using the wave field operations. For the transformation of the waves due to refraction and shoaling, a bottom profile is required as input. This bottom profile is defined in the same manner as in SWAN-One, with the water depth given at points with a certain distance from the offshore point, as well as the assumption of parallel depth contours. It is possible to define multiple bottom profiles, depending on the wave direction. However, the assumption of parallel depth contours is still present.
After the transformation, the output contains wave data at a certain depth, defined by the user (similar to the output of SWAN-One):

- Wave direction
- Wave height
- Peak period
- Spreading

Wave transformation
The APEX Wave Ray model performs well regarding the accuracy of wave transformation, as it takes shoaling, refraction and the influence of wind, bed friction and currents into account. It also presents the opportunity to incorporate diffraction.

Wave direction
A downside of the model is that the wave transformation is modelled along a profile with parallel depth contours, comparable to SWAN-One. This decreases the accuracy of the determined wave parameters when it concerns complex depth profiles. Although it is possible to modify the angle of the depth contours with respect to the shoreline, the model is still one dimensional.

Compatibility
Concerning compatibility with the breakwater model, the same problems arise as with SWAN-One (see Section 3.2.1). Computations have to either be done for each individual layout during a run or for numerous sections preliminary.

Computation time
The expected computation time of APEX Wave Ray is comparable to that of SWAN-One. Performing the calculations for each layout individual will significantly increase the computation time during runs. Running the model preliminary will take a significant amount of time, due to performing the runs and due to preparation.

3.2.4. Selection of models

The suitability of the wave models for implementation in the breakwater model is assessed using the same criteria aspects mentioned in Section 3.2:

- Compatibility with current model setup
- Wave direction accuracy
- Wave height accuracy
- Computation time

This assessment is based on analysis of each model, which is described in Sections 3.2.1, 3.2.2 and 3.2.3. These analyses have led to the following observations, visualised in Table 3.1.

	SWAN-One	REFRAC	APEX Wave Ray
Compatibility with current model setup	- -	+ +	- -
Wave direction	0	+ +	+
Wave height	+	0	+
Computation time	- -	+	- -

+ +	=	Very good
+	=	Good
0	=	Sufficient
-	=	Bad
- -	=	Very Bad

Table 3.1: The scores of the wave model performance for each wave model, upon which their suitability is judged

It is concluded that REFRAC is the most suited for integration with the model. The REFRAC model is very compatible with the model in its current form, it has the most accurate determination of the wave direction, its accuracy in determining the wave height is sufficient and due to the calculations being performed preliminary, it will not add to the current computation time, but even slightly reduces it.

3.3. Sedimentation

The implementation of sediment transport and sedimentation in the model is required due to its importance regarding the breakwater layout design and maintenance dredging. Based on the findings described in Chapter 2, the implementation of the sediment transport processes has been divided into three components:

1. Sedimentation due to longshore sediment transport
2. Sedimentation in the navigation channel
3. Sedimentation in the harbour basin

3.3.1. Longshore transport

Longshore sediment transport is important for the design of the primary and secondary breakwaters. As mentioned in Section 2.4.1, a function of the breakwaters is to prevent the transport of sediment into the harbour basin. To determine the required breakwater length to prevent sediment transport into the harbour basin, the accretion along the breakwaters must be determined. This accretion is estimated using the longshore sediment transport rates.

For the determination of longshore sediment transport rates, the bulk transport formulas are used. Three possible options have been explored in Chapter 2. Out of these three, the bulk transport formula that has been chosen for implementation is the Van Rijn equation (Equation 2.13).
The longshore sediment transport rates are used to predict accretion over a certain time period. This time period (in years) is given by the user. The main component that is of interest is the accretion length along the breakwater in shore-normal direction. The accretion will expand in seaward direction along the breakwaters over time. The length of the accretion along the breakwater in shore-normal direction will be used to determine the minimum length of the breakwaters, to prevent bypassing and sedimentation in the harbour.
A divide has been made between accretion at the updrift side of the port and accretion at the downdrift side of the port, as they need to be determined using different methods.

3.3.2. Updrift accretion and the minimum primary breakwater length

The updrift accretion is important for the design of the primary breakwater. The updrift accretion length in shore-normal direction along the breakwater is used to determine the minimum length of the primary breakwater to prevent bypassing. The minimum length of the primary breakwater is determined by adding the accretion length along the breakwater in shore-normal direction to the distance between the shore-line and the breaker line in shore-normal direction. The breaker line that is used in this calculation is the breaker line that corresponds to the mean wave height.

For the calculation of the accretion length along the breakwater in shore-normal direction, the Pelnard-Considère equation (Equation 2.14) is used.

$$L(t) = 2\sqrt{\frac{\phi' St}{\pi d}}$$

The longshore sediment transport rate that is used for this calculation (denoted by S) is the net sediment transport rate. This sediment transport rate is determined using the wave conditions and their probability of occurrence. Both the wave conditions and their probability of occurrence are provided by the user as input. The mean wave direction (denoted by ϕ' in radians) is also determined using the wave conditions and their probability of occurrence.
The profile height (denoted by d) is given by the user. This profile height can be determined with the theory provided in Section 2.4.1. The time period (in years) is also provided by the user.

Based on these parameters, the updrift accretion length in shore-normal direction along the breakwater (denoted by L_{acc}) is determined (shown in Figure 3.6a). With the use of this calculation, it is assumed that the shore profile is constant over time (Bosboom and Stive, 2015), as shown in Figure 3.6b.

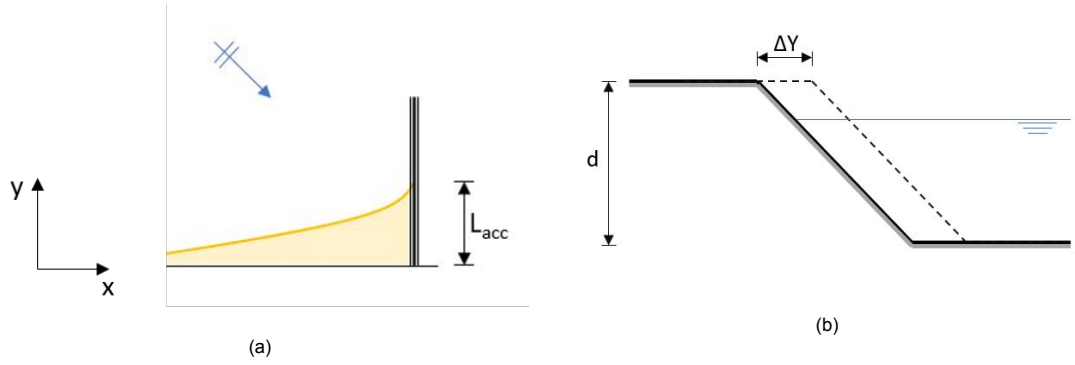

Figure 3.6: (a) The accretion length (denoted by L_{acc}) along the breakwater in shore-normal direction at the updrift side (b) The cross-shore profile that is assumed with a profile height d, in which ΔY resembles the accretion in shore-normal direction

The minimum length of the primary breakwater is determined using the accretion length along the breakwater in shore-normal direction and the distance from the shore to the breaker line known. This length is used as input for the generation of the layouts.

3.3.3. Downdrift accretion and the minimum secondary breakwater length

The accretion at the downdrift side of the port is important for the design of the secondary breakwater. The accretion length along the secondary breakwater in shore-normal direction is important in determining the required minimum length of the secondary breakwater to prevent bypassing. In the updated model, the minimum length of the secondary breakwater is determined by adding the accretion length in shore-normal direction along the breakwater to the distance between the shoreline and the breaker line. For this calculation, the same distance between the shoreline and the breaker line is used as for the calculation of the minimum length of the primary breakwater.

Estimating the accretion at the downdrift side of a port is complex. Diffraction effects, nearshore circular currents due to these diffraction effects and possible erosion have to be taken into account. Therefore, the accretion is usually determined with the use of a numerical model. However, the use of a numerical

model does not fit in the framework of the updated model. To make an estimation without the use of a numerical model, a method is used that is described by Van Rijn (Van Rijn, 2015). In this method, the longshore sediment transport rates on the downdrift side of the port are determined using Equations 2.13, 2.15 and 2.16. The sediment transport rates caused by waves that are coming in from the downdrift side are also accounted for.

The first step in determining the minimum secondary breakwater length is the determination of the sediment transport rates downdrift of the port. For the calculation of these sediment transport rates, the location of the diffraction point is of importance. The diffraction point is the point that causes diffraction effects. This diffraction point determines the size of the shadow zone and the distance between the shadow line and the secondary breakwater at the breaker line, which both influence the sediment transport rate at the downdrift side of the port (see Appendix E). The locations of the diffraction point and the shadow zone are shown in Figure 3.7a.

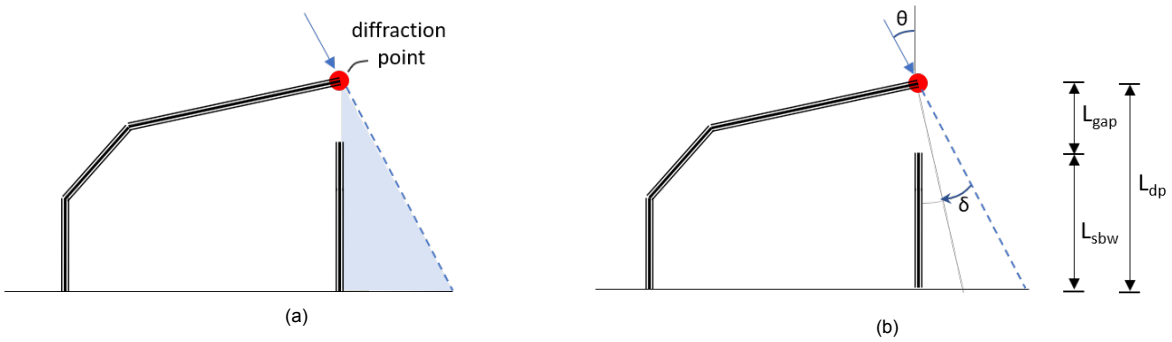

Figure 3.7: (a) A visualisation of the diffraction point location, with the shadow zone visualised as the blue area (b) The standard breakwater layout used for the determination of the minimum secondary breakwater layout

Due to the influence of the diffraction point location on the sediment transport rates, the location of the diffraction point also influences the accretion that occurs. The location of the diffraction point depends on the port layout. Therefore, the location of the diffraction point can differ for each layout alternative. The minimum lengths of the primary and secondary breakwater are used as boundaries for the possible locations of the breakwater nodes. Therefore, the minimum lengths of the primary and secondary breakwaters are required before the layouts are generated. As a result, the minimum primary breakwater length and the minimum secondary breakwater length have to be estimated before the layouts are generated.

To allow the model to make an estimation of the minimum secondary breakwater, a standard breakwater layout has to be assumed. The standard breakwater layout that is used is shown in Figure 3.7b.

In this standard breakwater layout, the diffraction point at the primary breakwater is assumed at the same alongshore location as the secondary breakwater. The distance between the shoreline and the diffraction point (denoted by L_{dp}) is assumed to be equal to the maximum length of the secondary breakwater (denoted by L_{sbw}) and the breakwater gap (denoted by L_{gap}). This is shown in Figure 3.7b. This breakwater gap is assumed to be 2 times the minimum navigation channel width. The minimum navigation channel width is determined before the model loop, based on the PIANC guidelines (PIANC, 2014). The maximum length of the secondary breakwater is assumed to be equal to L_{dp} - L_{gap}.

The accretion length along the breakwater is determined for various L_{dp} values, ranging from the breaker line to the outermost point for the primary breakwater on the y-axis (which is provided by the user in the input parameters). Each length of L_{dp} has a corresponding maximum secondary breakwater length ($L_{sbw} = L_{dp}$ - L_{gap}).
The required minimum secondary breakwater length to prevent bypassing is equal to the accretion length plus the distance from the breakerline to the shoreline. From a certain value of L_{dp}, the corresponding sum of (1) the accretion length and (2) the distance from the breakerline to the shoreline is smaller than the corresponding maximum secondary breakwater length (denoted by L_{sbw}). The value of L_{dp} and the corresponding maximum length of the secondary breakwater for which this first occurs

is determined by the updated model. This corresponding secondary breakwater length is taken to be the required minimum secondary breakwater length (L_{sbw}) for which bypassing will not occur.

For the determination of the accretion length, the longshore transport rates downdrift of the structure are determined using the method described by Van Rijn (Van Rijn, 2015). For the determination of the longshore transport rates downdrift of the structure, the wave conditions and their probability of occurrence are used (which are provided by the user).

Based on these longshore transport rates, it is determined where the longshore transport rate towards the structure is maximum. At this location, the gradient in the sediment transport rate ($\frac{dS}{dx}$) is zero. As a result, there is no coastline change at this location (Bosboom and Stive, 2015). This has been visualised in Figure 3.9.

In the area between the location where $\frac{dS}{dx} = 0$ (in Figure 3.9 denoted by A) and the secondary breakwater, accretion will occur. The amount of sediment that enters this area is determined from longshore sediment transport rate where $\frac{dS}{dx} = 0$. To estimate the accretion length along the breakwater in shore-normal direction, the following assumptions have been made:

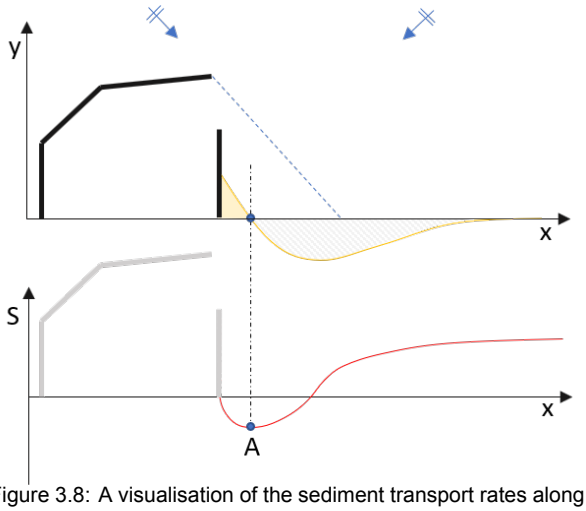

Figure 3.8: A visualisation of the sediment transport rates along the shoreline (bottom figure) in which A resembles the point at which the gradient of the sediment transport rate is zero. At this point, the coastline change is zero, as shown in the top figure

- The sediment transport rates are assumed to be constant over time.
- The accretion volume is schematized as a triangular area (shown in Figure 3.9) with a thickness that is equal to the profile depth :

$$V_{acc} = \frac{1}{2} L_{acc} W_{acc} d \qquad (3.1)$$

V_{acc}	=	Accretion volume	$[m^3]$
L_{ac}	=	Accretion length in shore normal direction	$[m]$
W_{acc}	=	Distance from structure to point where $dS/dx = 0$	$[m]$
d	=	Profile depth	$[m]$

  The base of the triangular area (denoted by W_{acc}) is equal to the distance between the secondary breakwater and the location where $\frac{dS}{dx} = 0$. The accretion length (denoted by L_{acc}) is the height of the triangular area.
- For the calculation of the sediment transport rates, the bed slope is assumed constant, with parallel depth contours.

These assumptions had to be made, to allow the model to make an estimation of the accretion length in shore-normal direction along the breakwater. It is noted that this estimation is likely to result in an overestimation, as the influence of the coastline change on the sediment transport rate is not accounted for in this method. These assumptions also introduce several other uncertainties and limitations, which are discussed in detail in Chapter 7.

Based on the calculated accretion length and the distance between the breakerline and the shoreline, the minimum secondary breakwater length is determined. This length is used as the input for the generation of the layout alternatives.

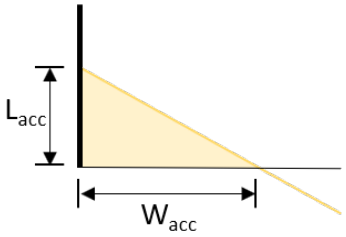

Figure 3.9: The schematization of the accretion area at the downdrift side of the port, along the secondary breakwater.

3.3.4. Channel sedimentation

Channel sedimentation has been incorporated in the updated model, to provide a more accurate indication of the dredging costs for a certain breakwater layout configuration. To determine the filling rate, different equations can be used. Three of these equations have been presented in Section 2.4.2. The Soulsby-Van Rijn equation takes both the current flow velocity and the influence of local waves into account in the determination of the filling rate. The Van Rijn equation and the Eysink-Vermaas equation only account for the current flow velocity, as described in Section 2.4.2. As local wave conditions can have a significant influence on the filling rate (Van Rijn, 2013), it has been chosen to implement the Soulsby-Van Rijn equation.

The filling rate of the channel partially depends on the seabed level and the relative depth of the channel with respect to the seabed. The channel depth changes over time due to the sedimentation that occurs over time. In return, the filling rate will adjust to this new depth. Incorporating this change in filling rate and depth in the model leads to additional computation time. Therefore, the initial filling rate is used for the calculation of the channel siltation volume over a certain time period, as the calculation of the sedimentation volumes with this filling rate is accurate enough for conceptual design purposes.

The filling rate is determined per channel section with a pre-defined length (see Figure 3.10). Determining the filling rate per channel section allows for differences in seabed levels and wave conditions along the navigation channel to be taken into account.

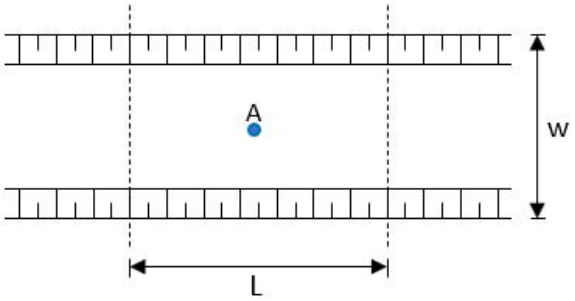

Figure 3.10: A channel section with a constant channel width (denoted by W) and a pre-defined length (denoted by L). The location A is the point where the representative wave height and wave direction for the channel section are determined.

To establish a mean filling rate, the filling rate is separately calculated for both ebb currents and flood currents, as discussed in Section 2.4.2.
For the incorporation of the local wave influence on the filling rates, the wave heights at the channel section location are required. The local wave heights are determined using the values produced by REFRAC, taken at the point in the center of the channel section (denoted by A).
The mean filling rate is determined per section, for each wave condition, taking into account the probability of occurrence of each condition.

Maintenance dredging operations are performed once per year or once every couple of years. The OPEX costs of the model are determined as costs per year. Therefore, the channel siltation volume over the entire channel is determined per year. The total volume of siltation over the channel sections is calculated per year and summed up to determine the siltation volume over the entire channel. From the total volume of the siltation, the costs are determined and added to the OPEX costs.

3.3.5. Basin siltation

The influence of basin siltation on the maintenance dredging costs that accompany a certain breakwater layout has been included in the OPEX costs determination. As discussed in Section 2.4.3, the method described in PIANC (2008) is not suitable for incorporation in the updated model. Therefore, an average yearly siltation rate is used.

The user provides an expected sedimentation rate in meters per year based on his own assessment. This rate is multiplied with the total basin area. This results in a siltation volume per year, which can be expressed in monetary terms and added to the Opex costs.

This method is also used in the original model for the determination of siltation in the basins and the navigation channel (Woerlee, 2019). In the calculation method, the sedimentation that occurs in the shielded areas (the harbour basin and if shielded, the inner channel) is computed using the yearly siltation rate. The total area of the components is multiplied with this sedimentation rate, which leads to a sedimentation volume per year. The navigation channel area is taken out of the equation, as channel sedimentation is calculated using the method described in Section 3.3.4. In this manner, the yearly sedimentation volume in the basins is calculated. As a result, the maintenance dredging costs due to harbour basin sedimentation are determined per year. These costs are added to the OPEX costs.

4

Model Adaptation

The bathymetry grid, the modelling of wave transformation with REFRAC and the sedimentation processes have been implemented in the model following the methodology presented in Chapter 3. To accomplish these implementations, several modifications and additions have been made to the original model. In this chapter, these additions and modifications are presented separately for each subject. The influence of these modifications and additions have also been assessed. The assessments and the corresponding results are described at the end of each section. In Section 4.1, the modifications and additions made to include bathymetry are described. Section 4.2 describes the modifications that have been made to integrate the REFRAC model. This section is followed by the description of the modifications and additions that have been made to implementation sediment transport and siltation, which is provided in Section 4.3. The impact on the computation time is addressed in Section 4.4.

4.1. Bathymetry

For the implementation of the grid, a separate bathymetry module has been added, within which the grid is created. To integrate a grid into the original model setup, several modifications had to be made to the existing modules. Therefore, the functions and methods used in the original modules have been analysed, to determine which modules had to be adapted to allow for the use of a grid with bathymetry data.

4.1.1. The bathymetry module

Before the updated model can be run, a grid has to be created by the bathymetry module. The grid is created using bathymetry data provided by the user. In addition, the user should provide the size of the grid and the size of the grid cells. These parameters are provided using the input file.
The bed level values of the grid are stored in a matrix, which is saved as both a compressed data file (for use in the model) and exported as a text data file (used for the REFRAC wave model). In addition, the manufactured grid is visualised as both a 3D-plot and a contour-plot, as can be seen in Figures 3.3a and 3.3b. These visualisations allow the user to check if the manufactured grid aligns with the user's desires.

4.1.2. Modifications of existing modules

The output generated by the new bathymetry module is a grid containing the bed levels at each grid point. This differs from the original model, where the bathymetry is assumed as a constant bed slope. The bed level at a location now depends on both the x- and y-coordinate, not just solely on the y-coordinate. This dependency on both the x- and y-coordinate has to be taken into account in the modules that contain calculations in which the water depth at a location is used. After analysis of the model, it is found that the following modules are influenced by the implementation of bathymetry:

- CAPEX/OPEX Module
- Downtime Module
- Functions Module

- Generator Module

A visualisation is given in Figure 4.1, along with the specific components of the modules that have to be modified.

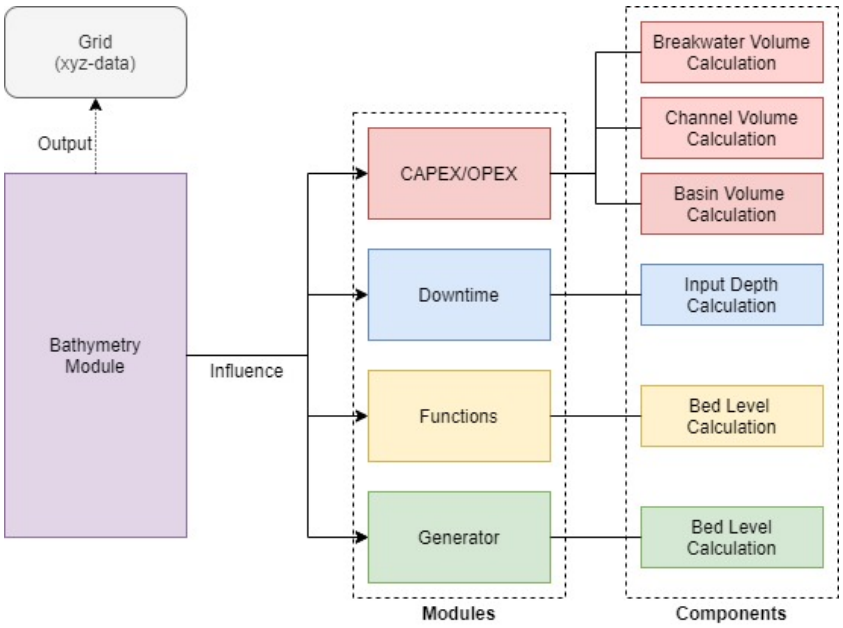

Figure 4.1: The influence of the bathymetry module on the other modules

For each of the modules, it has been analysed what modifications and/or additions had to be made to their components as a result of the bathymetric profile implementation. For some, a compromise had to be made between accuracy and computation time.

CAPEX/OPEX: breakwater volume calculation

The breakwater volume calculation in the original model is calculated using the x,y-coordinates of nodes that represent the two outer points of the breakwater segment (Woerlee, 2019). The volume of the segment is determined based on the length between these points (which is the segment length) and the depth at 2/3 of the segment (in seaward direction). The cross-sectional area of the breakwater at this depth represents the mean cross-sectional area of the breakwater of the segment. When it concerns a homogeneous slope with parallel depth contours, this calculation is exact and therefore highly accurate. With the introduction of more complex depth profiles, this method is no longer sufficient to calculate the volume of the entire segment, as the bed slope can vary between points in both x- and y-direction.

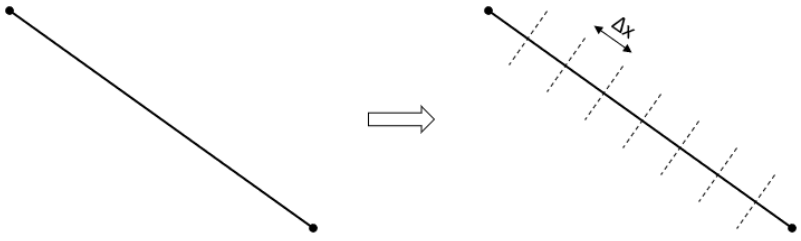

Figure 4.2: Creation of breakwater segment sections for determination of the volume

After modification, the depth at a desired point is determined using the data file containing the bed levels. From this data file, the depth can be determined using the bed level that corresponds to the x,y-coordinates of the desired point.

The volume of a breakwater segment is determined by dividing the segment into several sections with equal spatial step (denoted by Δx). The division of the segment is visualised in Figure 4.2. For each section, the volume will be determined based on the length of the section and the depth at 2/3 of the section, comparable to the calculation used in the original model.
For conceptual design purposes, a spatial step of 100 meters is considered sufficiently accurate.

CAPEX/OPEX: channel volume calculation

In the original model, the calculation of the channel volume is performed in the same manner as the calculation of breakwater segment volumes (Woerlee, 2019). The modifications that are made are therefore comparable. The inner channel and, if present, the outer channel are also divided into sections. For each of these sections, the volume that needs to be dredged is determined based on their length and the depth at 1/3 of the channel segment (in seaward direction). The spatial step has been set to 100 meters.

However, the point from where the required channel depth is reached also has to be determined, as from this point, dredging is no longer required. With a homogeneous bed slope with parallel depth contours, this point can be determined based on the y-coordinate. With the inclusion of depth profiles, a constant slope is not guaranteed. As a result, the original method is not sufficient anymore.
To determine the coordinates of the point where the required depth is reached, a function has been added. This function determines these coordinates based on the angle of the approach channel and the coordinates of the turning basin centre. From the coordinates of the basin centre, a line is constructed through the matrix that holds the bed level values. This method is visualised in Figure 4.3.

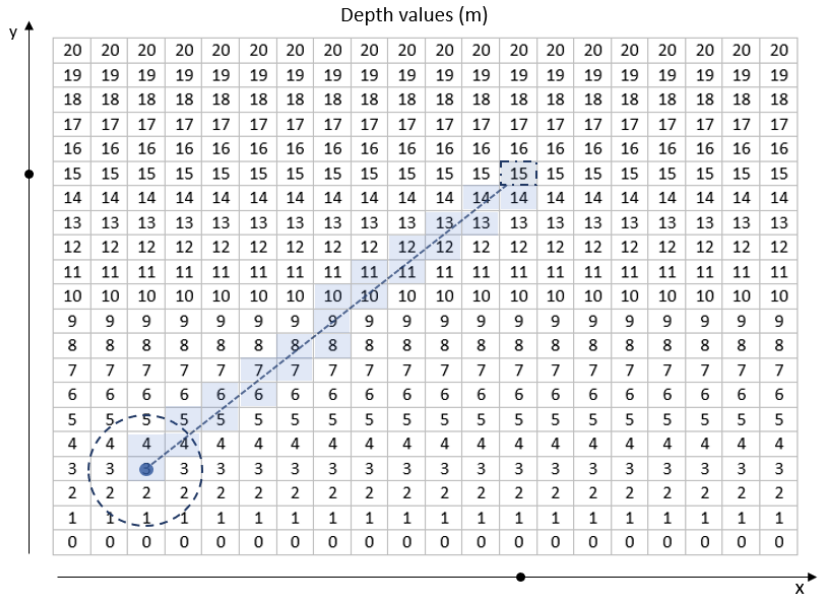

Figure 4.3: Visualisation of the line that is drawn through the array, based on which the x,y-coordinates are drawn, which in turn correspond to a certain depth. In the visualisation the required depth is taken at 15 m, at which the coordinates are determined.

All coordinates of the grid points that are on this line are stored. The depth values that correspond to these coordinates are then determined. Using these depth values, the point at which the depth is sufficient can then be found, providing the coordinates of that point.
It is possible that along the line, a point is found that has the required depth, but that further along the line, the depth is smaller than the required depth. This possibility has been incorporated into the function. When a point with required depth is found, the function still analyses the points further along the line, to assess if the depth at those points is larger or equal to the required depth. When a point meets these criteria, it is returned as the point from where dredging is no longer needed.
With the coordinates known, it is possible to determine the length of the inner channel, the end of the inner channel, the possible need for an outer channel and the end of this outer channel.

CAPEX/OPEX: basin volume calculation

In the original model, the basin volume is determined based on the radius of the turning basin and the position of the basin centre (Woerlee, 2019). The exact volume is calculated, which is possible due to the homogeneous slope and the parallel depth contours. This method has to be adapted with the implementation of the bathymetry profile.
After the implementation of bathymetry, the volume that has to be dredged due to the turning basin is still determined based on the turning basin radius and the basin centre. From the coordinates of the basin centre, multiple lines are constructed with the same length as the radius, to the edge of the basin. The construction of such a line is done multiple times, each time for a larger angle. In this manner, a ”spider web” is constructed based on which points are projected. These points are located in a manner that all points cover the same spatial area. This method is visualised in Figure 4.4. At these points, the depth is determined.

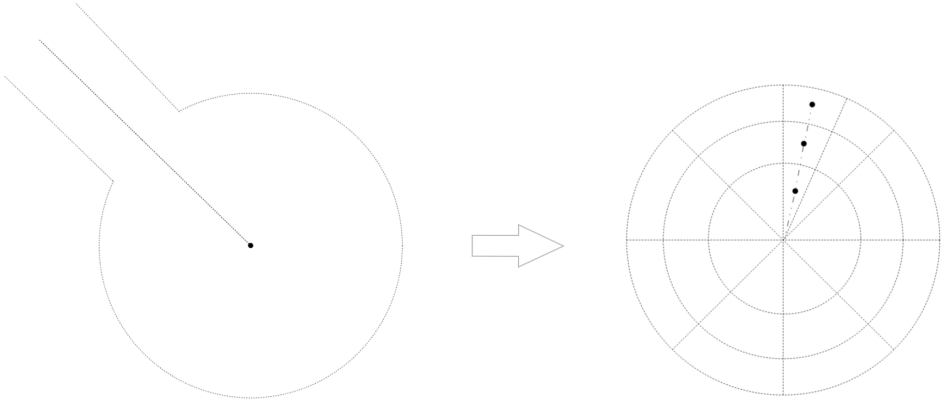

Figure 4.4: Regarding the turning basin, the depth is determined at certain points as shown on the right-hand site, to make a fast but accurate approximation of the depth and the median thickness of the layer that is to be dredged, which is done for the entire turning basin

These depth values are used to determine the mean depth of the area. All points that have a depth that is equal to or larger than the required turning basin depth are filtered out, leaving only the points where dredging is required. For these points, the mean depth is determined.
Using the ratio between the number of points where dredging is required and the total number of points, the area that is to be dredged is determined. This area is multiplied with the mean depth determined earlier, which gives an accurate approximation of the volume that is to be dredged.

Downtime: Input depth calculation

In the Downtime module, the implementation of bathymetry influences the determination of the water depth. The water depth in the original model is determined based on the y-coordinate of the point at which the depth is desired. This method has been modified, with the water depth now being determined based on the x,y-coordinates. The depth is determined using the corresponding bed level for the coordinates of the desired point. This bed level is drawn from the data file containing the seabed level data.

Functions: bed level calculation

In the Functions module, the bed level is required as a parameter for multiple functions. In the original model, the bed level is determined based on the y-coordinate of a point. This method has been modified to the bed level being drawn from the data file containing the bed level values, based on the x,y-coordinate of the point for which the bed level is desired.

Generator: bed level calculation

For the Generator module, the same situation arises as for the Functions module. The same modification is made, due to which the depth value is now determined using the x,y-coordinates of a point.

Generator: coordinates for exceptional cases

The Generator module's main function is creating the initial generation of layout alternatives, which in turn are defined by the generated coordinates of the nodes. For the creation of valid alternatives, the module also contains an exceptional cases function, to create valid coordinates for the primary breakwater nodes if the initial coordinates become invalid due to the configuration of other layout components. The creation of valid coordinates results in generated alternatives with coordinates outside of the user given bounds, which creates the need for a larger grid. The use of a grid that is larger than the area of interest poses two problems:

- It causes an increase in modelling time, as the size of the depth data file gets larger when the grid is enlarged.
- The current construction of the layout in leftward direction depends on negative indexing, which, when the grid is larger than the given bounds, will asses a different area than the rightward layout, which leads to inaccurate results.

Therefore, a modification has been made to the exceptional cases module. Due to this modification, the bed level assigned to the coordinates that would be out of bounds is equal to the depth at the boundary point it corresponds to.
Using this method, the inner workings of the model are not influenced and the eventual results are the same, as the model will evolve past these layout alternatives during convergence.

4.1.3. Assessment of the modification

It has been assessed if the model still produces sufficient results after the addition of the grid. This assessment has been executed by running the model for two test cases:

1. An area with a homogeneous constant bed slope (1:100) with parallel depth contours. This case allows the produced optimum breakwater configurations to be compared to the breakwater configuration produced by the original model, as the environment is identical.
2. An area that contains a sudden increase in bed slope and depth, with parallel depth contours. This case allows for the produced optimum breakwater configurations to be assessed on their reaction to a change in bed slope and depth and to observe if the produced breakwater configurations are in line with expectation.

In both test cases, the number of desired berths is three, with room for future expansion to five berths. A visualisation of these bathymetries is shown in Figure 4.5. For all test cases, the environmental conditions described in Table 4.1 have been used.

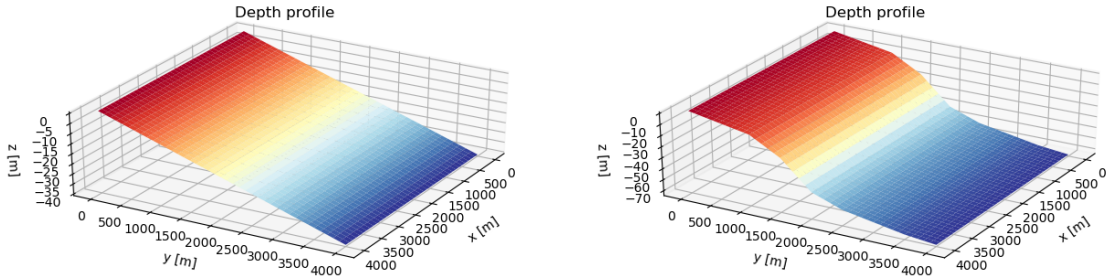

(a) (b)

Figure 4.5: (a) The bathymetry of the test case with a homogeneous slope (b) The bathymetry of the test case with a sudden increase in depth

$H_{0s}[m]$	$T_{0p}[s]$	$\theta_0[^o]$	$u_w[m/s]$	$\theta_w[^o]$	$u_c[m/s]$	$\theta_c[^o]$	P_r
4,2	8	340	15	200	0,2	200	0,005
3,9	8	340	15	200	0,2	200	0,015
3,5	8	340	15	200	0,2	200	0,04
3	8	340	15	200	0,2	200	0,15
2	8	340	15	200	0,2	200	0,22
3,7	8	280	15	200	0,2	200	0,005
3,4	8	280	15	200	0,2	200	0,015
3	8	280	15	200	0,2	200	0,06
2,5	8	280	15	200	0,2	200	0,22
1,5	8	280	15	200	0,2	200	0,27

Table 4.1: Environmental conditions used for test runs

First, the original model has been run, which results in an optimum breakwater configuration that is shown in Figure 4.6, with the corresponding data shown in Table 4.2. This breakwater configuration serves as a reference for comparison regarding the generated optimum configurations for the case with the homogeneous slope (Case 1).

Category	**Costs**
CAPEX/OPEX	**€196.7 million**
Breakwater Construction Costs	€78.1 million
Capital Dredging Costs	€52.6 million
Dredging Maintenance Costs	€1.8 million
Breakwater Maintenance Costs	€1.6 million
Downtime	**€7.6 million**
Downtime Costs	€7.6 million
Average downtime per berth	0.7 %

Table 4.2: Costs and downtime information of original model run

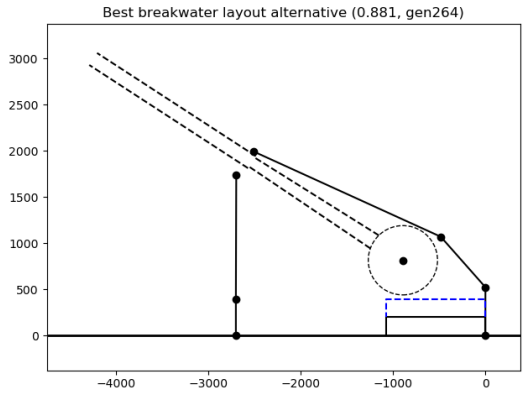

Figure 4.6: Layout produced in the original model for a slope of 1:100

Homogeneous slope

Based on the breakwater configurations produced for the test case with a homogeneous bed slope and parallel depth contours, a comparison is made with the breakwater configuration generated by the original model. The produced optimum breakwater configurations are shown in Figure 4.7 and their costs are displayed in Table 4.3.

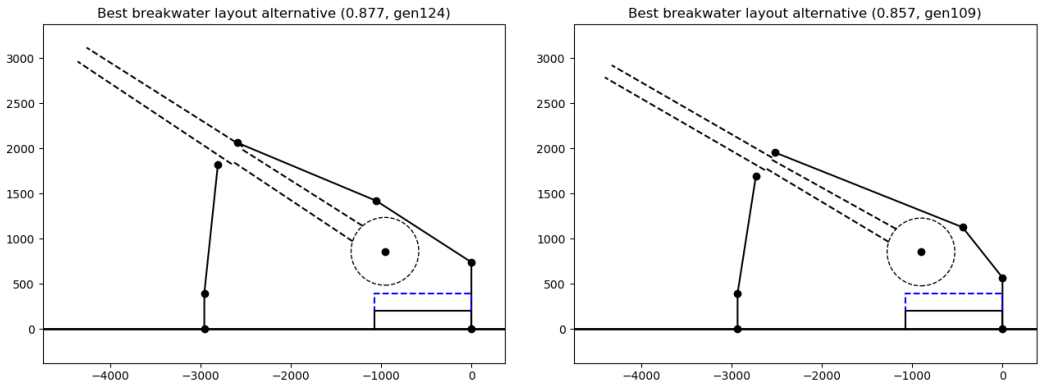

(a) (b)

Figure 4.7: (a) Optimal layout result from run 1(b) Optimal layout result from run 2

Category	Run 1	Run 2
CAPEX/OPEX (capitalised)	**€197.7 million**	**€202.5 million**
Breakwater Construction Costs	€85.1 million	€79.1 million
Capital Dredging Costs	€48.6 million	€61.4 million
Dredging Maintenance Costs	€1.5 million	€1.5 million
Breakwater Maintenance Costs	€1.7 million	€1.6 million
Downtime (capitalised)	**€7.6 million**	**€7.6 million**
Average downtime per berth	0.7%	0.7%

Table 4.3: Cost and downtime of the optimal layouts for the case with the homogeneous slope

It is observed that both the breakwater configuration produced in run 1 (shown in Figure 4.7a) and the breakwater configuration produced by run 2 (shown in Figure 4.7b) are similar to the breakwater configuration produced by the original model (shown in Figure 4.6.
The costs corresponding to the breakwater configurations produced by the updated model (presented in Table 4.3) do not show significant deviation from the costs corresponding to the layout produced by the original model (see Table 4.2). The occurrence of only minor deviations implicate that the addition of the bathymetry grid has been done correctly.
The costs corresponding to both layouts produced by the updated model with the implemented bathymetry grid show a lot of resemblances. Their differences are portrayed in Table 4.4.

Category	Difference (€)	Difference (%)
CAPEX/OPEX	4.8 million	2.4
Downtime	0.0	0.0

Table 4.4: Difference in costs between the optimal layouts for the case with the homogeneous slope

These differences are small and are considered acceptable. Based on the comparison with the original model and the comparison between the breakwater configurations produced by the model with implemented bathymetry, it is observed that the model still produces sufficiently accurate results after the made modifications.

4.1.4. Sudden slope increase

For the case with the sudden increase in slope and depth, the resulting optimum breakwater configuration should differ from the one for the homogeneous slope. Due to the sudden increase in depth, the breakwater layout is expected to be situated closer to the shoreline than the breakwater configurations produced with the homogeneous slope. This configuration is expected as it will reduce the breakwater construction costs. The generated layouts are portrayed in Figures 4.8a and 4.8b, with their costs displayed in Table 4.5.

Category	Run 1	Run 2
CAPEX/OPEX (capitalised)	**€194.8 million**	**€202.5 million**
Breakwater Construction Costs	€86.0 million	€92.3 million
Capital Dredging Costs	€47.2 million	€48.3 million
Dredging Maintenance Costs (per year)	€1.5 million	€1.3 million
Breakwater Maintenance Costs (per year)	€1.4 million	€1.8 million
Downtime (capitalised)	**€0.00**	**€0.00**
Average downtime per berth	0.0%	0.0%

Table 4.5: Cost and downtime of the optimal layouts for the case with the sudden increase in depth

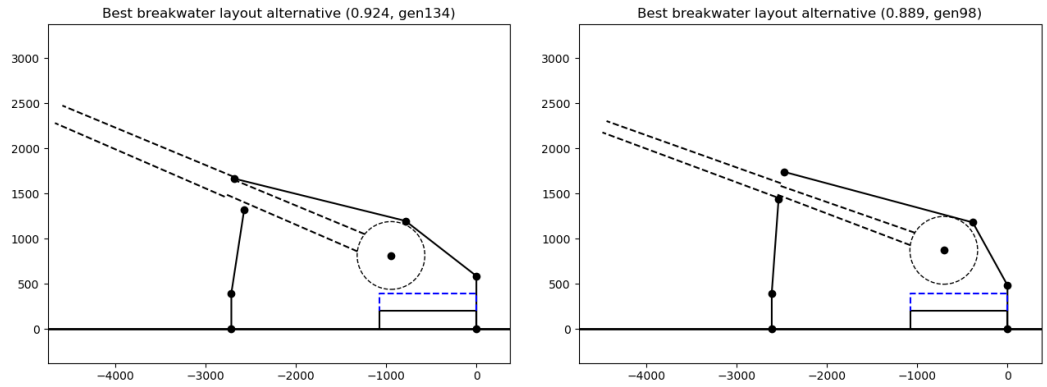

(a) (b)

Figure 4.8: (a) The optimal layout result from run 1 for the profile with a sudden increase in depth (b) The optimal layout result from run 2 for the profile with a sudden increase in depth

Both generated breakwater configurations show strong resemblance in their positioning and shape. Both breakwater configurations show that the breakwaters are constructed closer towards the shore, as is in the line of expectation due to the increase in depth behind the 1500 meter line (see Figure 4.5b. The primary breakwaters do not reach the 2000 meter line and the secondary breakwaters are both on the 1500 meter line. It can be seen that the different configuration also affects the dredging costs (see Table 4.5), as these are smaller than the dredging costs observed for test case 1. These results are in line with expectation, as less dredging will be required due to the sudden increase in depth. This can also be seen in the angle of the channel, which is larger for both generated configurations. Regarding the costs of both alternatives, it can be seen that these also show a lot of resemblances. Their differences are shown in Table 4.6.

Category	Difference (€)	Difference (%)
CAPEX/OPEX	7.6 million	3.9
Downtime	0.0	0.0

Table 4.6: Difference in costs between the optimal layouts for the case with the sudden increase in depth

As these differences are small and as both breakwater configurations have a large resemblance, the produced results are seen as acceptable.

4.2. Wave transformation

As described in Chapter 3, REFRAC is used to model the wave transformation with the implementation of the bathymetry grid.
The REFRAC model requires environmental conditions (defined by the user) and a bottom profile (which is generated by the Bathymetry module) as input (REFRAC Team, 1994).
After preparing the input files for REFRAC, the REFRAC model is run in the stage before the model loop, after the bathymetry module has been run. The generated output contains the wave heights at user defined coordinates and the wave angle along the generated wave rays (per unit wavelength). This data is imported into a separate REFRAC module that has been created. With the use of this module, the wave parameters are defined for all x,y-coordinates using interpolation, after which they are stored in separate wave data files.
The wave data is then imported into the Downtime module and the CAPEX/OPEX module of the updated model, where the wave data is used to determine the wave parameters at the requested coordinates. Based on these parameters, the estimated downtime and the channel sedimentation volumes of the layout alternatives are determined. A visualisation of the entire model is shown in Figure 4.9.

The wave heights are calculated based on the amount of energy present in the grid cell (Bouws and Battjes, 1982), as mentioned in Section 3.2.2. Therefore, the accuracy of the wave heights given by the model is partially dependent on the size of the grid cells.
REFRAC provides the user with the option to average the wave energy over a number of adjacent grid cells, in both the x- and y-direction (referenced to as AVG). With this operation, the wave energy can be smoothed, to prevent the occurrence of unrealistic wave heights at locations of cells where multiple rays cross. Averaging influences the accuracy, as the averaging occurs for all cells. It is therefore important to assess over which number of cells averaging should take place, to produce accurate results.
In earlier research, REFRAC has been used as validation for SWAN (Liu, 2009). In this research, an indication is given regarding the number of cells over which averaging should take place. It is also indicated that the number of cells over which averaging should take place has dependence on the size of the grid cells that is chosen.

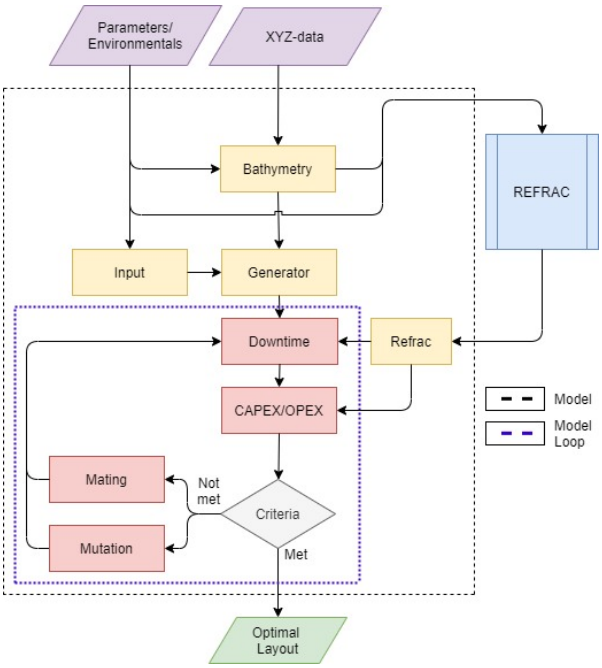

Figure 4.9: Visualisation of the model with addition of REFRAC

Apart from the information provided in the above-mentioned literature, an assessment has been made in which the wave height calculated by the original model are compared to the wave height found using the REFRAC model. Since the wave height calculation in the original model is performed using linear wave theory for a homogeneous slope with parallel depth contours, the same case is evaluated for the REFRAC model, to make a reliable comparison.

The transformation of incoming waves performed by REFRAC has been compared with the transformation of incoming waves using the linear wave theory (with the wavenumber k being calculated using *Chen and Thompson* (2008)) for different incident wave directions (denoted by θ_0). The combinations have been summarized in Table 4.7. The AVG parameter represents the cells over which averaging takes place. The first value is the averaging over the number of cells in the x-direction, on both sides of the cell. The second value is the averaging over the number of cells in the y-direction, on both sides of the cell.

Combination	**1**	**2**	**3**	**4**	**5**	**6**	**7**	**8**	**9**
$\theta[^o]$	15	15	30	30	40	40	40	45	45
$AVG[-]$	2 2	3 3	2 2	3 3	2 2	3 3	4 4	3 3	4 4

Table 4.7: Different combinations of angle and averaging for comparison of the REFRAC results with the results found using linear wave theory

This comparison has been done for incident wave heights (denoted by H_{s0}) of 3 meters and 4 meters. For each combination, the maximum difference in wave height between the wave height provided by REFRAC and the wave height provided using linear wave theory has been determined, based on which the maximum deviation has been determined (given in percentages). The results are portrayed in Tables 4.8a and 4.8b.
A visualisation of these results is given in Appendix C. It is observed that the values chosen for averaging do not lead to a wide range of differences in the wave height. All lead to a deviation of $5-6\%$. Averaging of 3 cells in x-direction and 3 cells in y-directions gives the best results (with exception of one situation). Therefore, this averaging is used as default value.

It should be noted that these results are valid for the currently used grid cell size for the model. If the grid cell size is to be adjusted, it should be assessed if this averaging still produces the best results.

θ [^{o}]	AVG [$-$]	ΔH_s [m]	$Deviation$ [%]
15	2 2	0.209	5.50
15	3 3	0.193	5.10
30	2 2	0.211	5.54
30	3 3	0.222	5.82
40	2 2	0.194	5.55
40	3 3	0.192	5.50
40	4 4	0.196	5.60
45	3 3	0.197	5.62
45	4 4	0.196	5.61

(a) Results of comparison with $H_s = 4\ m$

θ [^{o}]	AVG [$-$]	ΔH_s [m]	$Deviation$ [%]
15	2 2	0.162	5.85
15	3 3	0.158	5.74
30	2 2	0.158	5.54
30	3 3	0.167	5.82
40	2 2	0.161	6.04
40	3 3	0.158	5.74
40	4 4	0.160	5.79
45	3 3	0.143	5.63
45	4 4	0.147	5.55

(b) Results of comparison with $H_s = 3\ m$

Table 4.8: REFRAC Model Tuning Results

4.2.1. Assessment of the modification

To assess if the implementation of REFRAC into the updated model provides sufficient results, the test case for the homogeneous bed slope with parallel depth contours (see Section 4.1.3) has been run with the integration of the REFRAC model. The environmental conditions that were used are described in Table 3.1. The generated breakwater configurations are shown in Figure 4.10.

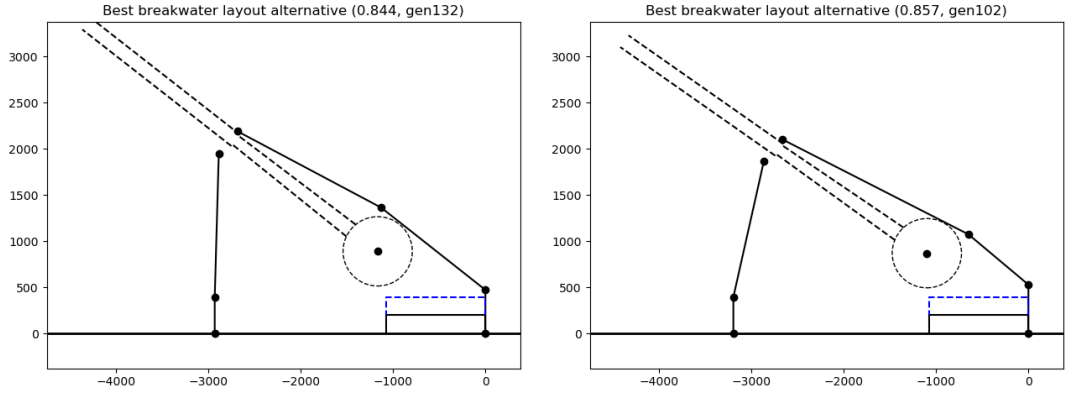

(a) (b)

Figure 4.10: (a) Run 1 for the model with REFRAC integration for a homogeneous slope (b) Run 2 for the model with REFRAC integration for a homogeneous slope

Category	**Run 1**	**Run 2**
CAPEX/OPEX (capitalised)	**€205.6 million**	**€202.5 million**
Breakwater Construction Costs	€88.4 million	€85.4 million
Capital Dredging Costs	€51.1 million	€51.8 million
Dredging Maintenance Costs (per year)	€1.5 million	€1.5 million
Breakwater Maintenance Costs (per year)	€1.7 million	€1.7 million
Downtime (capitalised)	**€7.6 million**	**€7.6 million**
Average downtime per berth	0.7%	0.7%

Table 4.9: Cost and downtime information for the REFRAC model runs

The generated layouts have a close resemblance to each other and to the layout generated by the original model, as well as the layouts generated for the same case in Section 4.1.3. The costs of both breakwater layout alternatives also show great resemblance, as can be seen in Table 4.9. Their differences are displayed in Table 4.10.

Category	Difference (€)	Difference (%)
CAPEX/OPEX	3.1 million	1.5
Downtime	0.0	0.0

Table 4.10: Difference in costs after integration of REFRAC for the case with the homogeneous slope

Based on these results, the conclusion is drawn that the model performance is sufficient and that the model with the integration of the REFRAC model leads to accurate results.

To assess the performance of the model with the integration of REFRAC for a complex and non-uniform depth profile, a case study has been performed. The case study is described in further detail in Chapter 5.

4.3. Sedimentation

For the implementation of sediment transport and sedimentation processes, a division has been made between the calculations that can be performed prior to the model loop stage (i.e. are not required in the iteration, which saves computation time) and the calculations that have to be performed in the model loop stage.

Calculations regarding longshore sediment transport and the corresponding accretion (described in Section 3.3) are performed prior to the iteration stage of the model. The equations used for these calculations have been added to the functions module. The input required for the equations is provided by the user-defined environmental conditions and the user-defined parameters, both given in the input sheet. Based on the accretion that occurs at both breakwaters, the required minimum breakwater lengths are determined. Therefore, the calculated values can be imported into the input module, as the breakwater lengths are required as input for the generation of the breakwater layout alternatives if sedimentation is incorporated.

The sedimentation of the channel and the siltation of the basins require input that is breakwater layout specific. Therefore, they have to be included in the model loop. The required equations have been added to the functions model. These equations are used for the calculation of the sedimentation volumes per year for each breakwater alternative. The calculation of these volumes have been included in the CAPEX/OPEX module. Based on these volumes, the OPEX due to channel sedimentation and harbour basin siltation is calculated and added to the total OPEX costs.

4.3.1. Assessment of channel siltation

The channel sedimentation volumes are determined as described in Section 3.3. This calculation method uses local environmental conditions as input and the generated result of the calculations is a siltation volume that is added to the OPEX calculation. To best assess its output, the calculation method has been analysed separately.
To assess if the model generates realistic values for the filling rate, a case study described in the book ”Dynamics of Marine Sands” (Soulsby, 1997) has been used. After performing the exemplary case and validating the results, it has been analysed if the generated filling rates are affected in a realistic manner when several parameter values are changed.

The influence of the following aspects have been analysed:

- The influence of varying water depth on the filling rate
- The influence of varying channel depth on the filling rate
- The influence of varying wave heights on the filling rate

- The influence of varying channel direction on the filling rate
- The influence of varying residual current flow velocity and direction on the filling rate

For these assessments, the default parameters are given in Appendix B.1. The values are based on the values that have been used in the example case. These default parameters have been used to determine the filling rate, unless mentioned otherwise.

Filling rate value

To assess if the filling rate generated by the model is realistic, a calculation has been performed with the same input parameters that are described in a test case in the book "Dynamics of Marine Sands" (Soulsby, 1997). The parameters used in the test case described in Table 4.11.

Parameter	Value	Unit	Description
θ_{ch}	90	^{o}	Channel angle w.r.t. shore-normal
θ_{ebb}	0	^{o}	Ebb current flow angle w.r.t. shore-normal
θ_{flood}	0	^{o}	Flood current flow angle w.r.t. shore-normal
u_{ebb}	0.8	m/s	Ebb tidal current flow velocity
u_{flood}	0.8	m/s	Flood tidal current flow velocity
H_s	0	m	Wave height
T_p	7	s	Peak period
d_{50}	2e-4	m	Median grain size
d_{90}	3e-4	m	90th percentile grain size
v	1.36e-6	m^2/s	Viscosity
z_o	0.006	m	Bed roughness
s	2.58	-	Relative density
β	0	^{o}	Angle of channel slope
h_{in}	5	m	Depth of seabed with respect to MSL
d_{ch}	10	m	Depth of channel with respect to MSL

Table 4.11: Parameter values for the filling rate test case

In the test case, the value for the wave orbital velocity has been determined using a graph. In the model, this value is determined with the use of an equation. These calculations lead to the results in Table 4.12.

Parameter	Test case value	Model value	Difference
Wave orbital velocity [m/s]	0.208	0.205	0.97 %
Filling rate [m/hr]	0.0110	0.0109	0.91 %

Table 4.12: Differences in wave orbital velocity and filling rate

It is observed that the difference is smaller than 1%. The difference between the filling rate calculated by the model and the filling rate given in the test case is 0.91 %. Therefore, it is observed that the model generates valid results for the filling rate value.

For the assessment of the effect of varying parameter values, several parameter values have been adjusted (such as the default channel angle and the default depth at the seabed) to observe if the function still performs well with parameters that are more likely to occur during calculations in the model. These parameters are given in Table B.1.

Influence of varying water depth

The influence of varying water depth on the filling rate has been assessed. The filling rate has been determined for the following parameters:

- Water depths for the seabed varying from 10 meter to 20 meter
- Water depths of the channel varying from 15 meter to 25 meters (with a constant depth difference between the channel and seabed (denoted by d), taken at 5 meter)

These cases have been performed for multiple mean ebb and flood current velocities, varying from 0.6 m/s - 1 m/s. The other default parameters are described in Appendix B.1.
The results are shown in Figure 4.11a. To take a more detailed look at the influence of the water depth on the filling rate, the results are also shown for a single value for the ebb and flood current velocities (shown in Figure 4.11b).

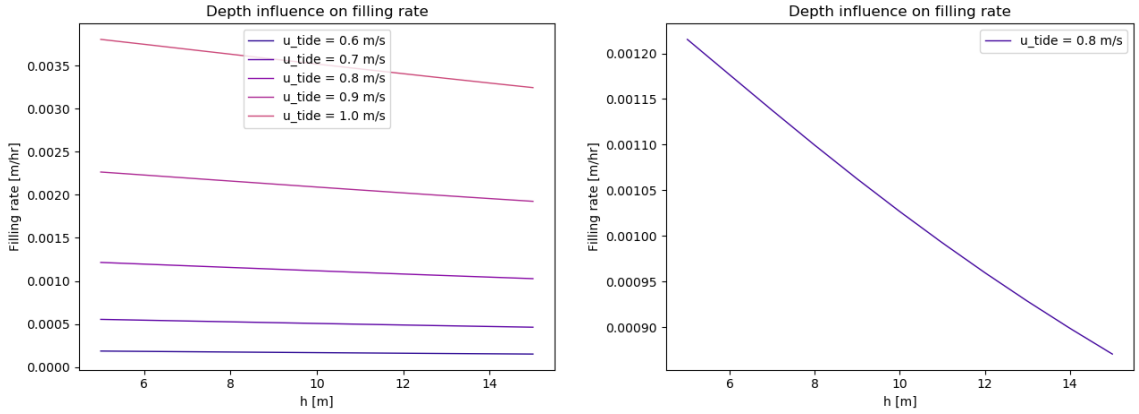

(a) (b)

Figure 4.11: (a) Filling rate for varying water depths, defined for multiple mean ebb/flood current velocities (b) Filling rate for varying water depths, defined for a mean ebb/flood current velocity of 0.8 m/s

It is observed that the filling rate decreases when the water depth becomes larger, which is logical as the relative difference in depth between the channel and the seabed becomes smaller. This result is in line with expectation, as the Soulsby-Van Rijn equation (see Appendix E.2) shows that increase in depth will lead to a decrease in sediment transport (denoted by q). It is also observed that a larger current velocity leads to an increased filling rate. From the Soulsby-Van Rijn equation, it can also be derived that an increase in the mean current velocity leads to an increase in sediment transport (denoted by q).

Influence of varying channel depth

The channel depth with respect to the bed level is an important factor in the determination of the filling rate. Therefore, it has been assessed if varying the channel depth with respect to the seabed level (denoted by d, see Figure 2.13) results in filling rates that are in line with the theory. Based on the equations that have been used (see Section 2.4.2), it is expected that an increase of channel depth with respect to the seabed will lead to an increase of the filling rate. Two test cases have been run, both with varying seabed levels and a constant channel bed level:

- A case with the channel depth at 15 meters below water level and the seabed level varying from 10 meters to 15 meters below water level.
- A case with the channel depth at 20 meters below water level and the seabed level varying from 15 meters to 20 meters below water level

The resulting filling rates of these two cases are presented in Figure 4.12.
Both figures show that the filling rate increases when the channel depth with respect to the seabed increases (denoted by Δh), as is in line with expectation. The filling rate will increase with increasing channel depth, which can be derived from the Soulsby-Van Rijn equation. The equation shows that an increase in water depth leads to a decrease in sediment transport. Consequently, a larger channel depth will lead to a smaller transport out of the channel (denoted as q_{out}) which will result in a larger filling rate (as Δq becomes larger).

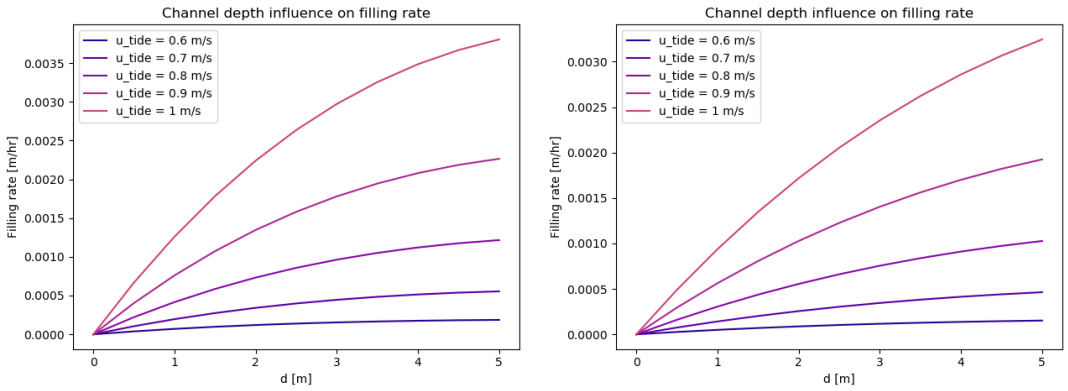

(a) (b)

Figure 4.12: (a) Filling rate for varying relative channel depths (denoted by d), defined for ebb/flood current velocities with the water depth at the channel bed being 15 m (b) Filling rate for varying relative channel depths (denoted by d), defined for ebb/flood current velocities with the water depth at the channel bed being 20 m

Influence of varying wave heights

It is expected that an increase in wave height will lead to an increased effect of the waves on the filling rate, which will result in an increase in sediment transport. The filling rate has been determined for wave heights ranging from 1 to 3 meters, of which the results are shown in Figure 4.13.

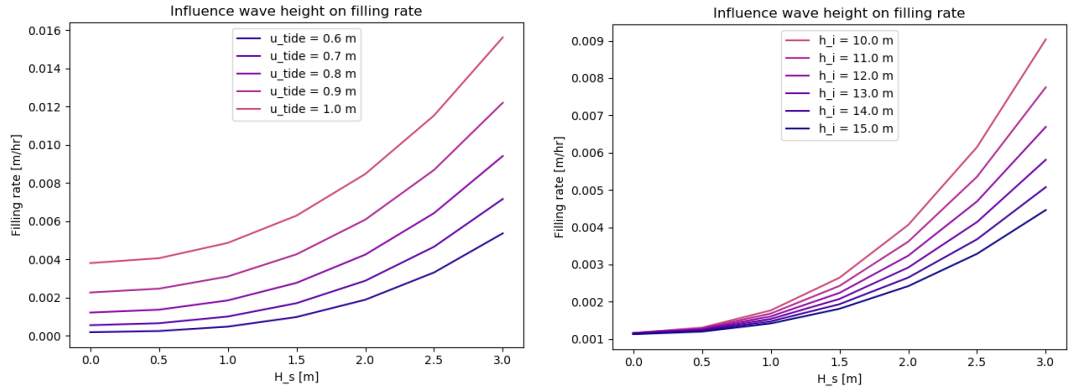

(a) (b)

Figure 4.13: (a) Filling rate for varying wave heights, defined for multiple ebb/flood current velocities (b) Filling rate for varying wave heights, defined for multiple seabed levels

It can be seen in Figure 4.13b that the influence of wave height on the filling rate is dependent on the local water depth and that the influence increases for larger wave heights. The increase in filling rate when larger wave heights occur is in line with expectation, as the wave orbital velocity will have a larger effect on sediment transport when the water depth is smaller. It should be noted that, as expected, the results show that the influence of the wave orbital velocity can be significant, which was already stated by Van Rijn (Van Rijn, 2013).

Influence of varying channel direction

The channel direction with respect to the current flow direction is of influence on the filling rate. The angle of the channel with respect to the current flow directions influences the transport of sediment into the channel. When the current flow direction is closer to perpendicular to the main channel axis, the filling rate becomes larger. To assess the effect of this relative angle, the filling rates have determined for a channel angle varying from 0 to 90 degrees. The results are shown in Figure 4.14.

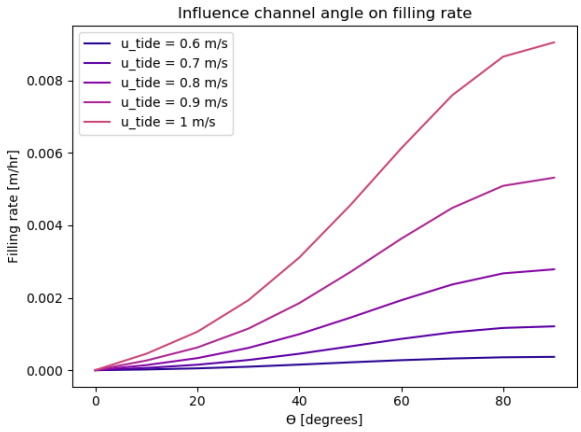

Figure 4.14: Filling rate for varying channel angles, defined for multiple ebb/flood current velocities

The results show that an increasing angle of the channel with respect to the current flow directions leads to an increase in filling rate. The increase in the filling rate when the flow direction comes closer to a direction perpendicular to the channel is in line with the expectation.

Influence of residual current velocity and direction

Apart from the tidal currents, the residual current also influences the filling rate. The tidal currents are set to 0. The residual current flow velocity is accounted for in the mean current velocity (see Equation 2.23). To assess if the effect of the residual current has been accurately integrated, calculations have been made. Residual current flow velocities ranging from 0.4-0.6 m/s are imposed and with the residual current flow directions varying between 0 to 90 degrees. The results are shown in Figure 4.15.

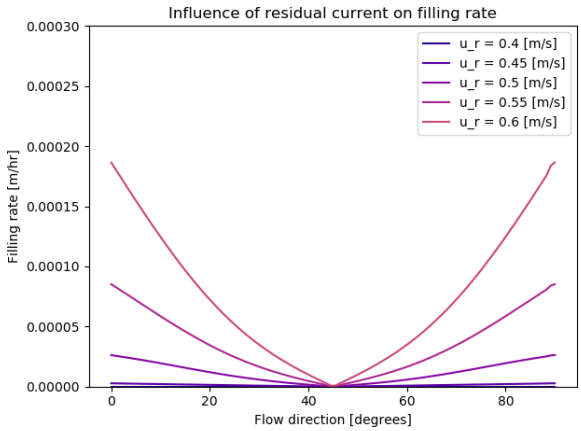

Figure 4.15: Filling rate for varying residual current flow directions, defined for multiple residual current velocities

The results show that an increase of the angle of the flow direction with respect to the channel direction results in larger filling rates. This is in line with expectation, due to the larger perpendicular orthogonal velocity components with regard to the channel.

Based on the assessments, it is observed that the function generates a value for the filling rate in the test case that is in line with the value presented in the test case. The filling rates calculated by the function when certain parameter values are changed, are in line with the theory that is used in the equations. The performance of the equations in a real-life situation is assessed during the case study, in Chapter 5.

4.3.2. Assessment of updrift and downdrift accretion

The computation of the updrift and downdrift accretion is executed following the method described in Section 3.3. The updrift accretion is approximated using the Pelnard-Considère equation (Eq. 2.14). The Pelnard-Considère equation is regarded as an approximation that is adequate for conceptual design purposes and will therefore not be analysed further.
The method used to determine the downdrift accretion has to be assessed, as this concerns a complex situation. For this assessment, an exemplary test case that has been used, presented by Van Rijn (Van Rijn, 2014).

Assessment of downdrift accretion calculation

First, the output of the model has been analysed for different wave directions and structure lengths. This analysis has been performed to analyse the effect of the wave direction and the structure length on the accretion length along the breakwater in shore-normal direction. By performing this analysis, it can also be observed if this effect is within the line of expectation. The analysis has been executed for:

- The distance to the diffraction point varying from 390 meter to 2000 meter.
- The wave direction varying from 15 to 45 degrees for a diffraction point distance of 1500 meters

The other parameters have been kept constant and are described in Appendix B.1. The results are visualised in Figures 4.16a and 4.16b.

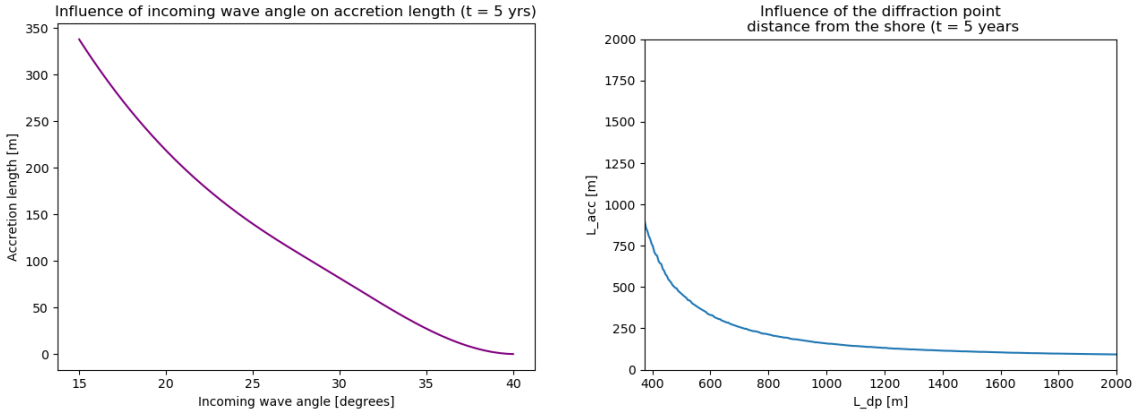

(a) (b)

Figure 4.16: (a) Influence of the incoming wave angle on the accretion length for a breakwater with the diffraction point at 1500 meters (b) Influence of the distance of the diffraction point from the shoreline on the accretion length

In Figure 4.16a it is observed that an increase in the incoming wave angle leads to a smaller accretion length. This is in line with expectation, as a larger angle of incidence leads to a smaller circular current velocity and a larger area over which the accretion will settle. As a result, the accretion length will be smaller.
Figure 4.16b shows the influence of distance of the diffraction point on the accretion. The decrease in accretion length is in line with expectation, as the increase in structure length will lead to a larger diffraction zone. This results in a smaller circular current velocity and a larger area in which the accretion will settle, comparable to the effect of larger incoming wave angles.

The required minimum length of the secondary breakwater is determined by calculating the accretion length along the secondary breakwater in shore-normal direction (denoted by L_{acc}) for a large range of values for L_{dp}, as shown in Figure 4.16b. The distance from the shore to the breakerline that belongs to the mean wave height is added to this accretion length. Based on their combined length, the minimum length of the secondary breakwater is determined (as is described in Section 3.3). The determining of the minimum secondary breakwater length is visualised in Figure 4.17.

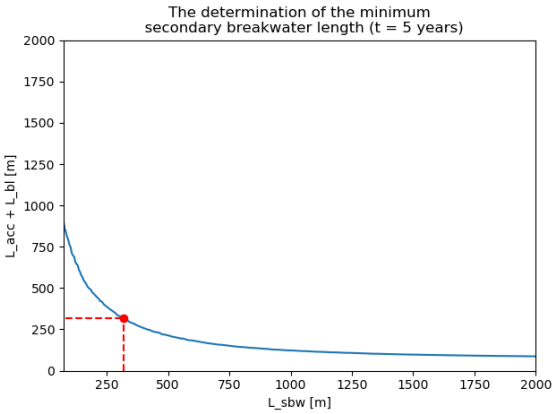

Figure 4.17: Visualisation of the determination of the minimum required secondary breakwater length

Test case

The test case describes a shore-normal breakwater along a straight coastline, with a length of 2800 meters. The parameters are described in Appendix B.2. The time period used in the calculation is 5 years.
For the exemplary test case, a full wave climate has been given. In the calculation performed in the example (Van Rijn, 2015), the wave climate is reduced to a single representative wave condition that occurs a certain amount of days per year. For the updated model, it is desired that only the environmental conditions have to be given as input and that the accretion is determined based on this wave climate. Therefore, the case has been tested using the full wave climate.
The results of the test case given in the paper have been produced using a combination of three models: LITTORAL, LONGMOR and DIFSAND (Van Rijn, 2015). These results and the results produced by the sedimentation module in the updated model have been summarized and are presented in Table 4.13.

Model	Total Net Transport [m3/yr]	Downdrift Accretion Length [m]
Van Rijn	$7.5 * 10^5$	110
BW Model	$7.24 * 10^5$	115

Table 4.13: Results of the test case, executed by the LITTORAL/LONGMOR/DIFSAND models and the updated model (denoted by BW Model)

Although the models use the same equations, it is observed that differences still occur. These difference can be explained based on the following:

- Van Rijn performs the calculations using three models: LITTORAL, DIFSAND and LONGMOR (Van Rijn, 2015). Within these models, certain aspects like a calibration factor and a friction factor are taken into account. In the method that has been installed in the updated model calculation, such additional factors are not included. This is expected to cause differences in the generated results.
- The LONGMOR model used by Van Rijn is a model that makes use of grid cells and performs calculates the coastline change for a certain time step, defined in days. The calculation implemented in the updated model is a schematized approach that determines the accretion length at the structure with a time step defined in years. This results in less accuracy, which in turn can lead to differences in the result.
- The circular current velocity is pre-defined in the method used by Van Rijn. In the updated model, this is implicitly calculated. This results in a overestimation of the circular current velocity of (2.5 %), which results in a slightly larger transport rate toward the structure in the downdrift area.

The results show that the difference in the calculated downdrift accretion lengths is around 4.5 %, which is relatively small and is seen as acceptable. The difference in net total transport is 4 %, which is acceptable. From these results, it can be observed that the method shows promise, as it produces

realistic results for this case.

4.4. Computation time

The additions and modifications implemented in the model have influence on the computation time. This influence has been observed during the model runs. The runs have been performed on a laptop with 4 cores (Intel i7) and 32 GB of RAM. For the original model, the computation time per generation is between 40 - 60 seconds. The number of generations till convergence during a run is in the range of 100 - 150 generations. The total run-time is in the range of 1 to 2.5 hours.

Influence of bathymetry implementation

With the implementation of the grid as described in Section 3.1.1, the added computation time is small. The grid is created preliminary, due to which no additional time is added to the model run itself. By storing the grid data in a matrix and saving it as a compressed data file, the added computation time due to loading the data is negligible. The data is loaded before the model loop, resulting in the added computation time being minimal. Within the loop, the depth values are drawn from the data file that is stored within the model. This results in little to no addition of computation time.

The modifications to the calculation of the breakwater segment volumes, the channel dredging volumes and the turning basin volumes do add to the computation time. The number of calculations that are executed is larger than in the original model, due to the splitting of the breakwater segments and the channel segments into multiple sections.
The function used to determine the point from where dredging regarding the navigation channel is no longer needed, adds to the computation time. This is due to the function having to assess all coordinates on the line, instead of just performing a single calculation The function used to determine the volume that needs to be dredged regarding the turning basin also leads to increase of the computation time.
The computation time with the implemented additions and modifications is in the range of 80 - 90 seconds per run. The convergence still occurs in the range of 100 - 150 generations. The total run-time is in the range of 2 - 3.5 hours, which is 1 hour longer.

Influence of the REFRAC integration

The integration of REFRAC into the model has influence on the computation time. The input files for REFRAC have to be prepared before REFRAC can be run. The preparation of these input files takes between 1 - 3 minutes. A run of the REFRAC model has a duration of several minutes, depending on the number of wave conditions and the accuracy desired by the user. After REFRAC has produced its output, these output files are converted to use-able data files in the REFRAC module, which takes around 5 - 10 minutes, depending on the number of wave conditions.
Within the model, the wave parameters at a location are determined using the wave data stored in the produced data files. These files are loaded into the model before the model loop. This operation does not add additional computation time compared to the calculations from the original model, but even slightly reduces it.
Regarding the integration of REFRAC, the added computation time is only due to the preliminary operations, which will result in around 10 - 20 minutes of added time. However, the reduction of computation time due to the wave data being drawn from the data file instead of through computation, compensates for the addition, leading to no additional computation time overall.
The run-time is still in the range of 2 - 3.5 hours, as there is no run-time increase.

Influence of the sedimentation implementation

The implementation of updrift and downdrift sediment transport effects, along with channel sedimentation and basin siltation, results in additional computation time.
The updrift and downdrift sediment transport calculations are performed in the input file, before the model loop. The total computation time increase as a result of these calculations is in the range of several seconds, which in the time frame of an entire run is negligible.
Both the calculation of the harbour basin siltation volume and the channel sedimentation volume are executed within the model loop. The modifications made regarding harbour basin siltation have negli-

gible influence on the computation time. The calculation of the channel sedimentation volumes does have a notable effect on the computation time. The additional time per run is in the range of 10 seconds. The computation time per run is increased to 90 - 100 seconds, while convergence still occurs in the range of 100 - 150 generations, which leads to the total computation time being in the range of 2.5 - 4 hours, which is only 0.5 hours longer. This run-time is considered acceptable.

5

Case Study: Anaklia

The results that the updated model produces after the implementation of the improved bathymetry, the integration of REFRAC for wave transformation and the implementation of sedimentation processes have been analysed by applying the updated model for a real port design project. This analysis has been done using a case study of the Anaklia Deep Sea Port. In this case study, the optimum breakwater layout generated by the updated model and the original model are compared to the actual conceptual design developed during the design process.

5.1. Anaklia Deep Sea Port

The Anaklia Deep Sea Port is a port that is currently in development. The site of the port is located on the coast of the Black Sea near Anaklia, Georgia. This location is shown in Figure 5.1. It will be the first Georgian deep water port, greatly increasing the size of vessels that can call at the country.

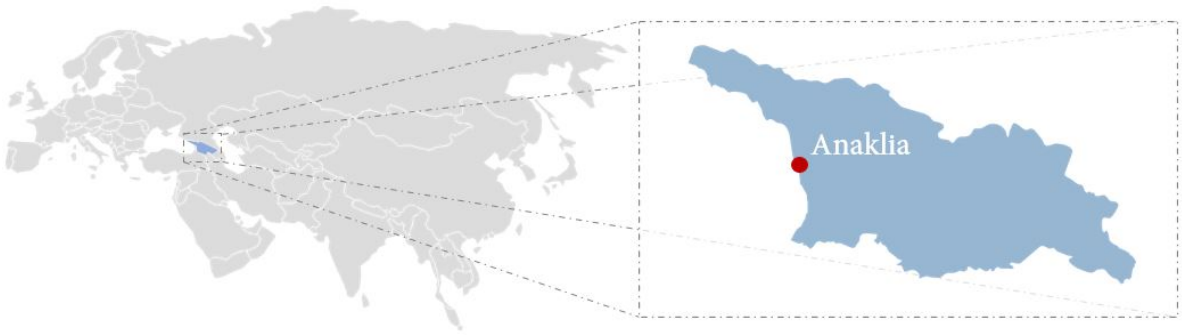

Figure 5.1: The geographical location of the Anaklia Deep Sea Port

The port is developed at this location due to the position of Anaklia. Anaklia is positioned in a strategic location on an ancient trade route (the Silk Road) and represents a critical transport node between Europe and China (Anaklia Development Consortium, 2020). The port will serve as a gateway for cargo to both landlocked countries in Central Asia and landlocked countries in the Caucasian regions. The port will unlock natural resources from, and a primary market in both Central Asia, the Caucasus region and Northern Iran.

The port is designed to handle containers, dry/break bulk and liquid bulk cargo. Therefore, the long term port design is in possession of (Anaklia Development Consortium, 2020):

- 7 berths for container vessels
- 2 berths for dry/break bulk vessels
- 1 berth for liquid bulk vessels

The main quay is designed as one long quay. The quay provides 7 berthing spaces for container vessels (Anaklia Development Consortium, 2020). The positioning of the berths for container vessels is shown in Figure 5.2, along with the port infrastructure, the port terminal layout and the breakwater layouts.

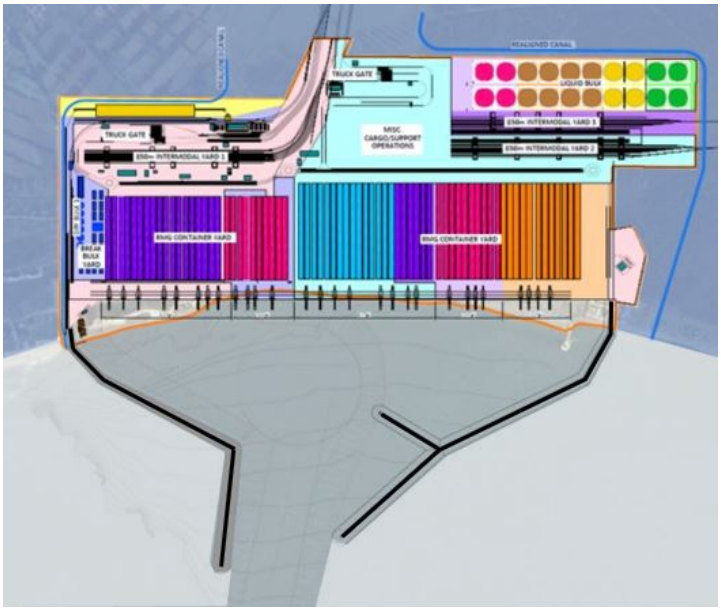

Figure 5.2: Conceptual design for the layout of the Anaklia Deep Sea Port (Anaklia Development Consortium, 2020)

The main type of cargo that will be handled in the port are containers. The focus on container cargo coincides well with the model in its current form, as containers are the cargo type considered by the model.

During the conceptual design phase, there are several requirements that had to be taken into consideration. Near the site of the port, a deep submerged canyon is present (see Figure 5.4). This canyon is located at the northern side of the port. This canyon has to be avoided, to prevent instability. Therefore, the breakwater has been designed at a safe distance from the canyon.
Another factor is the presence of a marine nature reserve, with a boundary perpendicular to the coast, just south of the port. The nature reserve is an area that is restricted and may not be encroached on, not even by the approaching ships. Due to the presence of this nature reserve, the approach channel has been designed with the incorporation of a bend, to avoid part of the navigation channel being located in this restricted area.

Due to the presence of the canyon, the focus on container vessels and the conceptual design containing a long and straight main quay and availability of bathymetry and environmental data, the Anaklia Deep Sea Port is seen as a good example to assess the performance of the model. The port design produced by the model has been compared to the available conceptual designs for the Anaklia Deep Sea Port.

5.2. Input parameters, environmental conditions and bathymetry

The port design and the location of the port have been modelled as accurately as possible. The environmental conditions at the port location, the bathymetry profile at the port location and the design parameters have been based on information provided in project reports and on the website of the Anaklia Development Consortium (http://anakliadevelopment.com/info/). The project reports have been provided by Arcadis Nederland B.V..

5.2.1. Design parameters

The port design features one large quay. The quay is designed to be 2250 meters long, with the distance between the breakwaters being 2920 meters (Anaklia Development Consortium, 2020). The quay consists of 7 berths, that are able to provide berthing space for container vessels.

The design vessel that has been used during design is a container vessel with the following specifications:

- Vessel Length: 300 meters
- Vessel Beam: 48 meters
- Vessel Draught: 15 meters

The parameters that are required for the determination of navigational components (such as the channel slope and the turning basin) are based on the information provided by the project reports. For the navigation channel, the channel slope is set to be 1:5.5 (Arcadis Nederland B.V., 2018). The turning basin diameter is designed to be 2 times the maximum vessel length, i.e. 600 meters. In the model, the default basin diameter is determined by multiplying the design vessel length with a factor 2.5. This factor is based on the PIANC guidelines (PIANC, 2014). These guidelines recommend a diameter of 2 to 3 times the design vessel length. Therefore, the factor of 2.5 has been modified to a factor of 2, such that in the model, the basin diameter is also 600 meters. The use of a factor of 2 is still within PIANC guidelines. The time required to fasten the tugs to the vessel is estimated to be 8 minutes (Arcadis Nederland B.V., 2018). The stopping lengths are estimated to be smaller than 1000 meters using simulations. In the model, the stopping length is determined using PIANC guidelines.

The cost values of the breakwater layer materials have been determined based on estimations of these costs that are provided in the project reports (Arcadis Nederland B.V., 2018). For the armour layer, both armour layer rocks and Xblocks have been used. In the model, the costs for armour layer materials is defined by the cost of the armour units. Therefore, the cost of the armour layer rocks and the Xblocks have been combined. As the size of the Xblocks varies over the breakwater length and the model uses a single size, a standard value has been assumed of 2 m^3. These cost values can be found in Table F.1 in Appendix F.

In the concession agreement and hence project requirements, it is specified that the wave height (H_s) at the berth may not exceed 0.5 meters (Arcadis Nederland B.V., 2018) for more than 5 % of the time. Therefore, this wave height has been set as the limiting wave height at the berth.

The type of unloading mechanism used at the berths are STS (Ship-To-Shore) gantry cranes (Anaklia Development Consortium, 2020). Based on information provided by the consortium, two cranes are assumed per berth (Anaklia Development Consortium, 2020). The average moves per hour for these cranes is 20-30 moves per hour (Ligteringen and Velsink, 2012). Therefore, the ceiling of average moves per hour is 60. When taking into consideration that this rate will not be reached all the time, the number of moves per hour have been set to 55. Regarding the berth occupancy, the default value of 0.65 is taken, which is seen as a good representative value for a port of this size and the number of berths present.

To gather information about local sedimentation and the sedimentation parameters, the project report "*Sedimentation Study*" (Arcadis Nederland B.V., 2018) has been used. This report shows that longshore sediment transport will not pose a problem regarding accretion along the breakwaters in shore-normal direction, due to the canyon acting as a sediment trap.

Therefore, only channel sedimentation is taken into account. Due to a lack of data, assumptions had to be made for the value of the bed roughness and the 90th percentile grain size. For the bed roughness, the default value of 0.06 m has been used. Based on the median grain size (which is 250 μm), a 90th percentile grain size of 500 μm has been assumed

All input parameters for the Anaklia case are given in Table F.1 and Table F.3, in Appendix F.

5.2.2. Environmental conditions

The environmental conditions are provided by the project reports. The reports provide detailed data on wave conditions, wind conditions and current flow conditions. The detailed data presented in the reports is too extensive and detailed for use in the updated model. The data has been reduced to twelve conditions, which are used as input for the updated model. The reduction to these twelve conditions has been done using the following criteria:

- The main wave directions, wind directions and current directions have to be well represented, to assure that the general conditions in the region are modelled accurately.
- The most unfavourable wave directions and their wave heights have to be included, to assure that they are accounted for in the design.
- The most extreme conditions that occur have to be included, as these are most likely to cause downtime.
- Excessive winds and currents have to be included, as they influence both downtime and sedimentation.

The extensive wave data for yearly offshore conditions has been visualised in a wave rose, shown in Figure 5.3a. As the coastline orientation is -135^o with respect to north, only the waves coming from 135 degrees with respect to North to waves coming in from 315 degrees with respect to north are taken into account.
For the wind conditions, extensive data is provided as well. The provided data contains the yearly wind conditions at 10 meters above the water surface. These conditions are portrayed in the wind rose shown in Figure 5.3b. For the wind conditions, all directions are taken into account.

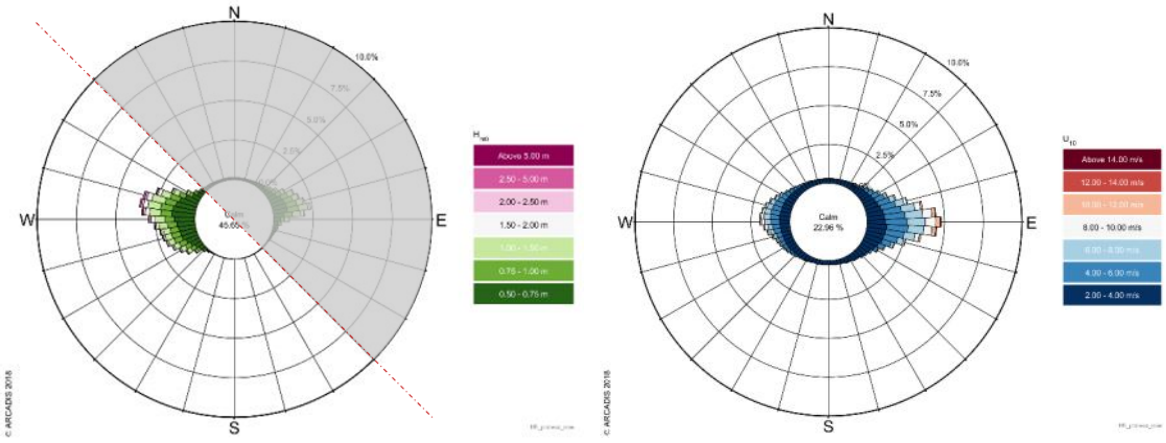

(a) (b)

Figure 5.3: (a) Wave rose containing offshore wave data (Arcadis Nederland B.V., 2018) (b) Wind rose containing wind data at 10 meters above MSL (Arcadis Nederland B.V., 2018)

For the current flow, a division is made between tidal currents and residual currents. According to the project report (Arcadis Nederland B.V., 2018), the tidal currents can be neglected. The residual current direction is alongshore (primarily from north to south), with a depth-averaged velocity that varies between the 0.2 m/s and 0.4 m/s. Therefore, a current flow velocity of 0.4 m/s has been used. These conditions are given in Table F.2, Appendix F.

5.2.3. Bathymetry

For the bathymetry profile, a detailed bathymetry data set was available for most of the area of interest. For the remaining bathymetry data, additional data from GEBCO (GEBCO, 2020) has been used. Based on this data, the grid has been created. This is visualised in Figure 5.4.

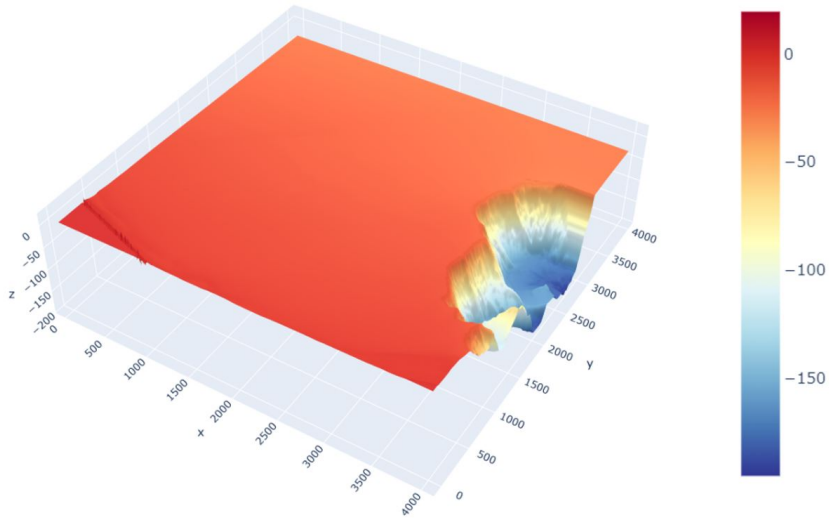

Figure 5.4: Visualisation of the Anaklia bathymetry as produced by the bathymetry module

5.3. Model runs

After defining the input parameters, defining the environmental conditions and creating the grid, the updated model has been run. Afterwards, the original model has been run, to assess their similarities and differences.

5.3.1. The updated model

The updated model has been run with all the input parameters defined in Appendix F. The REFRAC model has been run prior to the model runs. For illustrative purposes, the wave transformation due to REFRAC is shown for three of the wave conditions (θ_0 = 270^o, θ_0 = 225^o and θ_0 = 180^o with respect to North). The paths of the wave rays toward shore are shown in Figure 5.5 and the wave heights are shown in Figure 5.6. It is observed that the wave heights near the shoreline become unrealistic. These wave heights occur due to REFRAC not accounting for wave breaking.

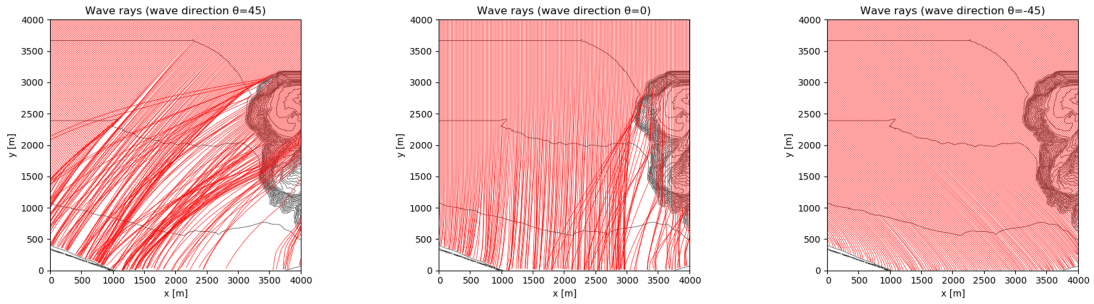

(a) (b) (c)

Figure 5.5: (a) The wave rays for incoming wave angle of 45 degrees w.r.t shore normal (270^o w.r.t. north) (b) The wave rays for incoming wave angle of 0 degrees w.r.t shore normal (225^o w.r.t. north) (c) The wave rays for incoming wave angle of -45 degrees w.r.t shore normal (180^o w.r.t. north)

It can be observed that the canyon has significant influence on the local wave heights and wave directions in the area of interest for waves that come in from 225 - 270 degrees with respect to north and less for the waves coming in from 180 degrees with respect to north.

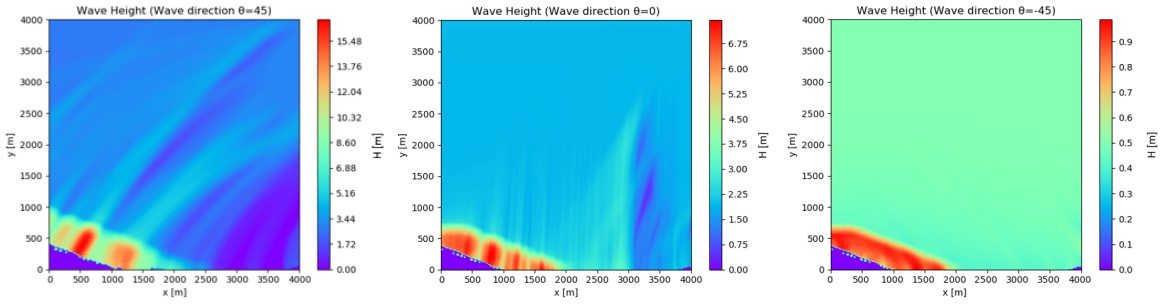

(a) (b) (c)

Figure 5.6: (a) The wave heights for a wave (H_s = 3 m) with incoming wave angle of 45 degrees w.r.t shore normal (270^o w.r.t. north) (b) The wave heights for a wave (H_s = 2 m)with incoming wave angle of 0 degrees w.r.t shore normal (225^o w.r.t. north) (c) The wave heights for a wave (H_s = 0.5 m) with incoming wave angle of -45 degrees w.r.t shore normal (180^o w.r.t. north)

The optimal port design produced by the updated model is shown in Figure 5.7, along with a visualisation of the layout on site. The monetary values and the downtime are displayed in Table 5.1.

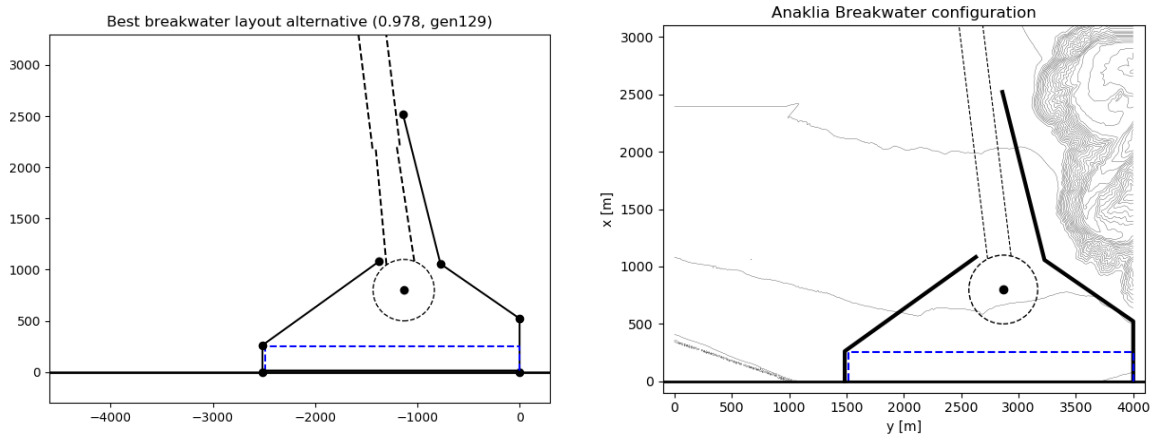

(a) (b)

Figure 5.7: (a) The port layout design produced by the updated model (b) The port layout design produced by the updated model, projected on the port development site

Category	Costs (€)
CAPEX/OPEX	**370.4 million**
Breakwater Construction Costs	58.2 million
Capital Dredging Costs	213.4 million
Dredging Maintenance Costs	3.7 million
Breakwater Maintenance Costs	1.1 million
Downtime	**38.5 million**
Downtime Costs	38.5 million
Average downtime per berth	1.7%

Table 5.1: Cost and downtime information for the Anaklia model run

For the case study, the model has been run four times. The two layouts with the highest score also showed resemblance, indicating to approach the optimal layout. The layout with the highest score is determined as the optimal layout. The run-time for the case study was 2.5 - 3 hours per run.
The generated optimal port layout is comparable to that of the initial conceptual design. A comparison of the port design produced by the model and the initial conceptual design is shown in Figure 5.8b. It is observed that the layout of the breakwaters, the alignment of the channel and the position of the turning basin coincide well with the conceptual design. The estimated distance between the primary and

secondary breakwater on the shoreline coincides well with distance shown in the conceptual design.

There are also notable differences between the initial conceptual design and the design produced by the updated model:

- The turning basin position is situated closer to the berth in the initial conceptual design. It is observed to have overlap with the berthing basin in the design generated by the updated model (visualised by the blue dashed line in Figure 5.8b).
- The third segment of the primary breakwater of the initial conceptual design is shorter than the third breakwater segment of the primary breakwater generated by the updated model.
- The primary breakwater in the initial conceptual design is constructed at a larger distance from the canyon than the primary breakwater produced by the updated model.
- The navigation channel in the initial conceptual design has a bend, which is not present in the navigation channel produced by the updated model.

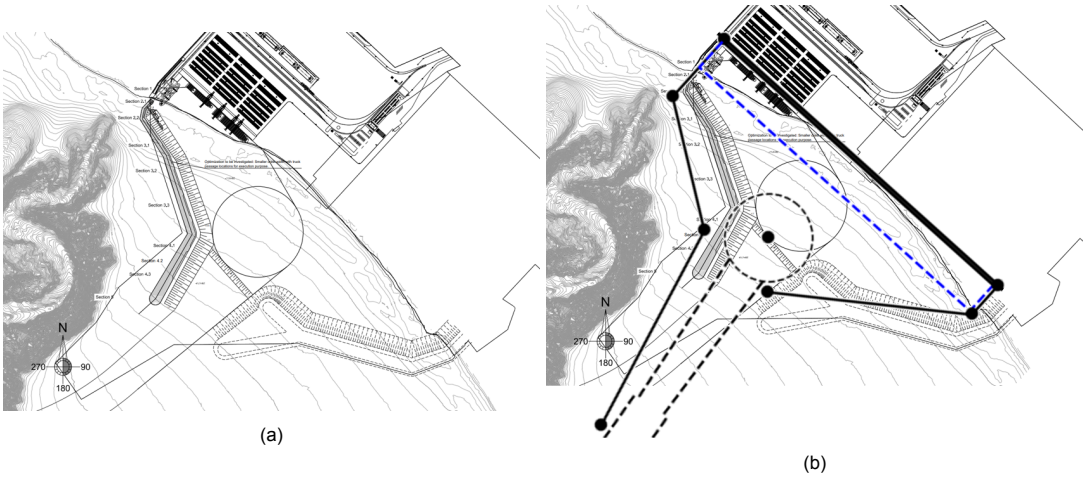

(a) (b)

Figure 5.8: (a) The initial conceptual designed for the Anaklia Deep Sea Port (b) Comparison between the initial conceptual design and the configuration of the breakwaters as produced by the updated model.

The difference in the position of the turning basin is likely due to the size of the berthing basin and due to dredging volumes. In the updated model, a criterion for the location of the turning basin is that the turning basin does not have overlap with the berthing basin. Due to the size of the berthing basin, the turning basin in the design produced by the updated model can not be placed at the same position as the turning basin in the conceptual design without overlap.
The dredging volume can also be a reason for the difference in between the result and the initial design. By placing the turning basin further away from the berth, the dredging volumes for the turning basin will reduce. If this reduction of volume is larger than the addition of dredging volumes due to the larger manoeuvring basin, this will lead to lower costs and therefore a higher fitness score.

The third breakwater segment of the primary breakwater in the design generated by the updated model is larger than the third breakwater segment of the primary breakwater in the initial conceptual design. This difference is due to the following: In the model, the length of this breakwater segment is partially dependent on criteria that determine if the channel has to be sheltered or not. For the wave environment that is present, the criteria determine that the inner channel has to be sheltered, to reduce navigational downtime. Therefore, the minimum length of this breakwater segment has to reach the end of the inner channel, which leads to a much longer breakwater segment than the breakwater segment of the initial conceptual design. The determination of the inner channel length is also of importance, due to the sheltering criteria. This channel length is based on the required stopping distance. In updated model, this distance is determined using PIANC guidelines (PIANC, 2014). Based on these guidelines, the determined stopping distance is 1410 meters. For the design of the conceptual design, real-time vessel movement simulations have been used (Arcadis Nederland B.V., 2018). The stopping distance in

the conceptual design is based on these simulations. Combined with a change in channel orientation, this results in a stopping distance that is smaller (< 1000 meters) than the one determined using the PIANC guidelines.

The primary breakwater is located closer to the canyon in the design produced by the updated model than the primary breakwater in the initial conceptual design. In the conceptual design, the primary breakwater has to attain a certain distance regarding its location with respect to the canyon. This distance is required to prevent possible instabilities. In the updated model, these types of restrictions are not accounted for. This results in the breakwater being constructed closer to the canyon.

As mentioned, the navigation channel in the initial conceptual design contains a bend that directs the channel towards deeper water and to avoid the nature preserve. This nature preserve is situated in southwest direction and has to be avoided. In the updated model, the incorporation of bends is not included. Due to the incorporation of bends not being included, a straight channel is present in the design produced by the updated model. The inclusion of certain area restrictions like the nature preserve is not present in the updated model. Due to the absence of these restrictions, the navigation channel of the design produced by the updated model is directed towards the nature preserve.

Downtime analysis

For the initial conceptual design, the expected downtime at the berths has been determined with the use of the numerical model PHAROS (Arcadis Nederland B.V., 2018). The PHAROS model accounts for diffraction, refraction, shoaling, bottom friction and reflection (Arcadis Nederland B.V., 2018; Deltares, 2020).
According to this wave penetration study, most of the downtime at the berths occurs at berths 3, 4 and 5. The largest percentage of downtime occurs at berth 5 (15 %).
The output corresponding to the layout produced by the updated model shows that the largest downtime occurs at berth 3 and 4. The largest percentage of downtime for the layout produced by the updated model occurs at berth 4 (7 %). For a visualisation of the berth locations and the downtime data produced by the model, the reader is referred to Appendix F.

The estimated percentage of the downtime presented in the reports is observed to be significantly higher than the downtime estimated by the updated model. Apart from the differences in the breakwater configuration, this difference in downtime can also be attributed to the updated model not accounting for reflection. According to the project report, the influence of reflection on the wave heights in the harbour basin is significant. To assess the influence of reflection, a model run is presented (with $H = 1m$, $\theta = 260^o$ w.r.t. North and $T = 7s$) in the reports, in which a small reflection coefficient is used. It is observed that the occurring wave heights become significantly smaller (e.g. a wave height reduction of 40 % at berth 5) with a smaller reflection coefficient.

Channel sedimentation

The breakwater configuration that has been developed by the model has a primary breakwater that stretches to the end of the inner channel, shielding the channel from waves. At the end of the breakwater, the channel depth with respect to the seabed level is smaller than 1 meter, leading to the channel sedimentation volumes being negligible.

In the project report (Arcadis Nederland B.V., 2018), the channel sedimentation rate has been determined for the initial conceptual design. To still be able to assess the performance of the channel sedimentation calculation in the model, the conceptual design has been recreated. The points at which the channel filling rate would be computed if the breakwater layout would be identical to the conceptual design are determined. Based on these points, it is possible to compute the yearly channel sedimentation volume (A visualisation is presented in Appendix F). By comparing this computed sedimentation volume with the estimated volumes given in the report, statements can be made about the performance of the model with respect to the channel sedimentation calculations.

For the conceptual design, the channel sedimentation volume has been estimated using Delft3D. The estimated channel siltation volume is given to be 15000 m^3 to 30000 m^3 per year (Arcadis Nederland

B.V., 2018). It is observed that under normal conditions, no sediment transport into the channel occurs due to the waves and currents not being able to mobilize the sand. Only during more extreme conditions, sediment transport into the channel is present.
The yearly channel sedimentation volume that is calculated by the model is 20952 m^3. This calculated volume is within the volume range given in the project report. The filling rate is observed to only be larger than zero for conditions where the offshore wave height is 2 meters or larger, which are more extreme conditions. Based on the channel sedimentation volume being within the expected range, as well as the observations that have been made with regard to when sediment transport occurs, it is concluded that the calculation of the channel sedimentation volumes is sufficiently accurate for concept design.

Revised concept design

The initial conceptual design has been revised. The main reasons for this revision were the nautical safety and the required reduction of downtime at the berths. Regarding the nautical safety, the initial concept design (shown in Figure 5.9) had a short stopping length, with a channel that was directed almost perpendicular to the berths. This design left little room for error, increasing the risk of collision. The desire to reduce downtime with respect to the first conceptual design was mainly due to the uncertainty that the downtime criteria would be met. This revision has led to a new conceptual design, shown in Figure 5.9a. The revised design has also been compared to the design produced by the updated model (shown in Figure 5.9b).

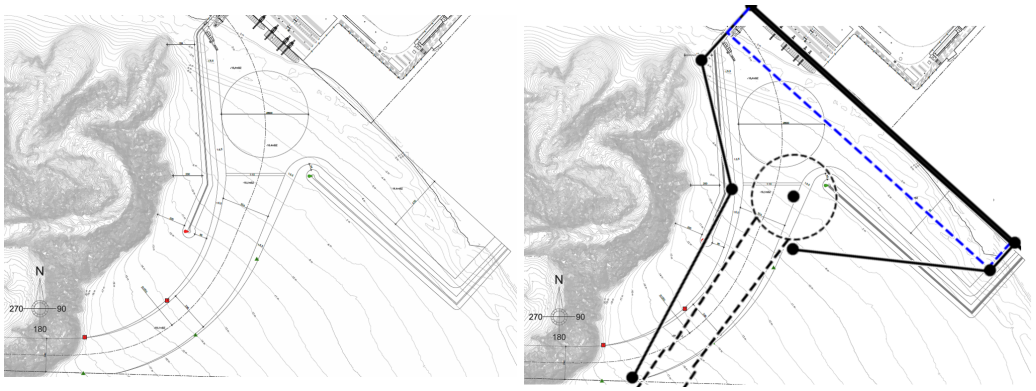

(a) (b)

Figure 5.9: (a) The revised design (b) Comparison between the revised design and the design produced by the updated model

It is observed that the shape of the primary breakwater of the revised design aligns well with the design produced by the updated model. The third breakwater segment of the primary breakwater in the design produced by the updated model is shorter, due to shielding of the inner channel. The shape of the secondary breakwater in the design produced by the updated model differs from the secondary breakwater in the revised design.
This difference is due to the shielding function of the primary breakwater for waves coming in from the south and diffracted waves coming in from the west, in combination with the location of the turning basin. An increase in downtime occurs if the secondary breakwater in the design produced by the updated model would be positioned in a manner that the secondary breakwater is positioned in the revised design.
Placement of the turning basin of the design produced by the updated model at the location of the turning basin in the revised design will lead to an increase in dredging cost. This increase in dredging costs is due to the increase in dredged volume regarding the turning basin and due to the needed increase in the channel angle, which will lead to an increase in dredged volume regarding the channel. The increase in dredged volume results in a lower fitness score.

5.3.2. The original model

The original model has been run with the input parameters that the original model allows the user to define (see Appendix A). The generated layout is compared to the optimal layout generated by the updated model. The optimal layout produced by the original model is shown in Figure 5.10b.

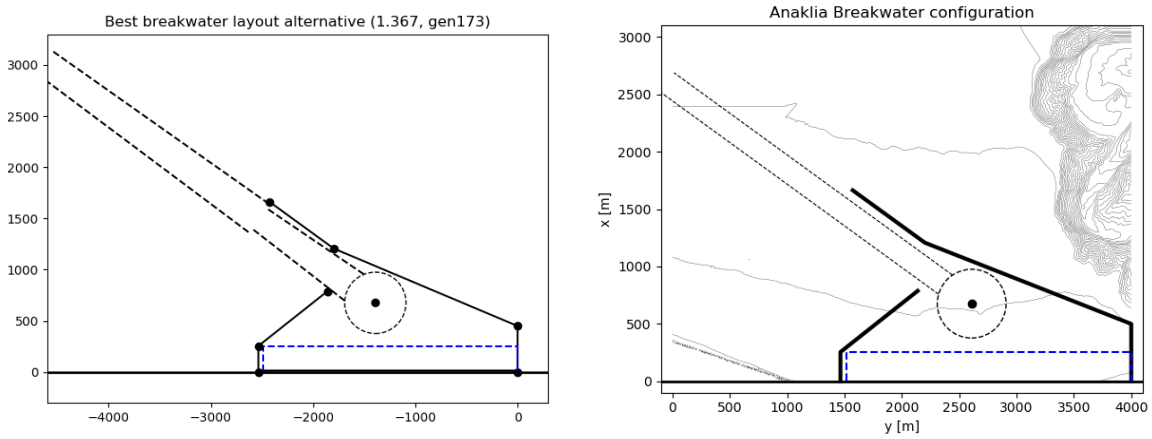

(a) (b)

Figure 5.10: (a) The optimal breakwater layout generated by the original model (b) The optimal layout as it is placed on the port development site

It is observed that the produced optimal layout coincides less with the conceptual designs presented in Section 5.3.1 than the optimal layout produced by the updated model. The notable difference that is observed is the orientation of the navigation channel and the shape of the primary breakwater (see Figure 5.11).

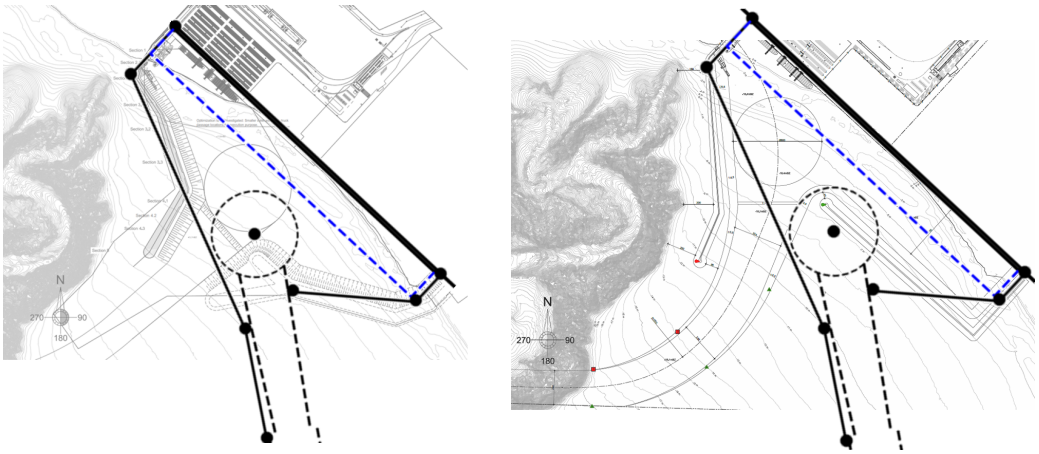

(a) (b)

Figure 5.11: (a) Comparison between the initial conceptual design and the design produced by the original model (b) Comparison between the revised design and the design produced by the original model

This difference is most likely caused by the difference in local wave parameters between the original model and the updated model. The use of the bathymetry profile and the REFRAC model allows the updated model to incorporate the canyon and its influence on the local wave height and wave direction (which can be seen in Figures 5.5 and 5.6).

In the original model, the canyon can not be incorporated due to the assumption of a homogeneous slope. The wave transformation is modelled using linear wave theory that assumes a homogeneous

bed slope with depth contours parallel to the shoreline. Therefore, the local wave parameters that are less accurate than the local wave parameters determined in the updated model.
Due to this difference, the local wave climate is not represented accurately. As a result, the generated optimal layout differs as well.

5.3.3. Concluding remarks

Based on the comparison of the port layout produced by the updated model with the existing conceptual designs, it is observed that the updated model produces results that coincide well with the conceptual designs. The updated model is able to include subjects of significant influence (such as complex bathymetry and its effect on wave transformations) in a sufficient manner. The assessment of the channel sedimentation calculations shows that the calculated sedimentation volume is within the estimated range that is mentioned in the project report (Arcadis Nederland B.V., 2018). This result shows that the method that is used in the updated model produces realistic results.

The layouts produced by the updated model and the original model have been compared. From this comparison, it is observed that the updated model produces an optimal layout that coincides better with the conceptual layouts than the layout produced by the original model. This difference is attributed to the absence of the ability to incorporate the canyon and its influence on the local wave conditions. This absence leads to a less accurate representation of the local wave conditions and therefore a less accurate representation of the optimal layout.

Based on the results of the updated model and the comparison of these results with the results produced by the original model, it is observed that the additions and modifications that have been made to the original model have resulted in the updated model producing more accurate layouts.
However, it has become clear that certain aspects have not been incorporated, which have proved to be of importance for the eventual design. The revision of the initial concept design portrays the importance of nautical safety measures (such as the alignment of the navigation channel with respect to the quay), which are currently not included. The same goes for the inclusion of area restrictions and the preference of clients (such as allowed downtime to reduce breakwater costs). The fact that these aspects are not accounted for has to be taken into consideration when using the updated model and its output. Another important factor is the occurrence of budget constraints in the first phases of project development, which may lead to a design that has less than optimal downtime.

6

Comparison of the original and updated model

In this chapter, the original model and the updated model are compared. The modifications and additions that have been made to the original model to develop the updated model are presented and the added value of these modifications and additions is described.
Thereafter, the original model performance and the updated model performance are compared and their differences are presented. The model performance of both models is compared based on their run-time, their consistency, their convergence and their applicability.
Based on the comparison between the models, the modifications and additions that have been made and the updated model performance are reflected upon.

6.1. Modifications and additions

The modifications and additions that have been made to the original model are attributed to the implementation of:

- The bathymetry profile grid
- The REFRAC model for modelling the wave transformation
- The sedimentation processes

In this section, it is described which modifications have been made with respect to the original model.

6.1.1. Bathymetry

In the original model, the breakwater volume calculation, the capital dredging volume calculation and the bed level determination are performed using methods that assume a constant bed slope with depth contours parallel to the shoreline. With the implementation of the bathymetry profile grid, the assumption of a constant bed slope with depth contours parallel to the shoreline is not valid anymore. To establish calculation methods that lead to correct results, modifications have been made to the breakwater volume calculation, the capital dredging volume calculation and the determination of the bed level.
The breakwater layouts can be generated in both positive and negative x-directions. In the original model, the x-coordinates are assigned to a negative x-value if the layout is generated in the negative x-direction. Modifications have been made in the module that is used for the generation of the layout alternatives, to maintain the option to generate breakwater layouts in both x-directions after implementation of the bathymetry profile grid.
Therefore, the implementation of bathymetry profiles results in modifications of the following aspects:

- Breakwater volume calculation
- Capital dredging volume calculation
- Bed level determination

- Layout generation

The modifications that have been made to these components (presented in Section 4.1) have resulted in the following developments:

Breakwater volume calculation
The modifications that have been made to the calculation of the breakwater volumes, ensure that varying seabed levels in both x- and y-directions are taken into account in these calculations in the updated model.

Capital dredging volume calculation
The modifications that have been made with regard to the capital dredging volume calculation ensure that in the updated model, variations in depth are taken into account. Therefore, the calculation of the required dredging for the construction of the navigation channel, as well as the turning basin, the manoeuvring basin and the berthing basin increases in accuracy with respect to the method used in the original model.

Bed level determination
The modification of the bed level determination allows the updated model to determine the seabed level based on the x,y-coordinates of the desired location. This modification allows the model to account for bathymetry profiles with the seabed level varying in both the x- and y- direction.

Layout generation
The modifications that have been made to the generation of the layout alternatives allows the updated model to use negative indexing. Negative indexing enables the updated model to still accurately construct the layouts in both directions along the x-axis after the implementation of the grid. In this manner, the option to construct the breakwater layout in both positive and negative x-direction is maintained.

The changes that have been made have increased the robustness of the bathymetry calculations. The updated model is able to account for all bathymetry profiles. All depth variations in both x- and y-direction can be accounted for, in both the seabed level determination, as well as for the volume calculations.
The changes that have been made also allow for future developments, like the integration of soil type variations in the area of interest.

6.1.2. Wave transformation
In the original model, wave transformation is modelled with the use of linear wave theory. With this approach, it is assumed that the bed slope is constant and that the depth contours are parallel to the shoreline. Due to the implementation of the bathymetry profile, it is not correct to assume that the bed slope is constant and that the depth contours are parallel to the shoreline. As a result, the modelling of wave transformations had to be modified as the method in the original model is no longer sufficient (described in Chapter 3). In the updated model, the modelling of wave transformations is performed using REFRAC. The integration of REFRAC allows for the updated model to better account for the influence of depth variations in both x- and y-direction in the modelling of wave transformations. The integration of REFRAC into the updated model has led to a modification in the method that is used for the determination of local wave parameters.

Wave parameter determination
In the updated model, the wave parameters at a specific location are determined using the wave parameter output generated by the REFRAC model. Using this output, the wave parameters are defined for each location and stored in a data file. Based on the x,y-coordinates at the desired location, the corresponding wave parameters are drawn from the data file. In this manner, local wave parameters are determined with a higher level of accuracy for simplistic and complex bathymetry profiles. The determination of the local wave parameters does not lead to additional computation time.

Due to the use of REFRAC for the modelling of wave transformations, depth variations in two dimensions (the x-axis and the y-axis) are accounted for. As a result, the local wave conditions can be determined with a higher level of accuracy for homogeneous and complex bathymetry profiles.

6.1.3. Sedimentation

In the original model, sedimentation is accounted for by a yearly siltation rate. This yearly siltation rate is multiplied with the channel area and the harbour basin areas, to determine a yearly siltation volume. This method gives a rough indication of the siltation volume in the channel and the harbour basin. The impact of the port on the longshore sediment transport is not included.

Longshore sediment transport can lead to accretion and eventually bypassing. To prevent bypassing, the breakwaters are usually designed with a minimum length. To incorporate this element of design, longshore sediment transport calculations have been included in the updated model.
A new calculation method to determine the channel sedimentation volume is also included in the updated model. This new calculation method has been included to improve the accuracy of the yearly channel sedimentation volume.

The implementation of sedimentation processes have led to modifications of the following components:

- Maintenance dredging volume calculation
- Layout generation

Maintenance dredging volume calculation

The implementation of the sedimentation processes has modified the calculation of maintenance dredging volumes.
The calculation of the channel sedimentation volume per year in the updated model is performed using the Souldby-Van Rijn equation. This modification has been made to make a more accurate prediction of the yearly channel siltation volume.
The calculation of basin siltation is performed by multiplying a yearly siltation rate with the total area of all basins.

Layout generation

With the implementation of sedimentation processes, longshore sediment transport is taken into account. The longshore sediment transport calculations are used to predict the length of the accretion along the breakwaters in shore-normal direction. The accretion length along the breakwater in shore-normal direction at both breakwaters is used to determine the minimum length of each breakwater. The minimum breakwater lengths are used as input for the generation of the layout alternatives. In this manner, a conservative prediction is made of the minimum breakwater lengths that are required to prevent bypassing.

These modifications allow the updated model to account for the impact of port construction on longshore transport and the possible accretion that can occur. The accretion that occurs at the breakwaters is an important aspect that has to be considered during port design.
In addition, the channel sedimentation volume is calculated in a more accurate manner, which results in a more accurate estimation of the dredging maintenance costs. In place of a highly simplified method, there is now an acceptable, robust modelling of sedimentation and its impact on costs.

6.2. Performance

The modifications and additions that have been made to the original model influence the performance of the updated model. Therefore, the performance of the updated model and the original model have been compared based on:

- Their convergence
- Their total run-time
- Their consistency
- Their applicability

Convergence

Both models make use of an optimisation algorithm to approach the optimal breakwater layout. When such an optimisation algorithm is used, it is important that the model converges during the optimisation. If convergence does not occur, no optimum is found.
For the original model, convergence generally occurs between 100 and 150 generations. For the updated model, convergence also generally occurs between 100 and 150 generations. The modifications that have been described in Section 6.1 do not influence the convergence.

Runtime

The modifications and additions that have been made to the original model have increased the model running time. The runtime of the updated model is 1.5 to 2 times larger (between 2.5 - 4 hours) than that of the original model. This run-time is considered acceptable, as it still remains much quicker than old fashioned layout development.
This difference in run-time between the original model and the updated model is mainly due to the different methods used for the calculation of the breakwater volumes, the capital dredging volumes and the channel siltation volume. These calculations lead to a small addition to the computation time. These calculations are all performed within the model loop. Due to the calculation being performed in the model loop, the small addition to the computation time by these calculations has a large effect on the total runtime. As a result, the total run-time has increased significantly.

Consistency

An important aspect is the consistency of the breakwater layouts that are produced by the model. The original model generally produces the same optimal layout for at least 2 out of 3 runs. Therefore, the user is advised to perform 3 - 4 runs. By performing multiple runs, the optimal layout can be determined. The updated model has the same consistency, generally producing the same optimal layout for at least 2 out of 3 runs. Therefore, it is still advised to carry out 3 - 4 runs to give confidence in the produced optimal layout.

Applicability

The applicability of the models depends on the locations at which the model can be applied and produce accurate results. The locations for which these criteria hold, are locations for which the model is able to model the local environmental conditions and the bathymetry correctly.

In the original model, a straight shoreline with a constant bed slope and depth contours parallel to the shoreline are assumed. Therefore, its applicability is limited to locations where these assumptions are valid. Moreover, the original model does not take longshore sediment transport into account. Many of the locations that have a consistent, uniform coastline are subject to substantial longshore transport. If at such a location longshore transport rates are present, the original model should be used with caution.

The updated model makes use of a grid to model the bathymetry. The incorporation of sedimentation processes allow the updated model to account for accretion due to longshore transport. This feature determines the sediment transport rates and the accretion length along the breakwater in shore-normal direction using a schematized method. This method uses linear wave theory and equations in which a constant bed slope with depth contours parallel to the shore is assumed. Moreover, a standard breakwater configuration has been assumed for these calculations.

Therefore, the updated model is applicable to most locations, except locations where external boundaries (such as exclusion zones) are present. If longshore transport rates are present, this can be taken into account. However, this feature should be used with caution, due to the assumption of a standard breakwater configuration and the assumptions that have been made in the calculation of the accretion along the breakwater in shore-normal direction (such as parallel depth contours or the shape of the accretion area).

6.3. Conclusion

From the comparison of the original model and the updated model, the following conclusions are drawn:

- The runtime of the updated model is larger than that of the original model
- The consistency of the updated model and the original model are similar
- The convergence of the updated model and the original model are similar
- The range of locations to which the updated model can be applied is larger than that of the original model

From the model comparison conclusions, it can be derived that the original model does perform better with regard to the model run-time. The run-time of the updated model is 1.5 to 2 times larger (around 2.5 - 4 hours), which is still within an acceptable range.
The consistency and the run-time of the updated model are similar to that of the original model.

The updated model has a significantly wider range of locations that it can be applied to. The original model can only be applied reliably to locations that can be modelled as a straight shoreline, with a constant bed slope and depth contours parallel to the shoreline. The incorporation of bathymetry and the modification of the modelling of the wave transformation have resulted in a model that is applicable to a much wider range of locations (such as locations with complex bathymetry profiles).
The incorporation of sedimentation processes allows the updated model to better account for possible morphological response due to port construction.
As the updated model has fewer simplifications and limitations than the original model, it can be used with more confidence. The modifications that have been made were necessary to improve the original model, making it more realistic and robust.

The updated model can still be significantly improved on several points. Improvements such as the improvement of cost modelling, the inclusion of budget restraints and the addition of restricted areas are steps that have to be taken to further develop the model. Moreover, additional validation of sedimentation processes and the modelling of the wave transformation are required to make more definite statements about their accuracy and reliability. These and other points of improvement are further discussed in Chapter 7.

7

Discussion

Increasing the applicability of the model is an important step in developing the original model (an initial proof of concept using genetic algorithms to generate a optimal breakwater layout) into a model that is more suited to realistic conditions.
By improving the applicability, the model is brought a step closer to being a widely applicable design support tool for the conceptual design of breakwater layouts. In this chapter, a critical reflection is given with regard to the results, the methodology that has been used, the accuracy of the added processes, the model performance and the subjects that have been selected for implementation. The uncertainties and limitations that have emerged during this research are also presented.

7.1. Selected processes

During the first stages of research, several subjects have been described that could be added to the original model or that could be improved upon (see Section 2.2). From these subjects, three subjects were selected for implementation: the addition of bathymetry, improvement of the modelling of wave transformation and implementation of sedimentation processes.

- The addition of the bathymetry profile has lead to a large increase in the applicability of the model. All types of bathymetry can now be accounted for. This addition has allowed the model to be applied to a much wider range of locations.
- Due to the integration of REFRAC, wave transformation is modelled more accurately for both simple and complex bathymetry profiles. Therefore, the updated model is able to use more accurate local wave parameters for the determination of the downtime. An accurate representation of the local wave parameters enables the updated model to produce reliable results for locations with simple bathymetry profiles and locations with complex bathymetry profiles.
- The implementation of the sedimentation processes has enabled the updated model to make a more accurate prediction of the yearly channel sedimentation volume corresponding to a breakwater layout alternative. A higher level of accuracy regarding the channel sedimentation volume per year results in a higher level of accuracy of the estimated operational costs per year. The implementation of sedimentation processes has also led to the incorporation of longshore sediment transport. The longshore sediment transport rates are used to determine the accretion length along the breakwaters in shore-normal direction. This allows for the model to give an indication of the minimum required primary and secondary breakwater lengths.

The implementation of the bathymetry profile and the integration of REFRAC have proved to be essential additions. The implementation of sedimentation processes adds to the accuracy of the OPEX calculation and has added design requirements to the model. As a result, the applicability of the model has increased due to the implementation of the selected subjects. The implementation of these subjects is therefore seen as a good choice.

The implementation of some subjects that have not been selected will also lead to improved applicability:

- Increasing the port layout complexity will result in the model to be applicable to different port layout designs. Inclusion of different cargo vessel types will result in the model being applicable to ports that call different cargo vessel types (instead of just container vessels). Therefore, implementation of these subjects is seen as a logical next step to further improve the model applicability.
- Improving the downtime cost estimation will lead to a more accurate estimation of the downtime costs. This subject can be divided into two separate subjects that can be further improved: the wave transformation inside the harbour basin and the correlation between the operational and navigational downtime. Both subjects have an influence on the estimated downtime and therefore on the downtime costs. The downtime cost estimation has significant influence on the fitness score of a layout alternative. Therefore, the accuracy of the downtime cost estimation also has influence on the accuracy of the generated optimal breakwater layout.

From the subjects that have not been selected, implementation of the following subjects will lead to an increase in accuracy of the generated optimal breakwater layout:

- Integration of the cross-sectional design tool will lead to a more accurate determination of the breakwater construction costs. The breakwater construction costs are of significant impact on the CAPEX. As a result, the accuracy of the breakwater construction costs also influences the accuracy of the optimal breakwater layout. Therefore, a more accurate estimation of these costs will increase the accuracy of the results produced by the updated model. It should be noted that the integration with the cross-sectional design tool can't be performed until the tool has been fully developed.
- The inclusion of client preferences and constraints is recognized as an important aspect in the further development of the model. During the Anaklia case study (see Chapter 5), it has been observed that one of the main differences between the produced layout and the conceptual designs (the length of the primary breakwater) is caused by a design choice based on budget restraints. Such restraints or restrictions can not be accounted for in the updated model. In further development, inclusion of such restraints will allow the model to produce layouts that better fit the client's preferences and possible constraints.

Implementation of these subjects is seen as valuable, as they will improve the accuracy of the generated optimal breakwater layout. Therefore, it is recommended to conduct further research on these subjects and implement them or improve upon them if possible.

From the results of the case study of the Anaklia Deep Sea Port (see Chapter 5), it has been observed that the following subject can also be of significant importance during the design process: the inclusion of nautical safety factors.
Nautical safety factors have not yet been included. From the results of the Anaklia case study (Chapter 5), it has been observed that aspects of nautical safety (such as the angle of approach of the navigation channel) can have significant influence on port design. Therefore, including the option to account for nautical safety factors will result in layouts being produced that concur more to the user's preferences.

7.2. Applicability

Compared to the original model, the updated model can be applied to a wider range of locations. This wider range of applicability is due to the introduction of the bathymetry grid and the use of REFRAC for the modelling of wave transformations. These additions allow the updated model to be applied to locations with complex bathymetry profiles that can not be modelled as a homogeneous slope with parallel depth contours.
The implementation of sedimentation processes has introduced the option to account for the morphological response of the shoreline due to port construction.

Regarding applicability, the limitations of the updated model are the limited port designs to which it can

be applied and the focus on one cargo vessel type: container vessels.
Similar to the original model, the updated model is only applicable to port designs that feature one long, straight quay at which all the berths are situated. This design requirement results in a limitation with regard to the port designs that the updated model can be applied to. To remove this limitation, the model should be able to incorporate more complex port design layouts. This can be achieved by providing the user with the option to incorporate a different quay design or to place berths at different locations than on the single main quay (e.g. placing berths on the breakwater). These additions will increase the applicability of the model with regard to different port designs.
The updated model still focuses solely on handling container cargo. This results in a limitation if certain berths within the port design are meant for vessels that carry other cargo types, such as dry/break bulk. Different cargo vessels will likely lead to different input parameter values, which will influence the estimated downtime (such as unloading rates and limiting wave heights). Including the option to assign berthing spaces to different cargo types (which will result in the berths having differing limiting factors and production) will remove this limitation and lead to a more accurate optimal breakwater layout design.

7.3. Methodology

The methodology that has been followed for the implementation of the bathymetry grid, the integration of REFRAC and the implementation of the sedimentation processes has been presented in Chapter 3.

7.3.1. Bathymetry

The implementation of the bathymetry grid has been done using a grid with rectangular grid cells, each with equal grid cell size. In this manner, the seabed level can be determined quick and accurately for each location. The choice for a grid with rectangular grid cells is supported by the fact that the generated bathymetry grid can be used as the bathymetry data that is required as input by REFRAC. For the use of the grid type in REFRAC, no further modification is required. As a result, the method used for the implementation of bathymetry is considered to be a sufficient method that fits well with the framework of the updated model.

7.3.2. Wave transformation

After review of three simple wave models (see Section 3.2), the REFRAC model has been chosen for the modelling of the wave transformation. The REFRAC model has been chosen, as it is most suited for integration concerning the updated model and the current framework. The updated model and REFRAC connect well due to the chosen grid type and the added module to convert the REFRAC output data to data that is useable in the model. The methodology that has been used enables the updated model to model the wave transformation with more accuracy compared to the method used in the original model. The use of a separate module provides the user with the opportunity to check the results produced by REFRAC, before using them in the model.
As a result, the methodology used for the integration of REFRAC is seen as a sufficient method.

The REFRAC model has to be run separately, as it is not part of the Python code but a separate model. The REFRAC model is run before the model loop, which is both an advantage and a disadvantage. The advantage is the fact that no additional computation time occurs during the model loop. The disadvantage is that the influence of the navigation channel on the wave transformation is not included (as the channel location and orientation can differ for each layout alternative).
This disadvantage can be removed if the wave transformation can be performed for each individual layout, allowing for incorporation of the navigation channel. The added value of this modification will differ per layout alternative, as the added value depends on the configuration of the breakwaters and the navigation channel. The general added value is expected to be significant, as refraction due to the channel can have a significant influence on wave conditions within the harbour basin and thus on the downtime (this is elaborated on in Section 7.4.2).
Therefore, it is recommended to review methods that allow for the navigation channel to be taken into account during the wave modelling. A possibility could be to install the functions used in REFRAC within the Python code, allowing for wave transformation to be modelled for each individual layout. Modelling the wave transformation for each individual layout is expected to add significantly to the computation

time. Therefore, it is of importance to assess if a possible method does not lead to excessive computation time that does not fit the updated model concept.

7.3.3. Sedimentation processes

The implemented sedimentation processes have led to the incorporation of longshore sediment transport processes and a more accurate calculation of the channel sedimentation volume. The incorporation of longshore sediment transport allows the updated model to provide an indication of the required minimum lengths of the primary and secondary breakwaters, as described in Chapter 3.

The calculation of the minimum required primary and secondary breakwater lengths is performed before the model loop. Therefore, a standard breakwater layout has been assumed to allow the model to make an estimation of the secondary breakwater length. This method introduces uncertainty, as the generated breakwater layouts can deviate from this assumed breakwater layout. As a result, the calculation of the accretion length and the minimum required secondary breakwater length are less reliable. Therefore, it is recommended to conduct further research on empirical methods to determine the minimum secondary breakwater length with more accuracy for variable layouts. A possibility could be to further develop the model in such a way, that the calculation with the schematized method can be executed for each individual layout during the optimisation.

In the updated model, the channel sedimentation volume is calculated using the Soulsby-Van Rijn equation (see Eq. 2.23). This method leads to a more accurate representation of this volume than the standard filling rate per year that is used in the original model. The Soulsby-Van Rijn equation has been chosen as this equation accounts for both wave orbital velocity as well as current flow velocity. The incorporation of the wave orbital velocity does lead to a larger computation time. From the results found in the analysis of the equation in Chapter 4 and the case study in Chapter 5, it is observed that waves can have a significant influence on the filling rate. Therefore, the use of the Soulsby-Van Rijn equation is seen as a correct choice.

7.4. Accuracy of added processes

7.4.1. Bathymetry

In the updated model, the bed level at a location is determined based on the x,y-coordinate of the location. Based on the x,y-coordinates, the corresponding bed level of that location is drawn from a data file that contains the bathymetry data. This method leads to an accurate determination of the bed level at that location.
The calculations of the capital dredging volumes and the breakwater volumes are determined by splitting the channel and the breakwater into sections, as described in Section 6.1. This method does not calculate the exact volume, which introduces a small uncertainty in the calculated breakwater volumes and capital dredging volumes. To approach the exact volumes, the section volumes have to be determined for sections with a length that approaches zero. Such a method is too time-consuming and leads to a large increase in run-time. As a result, a compromise has been made between computation time and accuracy.
Such a compromise is allowed, as the model is meant as a support tool for conceptual design. Therefore, it is not required to determine the exact volumes (see Section 1.3). The estimation that is made using the current method is considered sufficient for the conceptual design stage.

7.4.2. Wave transformation

For the updated model, the local wave parameters are determined with the use of REFRAC. A REFRAC run duration is relatively short, as the model produces its output in a matter of minutes. With the use of REFRAC, wave transformation due to refraction and shoaling can be modelled for both homogeneous and complex bathymetries. The resulting local wave parameters have been compared to the wave parameters produced by the method from the original model for a case with a homogeneous bed profile (see Chapter 4), which showed only small deviations (< 5%). Literature (Liu, 2009) and the Anaklia case study (see Chapter 5) show that REFRAC is also able to model wave transformation for complex

depth profiles. REFRAC produces the most reliable results for locations where waves with little to negligible directional spreading are dominant (as REFRAC doesn't account for directional spreading) and where shoaling and refraction are the dominant wave processes concerning wave transformation. Consequently, the updated model can best be applied to locations where such conditions are present.
It should be noted that for most port design projects, extensive wave studies have been performed in the initial stages of design, using complex wave models such as SWAN (SWAN, 2020). The results produced by these complex wave models have a higher level of accuracy than the results produced by REFRAC. To quantify the difference in accuracy between the results produced by REFRAC and results produced by more complex wave models that are able to account for additional wave processes, additional research has to be conducted.
Adding the possibility to use the wave data generated by wave models with a higher level of accuracy will increase the accuracy of the updated model. The wave data generated by the wave models has to be transformed into data that can be used in the model. Such a transformation of data is performed in the updated model for the results produced by REFRAC. By programming additional modules for transformation of wave data produced by other wave models, the wave data from these other models can also be used in the updated model.

The wave conditions within the harbour basin are approximated by incorporating diffraction effects. The diffraction effects on the incoming waves inside the harbour basin are determined using diffraction coefficients. These diffraction coefficients are determined based on the Goda diffraction diagrams (Goda, Takayama, and Suzuki, 1978). This method provides the diffraction coefficients at the berth based on several assumptions, which are mentioned in Section 2.3.
The assumption of a constant basin depth is not necessarily true. In addition, wave processes such as wind-growth, shoaling, refraction and wave reflection can also influence the wave conditions within the harbour basin. Due to these processes not being accounted for, the calculated wave heights at the berth can differ from reality. An example is shown in the Anaklia Deep Sea Port case study (see Chapter 5), where it is observed that reflection can have a significant influence on the wave heights within the harbour basin. Minor changes in the wave height (in the range of decimeters) can have a significant effect on the estimated downtime. Therefore, not accounting for these processes can result in a less accurate determination of the downtime at the berth.
Due to this uncertainty, expert judgement is required to review the produced optimal breakwater layout and the possible influence of the processes that are not incorporated. Special attention should be given to the possible impact of reflection (depending on the type of quay, the reflective quality of the breakwater material (which depends on the slope and material (Zanuttigh and van der Meer, 2007)) on the wave conditions within the harbour basin, as reflection is considered to have the most dominant influence within the harbour basin besides diffraction (Holthuisen, 2007).
A more accurate estimation of the wave conditions inside the harbour basin will require more complex modelling. The wave conditions within the harbour basin have to be determined for each layout alternative separately. Introduction of numerical modelling will likely result in excessive run-time. Therefore, it is recommended to explore other possible methods that can be applied (such as empirical equations or factors) to better incorporate these additional processes, while keeping the run-time increase as small as possible.

As mentioned in Section 7.3.2, refraction due to the change in depth at the channel location is not taken into account. Channel refraction can have a significant influence on the wave conditions. Due to the deepening of the channel, the wave directions will adjust. This adjustment will result in the wave direction being closer to the direction of the main channel axis (Van Rijn, 2013). For certain angles of wave incidence (depending on the channel depth and the wave period), this can result in the channel "trapping" the waves. This can lead to increased wave penetration and a possible increase in wave height due to converging wave rays on the channel slopes, which is called wave tunnelling (Dusseljee et al., 2014; Riezenbosch, 2013). As downtime at the berths is fairly sensitive to small wave height increases (an increase in the range of decimeters can make a significant difference), channel refraction is not negligible in the initial stages of design and can lead to inaccuracy in the estimated downtime. The size of the inaccuracy will depend on the breakwater layout alternative, as both the location of the breakwaters, the depth of the channel with respect to the seabed and the angle and position of the channel are of influence.

Therefore, expert judgement is required to assess the expected influence of wave refraction and shoaling due to the navigation channel for the produced layout.
To incorporate channel refraction into the updated model, a method has to be used that is able to include the navigation channel in the modelling of the wave transformation for each layout alternative separately. A possibility is to model the wave transformation for each layout alternative individually. Modelling the wave transformation for each layout alternative is expected to increase the run-time. Therefore, it is recommended to conduct further research on which possible methods could be used to include channel refraction and if these methods fit the current model concept with regard to run-time.

7.4.3. Sedimentation processes

Longshore sediment transport

Longshore sediment transport processes have been included, to predict the accretion length in shore-normal direction at both breakwaters. Therefore, the morphological response updrift and downdrift of the structure have been taken into account. The downdrift morphological response is complex, because both accretion due to secondary currents and erosion have to be taken into account. A schematized method has been used to make an estimation of the morphological behaviour downdrift of the structure without the use of a numerical model. A test case has been performed in Section 4.3, to assess the results presented by the schematized method. The calculated net longshore sediment transport and accretion length showed only a minor deviation (4 - 4.5%) from the net longshore sediment transport and the accretion length given in the test case, which shows promise. To establish this schematized method, several assumptions have been made. These assumptions have been described in Section 3.3.
Due to these assumptions, several uncertainties arise:

1. For the calculation of the accretion at the downdrift side of the port, it is assumed that the primary breakwater tip has the same x-coordinate as the starting point of the secondary breakwater. The distance between the length of the breakwater and the secondary breakwater is assumed to be two times the channel width (shown in Figure 3.7b). These assumptions are not necessarily the case for the generated breakwater layouts. As shown in Figure 3.7a, the position of the tip of the primary breakwater with respect to the secondary breakwater influences the size of the diffraction zone. The nearshore circular current partly depends on the size of the diffraction zone. As a result, the accretion length along the breakwater in shore-normal direction is also dependent on the size of the diffraction zone. A larger difference between the actual layout and the assumptions will result in a larger uncertainty in the predicted accretion length along the breakwater in shore-normal direction.
2. In the schematized method (based on Van Rijn (Van Rijn, 2015)) used for the calculation of the downdrift accretion, the nearshore circular current velocity is assumed to have the shape of a circle. Research on these circular patterns (Rietberg, 2017) has shown that this circular current can also take the form of an ellipse, depending on the incoming wave angle. Moreover, the possible influence of coastline changes on the nearshore circular current is not taken into account. As a result, uncertainty in the longshore velocity component in the longshore direction is introduced. This uncertainty can lead to differences in sediment transport rates compared to reality.
3. The calculation of the downdrift accretion is based on the assumption that the point where coastline change is zero will not change in its horizontal position. In reality, it is not unlikely that this point will change position, which can lead to larger accretion lengths along the breakwater in shore-normal direction (when the point moves toward the structure) or smaller accretion lengths along the breakwater in shore-normal direction (when the point moves away from the structure).
4. In the calculation of the accretion length, it is assumed that the accretion assumes the shape of a triangle. In reality, the shape of the accretion area is never a perfect triangle. This introduces an uncertainty in the accretion length along the breakwater in shore-normal direction.

The assumption of a standard breakwater layout (1) causes a limitation in the applicability of the longshore sediment transport feature. If the optimal breakwater configuration deviates significantly from the assumed breakwater layout, the calculated minimum secondary breakwater length becomes less reli-

able (resulting in either an underestimation or an overestimation of the minimum required breakwater length, depending on the location of the diffraction point with respect to the secondary breakwater). If this occurs, it is recommended to perform additional runs without using the minimum required primary and secondary breakwater length (generated by the longshore sediment transport module) as input for the generation of the layouts.

To increase reliability and applicability, it is recommended to further study the development of accretion at the downdrift side of structures. If a method can be developed that can be used for all breakwater layout alternatives, the use of such a method will remove the current limitation. Another option is to further develop the model in such a way that the minimum secondary breakwater can be determined for each layout alternative individually during the model loop. This will remove the limitation and increase the overall reliability of the method, but will increase the computation time.

The assumptions that have been made with regard to the morphological response (2, 3 and 4) lead to uncertainties in the estimated accretion length along the secondary breakwater in shore-normal direction. As a result, it can occur that an overestimation or an underestimation of the secondary breakwater length is made. In case of a overestimation, the length of the secondary breakwater is unnecessarily long, which results in unnecessary breakwater construction and maintenance costs. In the case of an underestimation, sediment bypassing will occur which results in increased maintenance dredging costs.

To quantify the uncertainties that arise, it is recommended to conduct further research on both the diffraction effects and the morphological response downdrift of structures. By assessing the diffraction effects and the resulting currents included in the updated model, the uncertainties with regard to the circular current velocities can be quantified.

By assessing the morphological response downdrift of structures with the use of numerical models (such as Unibest-LT or Delft3D), the uncertainty of the schematized method for estimating the accretion length in shore-normal direction along the secondary breakwater can be quantified. Based on further research, required additions can be added or changes can be made to the method if necessary.

It should be noted that tidal currents have not been accounted for in the calculation of longshore sediment transport. These currents can lead to additional longshore sediment transport rates. As a result, larger uncertainty in the longshore sediment transport rates can occur at locations where it is observed that longshore tidal current velocities are present. Therefore, it is recommended that possible effects of these current flows on the estimated morphological response of the shore are further studied and integrated into the model if possible. This addition will further increase the accuracy of the updated model.

Channel sedimentation

The calculation of channel sedimentation volumes has been incorporated to increase the accuracy with which the channel sedimentation volumes are determined. To assess if the method that has been used produces accurate results, an assessment has been performed for the Anaklia Deep Sea Port in Chapter 5. The calculated channel sedimentation volume per year was within the estimated range provided by the project reports. This result implies that the method used for the calculation of channel sedimentation provides a reliable estimate of the channel sedimentation volume.

Although the results are promising, it is not possible to make a definite statement about the reliability and accuracy of the method based on a single test case. It is recommended to assess the method using multiple cases with varying conditions (such as high tidal current velocities or a combination of both tidal and residual current velocities). By testing the method with multiple cases with varying conditions, possible weak points or inaccuracies can be determined. Thereafter, it is possible to further develop the method to remove possible weaknesses and inaccuracies.

Harbour basin

As mentioned in Chapter 3, the incorporation of harbour basin siltation in the updated model is similar to the incorporation of harbour siltation in the updated model. In Section 2.4.3, a different method has

been explored that is used to estimate harbour basin siltation rates. However, this method requires empirical coefficients that have to be determined based on the port design and basin sedimentation observed for similar port designs. Due to these empirical coefficients being very case-specific, this method proved to be insufficient for application in the updated model. The method that is currently used (a yearly siltation rate multiplied with the basin area) provides a rough estimation and requires input in the form of a siltation rate value provided by the user. Such a rough indication is seen as sufficient for the conceptual design phase that the updated model is meant for, as the influence of harbour basin siltation on the conceptual breakwater design often insignificant.

7.5. Model performance

The implementation of the bathymetry profile, the integration of REFRAC and the implementation of sedimentation processes have influence on the performance of the model. The updated model performance is judged on its convergence, its consistency and its run-time.

The convergence of the updated model is similar to that of the original model. As described in Chapter 4, convergence generally occurs between 100 and 150 generations. It does occur that the updated model converges before 100 generations or after 150 generations. When convergence before 100 generations occurs, the model results are more likely to correspond to a local optimum. For convergence after 150 generations, the generated layout is often the optimum layout.

The consistency of the updated model is partially dependent on the input, similar to the original model. As observed in Chapter 4, the updated model produces consistent results. The updated model produces the same optimum layouts. The optimal layout is generated for 2 out of 3 runs on average. Therefore, multiple runs have to be executed to determine the optimal layout. The updated model seems to become less consistent when the input wave climate becomes larger and more complex. This has been observed in the Anaklia case, where the optimal layout has been produced by 2 out of 4 runs on average. The other runs showed that the model got stuck in local optima. This implies a reduction in consistency, which is in line with the observations of the original model, where a decrease in consistency was also observed with more complex wave conditions.
Although the optimum layout is still found by performing multiple runs, increased consistency is preferred. A higher consistency will not only lead to a more efficient model, but also to a model with more confident results. To increase the consistency of the model, more research has to be conducted with regard to model tuning. If the ideal set of optimisation parameters can be found, model consistency can be enlarged. If the model can become consistent enough to not require multiple runs, it will increase the efficiency of the model.

The run-time of the updated model is significantly larger than the run-time of the original model (2.5 - 4 hours). This increase in run-time is mainly due to the calculations that are made to determine the capital breakwater volume, the capital dredging volume and the channel siltation volume. The run-time of the updated model is still within acceptable range, as a conceptual design of a port layout by a port engineer usually takes several days. Therefore, a run time of 2.5 - 4 hours is still seen as acceptable. Moreover, the updated model is run in the background, which allows the user to perform other tasks during model runs.
Although the run-time is within acceptable range, it can likely be improved. With the right Python expertise and more efficient programming, a significant reduction of the run-time should be able to be achieved.
Further research on the optimal set of optimisation parameters will also lead to a decrease in run-time. The possibility is presented to the user to determine the direction in which the breakwater layout will be constructed. Due to this feature, it is highly likely that the population size (the number of layouts that are initially created) can be decreased and still lead to consistent results if the correct optimisation parameters are used. With a smaller population size, a smaller number of layout alternatives have to be assessed. As a result, the run-time will decrease.

8

Conclusions and recommendations

In this chapter, the main findings of this research are summarized. The main research question "*How can the original model be improved to increase the applicability of the model and produce results that are sufficient for conceptual design?*" is answered based on these findings. In addition, it has become apparent that there are still several aspects that have to be improved or added before the model can be used as a valuable support tool for the conceptual design of breakwater layouts. Therefore, recommendations for model improvement and further research are given in the second section of this chapter.

8.1. Conclusions

The main objective of this research was to improve the overall applicability of the original model. Possible subjects of improvement have been reviewed, from which three subjects were selected for implementation. These subjects (the incorporation of bathymetry, a modification of the modelling of wave transformation and the implementation of sedimentation processes) were selected as they were expected to improve the applicability of the model. The selected subjects have been implemented in the model, to further develop the model to produce accurate results for a wide range of locations.

The incorporation of bathymetry has been accomplished with the addition of a grid. The grid area of this grid is rectangular and consists of rectangular grid cells.
It has been observed that this method provides quick and accurate determination of the depth values for the desired locations. In addition, the grid in its current form has the advantage that it can also be used in a wave model such as REFRAC, without any modification. It can be concluded that the addition of the grid in its current form is a reliable and efficient method for the inclusion of bathymetry.

For modelling of the transformation of waves travelling from deep water conditions towards the shoreline, it has been recognized that shoaling and refraction are essential processes that have to be accounted for (to a depth where wave breaking and bottom friction/dissipation does not become dominant). Both of these wave processes are partially depth-dependent. For complex bathymetry profiles, the method used to model wave transformation in the original model will not lead to an accurate representation of the local wave conditions. Therefore, it was concluded that a different method for the modelling of wave transformations had to be used.
For the modelling of the wave transformations from deep water conditions towards the shore, three different wave models have been reviewed (SWAN-One, APEX Wave Ray and REFRAC). Out of these three options, the REFRAC model was recognized as the wave model that is most suited for integration in the updated model. The REFRAC model accounts for both shoaling and refraction. REFRAC has the ability to model refraction and shoaling relatively quick (a matter of minutes) for both homogeneous and complex bathymetry profiles. Based on the results of the assessments and the case study (performed in Chapter 4 and Chapter 5), it is observed that the updated model and the original model produce similar results for a homogeneous bathymetry profile and that the updated model produces more accurate results for a complex bathymetry profile (as observed in the Anaklia Deep Sea Port case

study, presented in Chapter 5). Therefore, it is concluded that the integration of REFRAC is a valuable addition that leads to more accurate local wave parameters.

Limitations and uncertainties do arise with the use of REFRAC. The model accounts for shoaling and refraction, but does not account for the influence of wind, currents and bottom friction on wave transformation and does not incorporate wave breaking. This does not pose a problem for its use in the updated model, as the local wave parameters of interest are situated where shoaling and refraction are assumed to be dominant. This limitation should be kept in mind regarding future development of the model. In addition, REFRAC can not account for directional spreading. As a result, it will produce the most reliable results for incoming waves with little to no directional spreading.
Moreover, the REFRAC model is used to model the wave transformation before the model loop. Therefore, channel refraction is not taken into account, which can have an impact on the local wave conditions. The influence on the local wave conditions can have a significant impact on the estimated downtime (see Section 7.4.2). The influence of channel refraction in the conceptual design stage is not negligible and has to be kept in mind when reviewing the produced optimal layout.

For the approximation of the wave conditions within the harbour basin, diffraction effects are taken into account. The diffraction effects inside the harbour basin are accounted for using the Goda diagrams. This method provides a fast determination of the diffraction coefficients at a desired location in the harbour basin. As a result, the diffraction effects in the harbour basin can be accounted for in the model without extensive computation time. Therefore, this method is sufficient for the current framework of the model and its application to the conceptual design stage.
With the use of this method, the influence of wind, shoaling, refraction and reflection inside the harbour basin are not accounted for. The influence of these processes (mainly the influence of reflection) on the wave conditions can be significant, reducing the reliability of the estimated downtime by the updated model. Therefore, expert judgement is required to estimate the impact of these additional processes on the downtime for a produced layout alternative.

The implementation of sedimentation processes has resulted in the incorporation of longshore sediment transport and a modification in the calculation of the channel sedimentation volumes.
The longshore sediment transport rates are used to determine the accretion length along the breakwater in shore-normal direction. This length is calculated for the primary breakwater and the secondary breakwater. The calculation of the updrift accretion is performed using the Pelnard-Considère equation. The calculation of the downdrift accretion is performed using a schematized method. This method allows for the model to account for nearshore circular currents that occur in the diffraction zone. This method has been assessed using a test case. The net longshore sediment transport and the accretion length determined by this method only showed a minor deviation (4 - 4.5 %) from the net longshore sediment transport and the accretion length provided in the test case results (presented in Chapter 4). It is concluded that the method does show promise based on these observed results. Although the overall reliability can not be confirmed (due to the assumptions with regard to the morphological processes, the assumption of a standardized breakwater configuration and the lack of validation for multiple cases), the method does appear suitable for the conceptual design stage.
Limitations arise due to necessary assumptions made regarding the breakwater layout. Differences between a produced optimal breakwater layout and the assumed standard breakwater layout will result in uncertainties in the calculated accretion lengths for the generated layout. When this module is used, the produced layout should be reviewed with expert judgement to assess if the produced layout deviates significantly from the assumed standard layout. If this is the case, it should be reviewed how this uncertainty affects the optimal layout and if the calculated accretion lengths are within realistic range. This can be done with the use of numerical models like Unibest and Delft3D.

The calculation of the channel sedimentation volume has been modified. Due to the modification, this volume is calculated using the Soulsby-Van Rijn equation. The use of this equation results in a more accurate estimation of the channel sedimentation volume that the method used in the original model. From the results obtained in the case study of Anaklia (see Chapter 5), it is observed that the calculated sedimentation volumes are within the estimated range provided by the project reports. Therefore, the method shows promise that it produces an accurate estimation of the channel sedimentation volume.

To make a definite statement about the accuracy and reliability of the method, the method will have to be assessed with multiple cases such that the effect of varying environmental conditions can be evaluated.

The determination of harbour basin siltation is performed by multiplying a user-defined yearly siltation rate with the harbour basin areas. This method gives a rough estimation of the yearly sedimentation volume. This estimation is considered to be sufficient, as the updated model is meant as a support tool in the first stage of design and the impact of harbour siltation in this stage of design is considered insignificant.

The results produced by the updated model have been assessed by comparing them with results produced by the original model and with conceptual designs of a port that is currently in development. This has been done by running test cases (presented in Chapter 4) and by performing a case study (presented in Chapter 5). From the results, it is observed that the updated model produces similar layouts as the original model for a homogeneous bathymetry profile. For a complex bathymetry, it is observed that the updated model produces layouts that coincide better with the conceptual designs than the layouts produced by the original model. Therefore, it can be concluded that the bathymetry grid and the wave modelling by REFRAC have been implemented correctly and are valuable additions to the model.

During the case study, the following points of improvement emerged:

- The inclusion of nautical safety constraints
- The inclusion of better cost estimation and possible CAPEX limits
- The possibility to account for various types of cargo vessels
- The inclusion of berthing spaces on other locations than the main quay

These points of improvement have been derived based on the differences between the produced layout and the actual conceptual designs.

The run-time of the updated model is significantly larger than that of the original model (1.5 to 2 times larger), but is still considered acceptable. The increase in run-time is mainly due to the modifications to the calculation of the breakwater volume, the capital dredging volume and the channel sedimentation volume. It is observed that the updated model produces results with a convergence and consistency that is similar to that of the original model.

In conclusion, the updated model has a larger applicability than the original model. The updated model in its current state can serve as a support tool for breakwater design in the conceptual design phase for port development projects that are to have:

- A large single quay parallel to the coastline
- Container cargo and container vessels as their main focus.
- No CAPEX cap or other budget restrictions.
- No area restrictions with regard to navigation, wet infrastructure construction or breakwater construction.
- Incoming waves that can be modelled as monochromatic waves, with no directional spreading.
- No significant influence of currents, wind or bottom friction on the wave transformation.

When using the updated model, expert judgement is required to critically assess the produced layout with regard to the wave conditions within the harbour basin. Special attention should be given to the possible impact of (channel) refraction and wave reflection on these wave conditions.

The updated model also provides the option to account for longshore transport, which allows application of the model to locations where the morphological response of the shoreline is expected to be of impact on the breakwater layout design. The use of this feature should be combined with expert judgement, as this method still has uncertainties and limitations (as described in Section 7.4) and requires further validation.

8.2. Recommendations

During this research, several points of improvement have emerged. These points of improvement can help to further increase the applicability or help to increase the accuracy of the model. These recommended points of improvement are listed below and have been divided into recommendations regarding applicability and recommendations regarding further research.

8.2.1. Applicability

The recommendations listed below are points that can be added or improved upon concerning the applicability of the updated model. The order in which the recommendations are presented is according to their importance. The most important recommendations are presented first.

- **Inclusion of client preference and constraints** During the analysis of the Anaklia case, it became apparent that client preference can significantly influence the conceptual design of the port and the breakwater layouts. This preference can be due to factors such as budget constraints, a user-defined stopping length or a allowed percentage of downtime. The latter will be of larger influence for cargo types that require less strict schedules than container vessels. In the current model set up, these kinds of preferences can not be taken into account.

  To increase concurrence of generated optimal layouts with the client's preference, the option to include this preference has to be implemented in the model. An example of such client preference is allowing for more downtime to reduce the costs of breakwater construction.

- **Incorporation of different quay layouts and berthing spaces** The updated model is only applicable to port designs that feature one straight quay at which all the berths are situated. In addition, the orientation of the quay has to be parallel to that of the shoreline. In reality, a port design can have several quays. Moreover, quay orientations are not necessarily parallel to the shoreline. In addition, the berths can be located at the quay but also at the breakwaters. With the current model set up, possible space for berths on the breakwaters can only be created on the first breakwater segment by imposing a minimum segment length for this breakwater segment.

  To make the model applicable to a wider range of port designs, the port layout complexity that the model can account for has to be increased. Therefore, it is recommended to include more complex port layouts and possible berth locations in the model.

- **Incorporation of different types of cargo vessels** The updated model in its current form is focused solely on container vessels. In reality, large ports often handle multiple types of cargo. To allow the model to be applied to ports that (also) handle different cargo types, the model has to be modified. After modification, the model has to be able to account for loading/unloading of different cargo and different cargo vessel types.

  Different cargo and different cargo vessel types can be accounted for by allowing limiting wave heights and parameters connected to berth productivity to be defined for each berth separately. In this manner, berths can be assigned as berthing spaces for specific vessel types.

- **Inclusion of data from available wave studies** For most port design projects, detailed wave studies have been performed with the use of complex wave models. These models are used to determine the nearshore wave climate at the project location as accurately as possible. The local wave parameters determined by these complex wave models are often of a higher level of accuracy than the local wave parameters that have been determined with the REFRAC model.

  To increase the level of accuracy of the local wave parameters that are used for determining the channel sedimentation rate and the downtime, it is recommended to install a module in the model that can transform the output of complex wave models into useable data. This transformation can be performed in a manner that is similar to the transformation of the REFRAC data. The REFRAC data is transformed into useable data in a separate module before the model loop, which has proven to be a sufficient method.

- **Inclusion of nautical safety aspects** It has been observed in the Anaklia Deep Sea Port case study (Chapter 5) that nautical safety can have a significant influence on port design. As a result,

nautical safety also influences the breakwater layout design. By providing the user with the option to incorporate nautical safety aspects (such as the angle of the navigation channel with respect to the quay), the model will produce layout options that have a larger concurrence with the designer's preferences. It is therefore recommended to further study what nautical safety aspects can be of significant influence on port design and to add these nautical safety aspects to the model criteria.

- **Project phasing** Port development is often performed in phases. In the updated model set-up, the phasing of port development projects is only taken into account in the spacing between the breakwaters on the shoreline. This spacing is based on the input parameter: "number of berths in future" (see Appendix A). By performing multiple runs, each with the number of berths that concur to their respective phase, the optimal layout for each phase can be produced. By comparing these layouts, it is possible to approximate the best layout with regard to project phasing. However, this method is far from ideal.

  To include project phasing, it is recommended to investigate the possible methods to include project phasing in a single run. A possibility that can be explored is to take all phases into account in a model run. This indicates that the model should approximate the overall costs corresponding to the layout of the current phase, as well as the total costs that correspond to the layout after possible breakwater expansions that might be needed for future phases. Therefore, it is expected that the inclusion of project phasing will be fairly complex and will result in a longer run-time.

  Another option could be to develop the model in such a way that the optimal layout generated for an earlier phase can be used as starting point for extension of the breakwaters in the next phase. The advantage of such a phase by phase approach is that it allows for incorporation of CAPEX constraints (when this is included in the model) that are often present in the first development phase.

- **Reduction of model run-time** The run-time of the updated model is significantly larger than that of the original model. To increase the efficiency of the updated model, it would be convenient if the model run-time could be decreased. It is expected that a decrease in run-time can be obtainable by more efficient programming. For example, it is expected that the method used for the calculation of the turning basin volume can be programmed more efficiently.

8.2.2. Further research

The recommendations listed below are points that can be added or improved upon concerning the applicability of the updated model. The order in which the recommendations are presented is according to their importance. The recommendations that are most important are presented first.

- **Wave transformation within the harbour basin** In the updated model set-up, diffraction is accounted for concerning wave transformation within the harbour basin. The influence of wind, shoaling, refraction and reflection are not accounted for.

  As the influence of these processes on the estimated downtime can be significant, possible methods to account for these processes in the modelling of the wave conditions within the harbour basin should be explored. The use of numerical models does not fit the framework of the updated model. It is therefore recommended to research if simple equations or factors can be used to incorporate the influence of these processes in the wave transformation.

- **Wave transformation toward the shore** For the modelling of the wave transformation from deep water conditions towards the shoreline, the REFRAC model is used. As mentioned in Chapter 7, the accuracy of the wave heights produced by REFRAC has not yet been quantified and only indications have been given.

  Therefore, it is recommended to assess the accuracy of the REFRAC model. Such an assessment can be done by comparing the results generated by REFRAC and a complex wave model (such as SWAN) for multiple cases. The results should allow for a definite statement on the accuracy of REFRAC.

  Moreover, the modelling of the wave transformation is performed before the model loop. As a result, refraction due to the navigation channel is not taken into account. The influence of

channel refraction on the wave conditions can have a significant impact on the wave conditions at the berth and thus on the estimated downtime.

Therefore, a recommended step in further development of the model is to explore possible methods to model wave transformation with incorporation of the navigation channel. An option is to include the functions that are used in REFRAC in the Python code, allowing for modelling of wave transformation for each layout alternative separately. During the selection of a suitable method, it has to be kept in mind that the run-time should still fit the model concept.

- **Downtime determination** The downtime that corresponds to a layout alternative is of significant influence on the fitness score of that layout. The determination of the downtime currently incorporates navigational and operational downtime at the berth. The assumption is made that operational downtime at the berth always occurs when navigational downtime occurs, which is not always true. As a result, the accuracy of the estimated downtime costs is influenced and thereby also the accuracy of the fitness score of the layouts.

  To increase the accuracy of the downtime determination, the interaction between navigational and operational downtime should be studied. Port specific parameters like service times and waiting times might prove to provide an indication of the time that the port is operational while navigational downtime occurs. Improvement of the accuracy of the determined downtime will improve the accuracy of the model.

- **Tuning of the optimisation parameters** For the optimisation, the updated model uses the same optimisation parameters as the original model (see Section 2.1). These optimisation parameters are the population size, the mutation size and the mutation rate. These optimisation parameters result in the same convergence and consistency as the original model.

  However, the updated model provides the user with the possibility to determine the direction in which the breakwater is constructed, as well as the possible determination for the need for a secondary breakwater. When these decision variables are assigned a constant value, it is possible to tune the optimisation parameters, to increase the consistency and possibly decrease the run-time of the model (by reducing the initial population).

  Therefore, it is recommended to further study the influence of the number of decision variables on the optimisation parameters in this specific model. In addition, it is recommended to conduct further research on the best set of optimisation parameters when a specific decision variable (such as the layout direction or the need for a secondary breakwater) is assigned a constant value. By further study and tuning of these parameters, the model performance is expected to be significantly improved.

- **Downdrift accretion and secondary effects** To create a schematized method for the inclusion of downdrift accretion, multiple assumptions have been made. These assumptions result in uncertainties in the accretion lengths in shore-normal direction along the breakwaters.

  To increase the accuracy of the calculated accretion lengths, it is recommended to further study downdrift accretion and analyse the processes that are of importance. In addition, it is recommended to assess the current schematized method. For example, such an assessment can be done by comparing the results produced by the schematized method with results produced by the UNIBEST model or the Delft3D model. By performing such an assessment, the accuracy of the method can be quantified and the weak and strong points of the schematized method can be recognized. As a result, the method can be modified to produce more accurate and reliable results.

  In addition, it is recommended to explore possible methods to determine the required minimum secondary breakwater for each layout alternative individually. To accomplish this, modifications will have to be made to the generator module of the updated model. It is likely that such modifications will also affect other modules or functions. Therefore, the model has to be studied before such modifications can be made.

  Inclusion of longshore tidal current effects on the longshore sediment transport rate will increase the accuracy of the longshore sediment transport rates that are calculated. As a result, the accuracy of the estimation of updrift and downdrift accretion will increase. Therefore, further study on how to include these longshore tidal currents is recommended.

- **Channel sedimentation** The calculation of the yearly channel sedimentation volume is done using the Soulsby-Van Rijn equation. This method has been assessed in the Anaklia case study and shows promising results.

  However, it is not possible to give a definite statement about its accuracy based on a single case. Therefore, it is recommended to perform multiple case studies of cases with different environmental conditions. Based on the results of these case studies, inaccuracies can be recognized and a definite statement about the accuracy of the method can be made.

Bibliography

AACE International (2019). *COST ESTIMATE CLASSIFICATION SYSTEM – AS APPLIED IN ENGINEERING, PROCUREMENT, AND CONSTRUCTION FOR THE PROCESS INDUSTRIES TCM Framework: 7.3 – Cost Estimating and Budgeting*. Tech. rep. AACE International.

Anaklia Development Consortium (2020). *The Anaklia Port Project*. `http://anakliadevelopment.com/info/`, Last accessed on 2020-5-19.

Arcadis Nederland B.V. (2018a). *Anaklia Deep Sea Port: Appendix A - Requirement register*. Arcadis Nederland B.V.

Arcadis Nederland B.V. (2018b). *Anaklia Deep Sea Port: Assessment and re-evaluation of the marine layout*. Arcadis Nederland B.V.

Arcadis Nederland B.V. (2018c). *Anaklia Deep Sea Port: Contract 2000 - Dredging/Breakwater*. Arcadis Nederland B.V.

Arcadis Nederland B.V. (2018d). *Anaklia Deep Sea Port: Sedimentation study*. Arcadis Nederland B.V.

Arcadis Nederland B.V. (2018e). *Anaklia Deep Sea Port: Wave Penetration Study*. Arcadis Nederland B.V.

Arcadis Nederland B.V. (2018f). *Anaklia Deep Sea Port: Wind and Wave Study*. Arcadis Nederland B.V.

Bayram, Atilla, Magnus Larson, and Hans Hanson (2007). “A new formula for the total longshore sediment transport rate”. In: *Coastal Engineering 54*, pp. 700–710.

Bosboom, Judith and Marcel J.F. Stive (2015). *Coastal Dynamics 1*. DAP (Delft Academic Press).

Bouws, Evert and Jurjen A. Battjes (1982). “A Monte Carlo Approach to the Computation of Refraction of Water Waves”. In: *Journal of Geophysical Research* 87(C8), pp. 5718–5722.

Cerdeiro, Diego A. et al. (May 2020). “World Seaborne Trade in Real Time: A Proof of Concept for Building AIS-based Nowcasts from Scratch”. IMF Working Paper.

Deb, Kalyanmoy et al. (Apr. 2002). “A Fast and Elitist Multiobjective Genetic Algorithm: NSGA-II”. In: *IEEE Transactions on Evolutionary Computation* 6(2), pp. 182–197.

Deltares (2020). *PHAROS: Technical Specifications*. `https://www.deltares.nl/en/software/pharos/#technical-specifications`, Last accessed on 2020-6-12.

Dusseljee, D.W. et al. (June 2014). “Impact of harbor navigation channels on waves: A numerical modelling guideline”. In: *Proceedings of the 34th international conference on coastal engineering*. Coastal Engineering Research Council.

Eysink, W.D. (1989). “Sedimentation in harbour basins. Small density differences may cause serious effects”. In: *Proceedings of the 9th International Harbour Congress*.

GEBCO (2020). *The General Bathymetric Chart of the Oceans*. `https://www.gebco.net/`, Last accessed on 2020-5-19.

Goda, Yoshimi, Tomotsuka Takayama, and Yasumasa Suzuki (1978). “Diffraction diagrams for directional random waves”. In: *Coastal Engineering Proceedings, 16*, pp. 628–650.

Helm-Petersen, Jacob (1998). “Estimation of Wave Disturbance in Harbours”. PhD thesis. Denmark.

Holthuisen, Leo H. (2007). *Waves in Oceanic and Coastal Waters*. Cambrige University Press.

Kamphuis, J. W. (2000). *Introduction To Coastal Engineering And Management*. World Scientific Publishing Co Pte Ltd.

Ligteringen, H. and H. Velsink (2012). *Ports and Terminals*. Delft Academic Press.

Liu, Jingyi (2009). “Swell propagation in a natural coastal channel in the SWAN model”. MSc. Thesis. TU Delft.

Mangor, Karsten et al. (2017). *Shoreline Management Guidelines*. DHI.

Mil-Homens, Joao (2016). “Longshore Sediment Transport: Bulk Formulas and Process Based Models”. PhD thesis. Delft University of Technology.

Pelnard-Considère, R. (1956). “Essai de théorie de l’évolution des formes de rivage en plages de sable et de galets”. In: *4th Journees de l’Hydaulique, Les Energies de la Mer, Question III* 3(1).

PIANC (1995). *Criteria for movements of moored ships in harbours: A practical guide: Report of Working Group no.24,of the Permanent Technical Committee II*.

PIANC (2008). *Minimising Harbour Siltation*.

PIANC (2014). *Harbour Approach Channels Design Guidelines*.

PIANC (2016). *Criteria for the selection of breakwater types and their related optimum safety levels*.

REFRAC Team, the (1994). *REFRAC User Manual*. English. Version Version 20.02. Delft University of Technology. 11 pp. 1994.

Rietberg, D.C. (2017). “Wave dynamics behind a shore-normal breakwater: towards better understanding and modelling of coastal impacts at sandy coasts”. TU Delft.

Riezenbosch, Hendrik Jan (Dec. 2013). “Greenfield Deep-Sea Port Design: An investigation of chal lenges and opportunities”. MA thesis. Delft University of Technology.

Rijksinstituut voor Kust en Zee (2004). *Golfbelasting in havens en afgeschermde gebieden : een gedetailleerde methode voor het bepalen van golfbelastingen voor het toetsen van waterkeringen*. Tech. rep. Rijksinstituut voor Kust en Zee.

ROM 3.1-99 (2007). *Recommendations for the Design of the Maritime Configuration of Ports, Approach Channels and Harbour Basins, Spain*. Chap. Part VIII.

Rustell, Michael (2016). “Knowledge Extraction and the Development of a Decision Support System for the Conceptual Design of Liquefied Natural Gas Terminals under Risk and Uncertainty”. PhD thesis. University of Sully.

Soulsby, Richard (1997). *Dynamics of Marine Sands*. Thomas Telford Publications.

SWAN (2020). *USER MANUAL SWAN Cycle III version 41.31A*. `http://swanmodel.sourceforge.net/`, Last accessed on 2020-6-12.

TU Delft (2018). *SwanOne User Manual*. English. Version 1.3. Delft University of Technology. 18 pp. 2018.

Van Rijn, L.C. (2013a). *Basics of Channel Deposition/Siltation*. https://www.leovanrijn-sediment.com/papers/Channelsedimentation2013.pdf, Last accessed on 2020-5-19.

Van Rijn, L.C. (2013b). *Design of hard coastal structures against erosion*. Tech. rep.

Van Rijn, L.C. (2014). "Simple general expression for longshore transport of sand, gravel and shingle". In: *Coastal Engineering Vol. 90*, pp. 23–39.

Van Rijn, L.C. (2015). *Coastal erosion in lee zone of structure; DIFSAND-model and LONGMOR-model*. https://www.leovanrijn-sediment.com/papers/Erosionleezonestructure2015.pdf, Last accessed on 2020-5-19.

Van Rijn, L.C. (2020). *Engineering tools and databases on Sediment Transport and Morphology*. https://www.leovanrijn-sediment.com/page4.html, Last accessed on 2020-6-12.

Woerlee, Sebastiaan (2019). "Breakwater layout optimisation using a parametric model: Development of a decision-making tool for the conceptual design of breakwaters". MSc. Thesis. TU Delft.

You, Zai-Jin (2008). "A close approximation of wave dispersion relation for direct calculation of wavelength in any coastal water depth". In: *Applied Ocean Research* 30(2), pp. 113–119.

Zanuttigh, Barbara and Jentsje W. van der Meer (Apr. 2007). *Wave Reflection From Coastal Structures*. Tech. rep. Coastal Engineering 2006.

A

Input parameters original model

A.1. Environmental conditions

Category	Symbol	.py symbol	Unit	Description
Wave parameters	H_{s0}	H_s0	m	Offshore significant wave height
	T_{p0}	T_p0	s	Offshore peak period
	θ_0	\theta0	^{o}	Offshore wave direction
Wind parameters	$u_{w,10}$	u_w	m/s	Wind speed at 10 m above MSL
	θ_w	theta_w	^{o}	Wind direction
Current flow parameters	u_c	u_c	m/s	Current flow velocity
	θ_c	theta_c	^{o}	Current flow direction

Table A.1: The environmental conditions input parameters

A.2. Design parameters

Category	Symbol	.py symbol	Unit	Description
Constraints	x_{max}	x_max	m	outermost point for primary breakwater on x-axis
	y_{max}	y_max	m	outermost point for primary breakwater on y-axis
	L_{max}	l_max	m	outermost distance for secondary breakwater in x-direction
Navigation	H_c	h_ch	m	limiting wave height in sheltered channel
	H_{berth}	h_berth	m	limiting wave height at berth
	$v_{s,min}$	v_smin	m/s	minimum vessel speed
	t_{tug}	t_tug	min	tugging time
	$u_{cw,n}$	u_cwn	m/s	limiting cross-wind speed for navigation
	$u_{lw,n}$	u_lwn	m/s	limiting longitudinal wind speed for navigation
	$u_{w,o}$	u_wo	m/s	limiting wind speed for operations
	$u_{cc,n}$	u_ccn	m/s	limiting cross-current speed for navigation
	$u_{lc,n}$	u_lcn	m/s	limiting longitudinal current speed for navigation
Vessel	L_s	ls	m	length over all of design vessel
	B_s	bs	m	beam of design vessel
	D_s	ds	m	draught of design vessel
	v_s	vs	m/s	entrance speed of a vessel

Costs	C_{core}	c_core	€/m^3	unit price for breakwater core material
	C_{under}	c_under	€/m^3	unit price for breakwater underlayer material
	C_{armour}	c_armour	€/unit	unit price for breakwater armour layer material
	C_{dd}	c_dd	€/m^3	dredging-dumping costs of sediment
	C_{df}	c_df	€/m^3	dredging-filling costs of sediment
	C_{TEU}	c_teu	€/TEU	(un)loading unit rate per twenty-foot equivalent unit
	C_{land}	c_land	€/m	land cost per running meter of coastline stretch
	$\Phi_{bw,m}$	psi_bwm	-	ratio of annual breakwater maintenance costs w.r.t. construction
	r	r	-	discount rate for present-day value
	T_L	t_life	yr	design lifetime of breakwater
Terminal	n_b	n_b	-	number of berths second phase
	n_{bf}	n_bf	-	number of berths in future
	y_f	yf	m	fill-up distance in y-direction
	m_b	mb	-	berth occupancy factor
	P_b	pb	MPH	hourly production per berth
	f_{TEU}	f_teu	-	TEU-factor
Bathymetry	z_0	z0	m	ground level above MSL at y = 0
	$1:\alpha_b$	alpha_b	-	slope of the sea bed
Coast	θ_s	theta_s	°	orientation of offshore-directed normal to coastline w.r.t. North
Environment	s_{max}	smax	-	maximum directional spreading parameter
Water levels	HAT	hat	m	high astronomical tide level above MSL
	LAT	lat	m	low astronomical tide level below MSL
Breakwater	h_l	h_l	m	level of leeward armour layer below MSL
	h_c	h_c	m	core height above HAT
	t_u	t_u	m	thickness of underlayer
	t_a	t_a	m	thickness of armour layer
	B_{crest}	b_crest	m	breakwater crest width
	$1:x_f$	xf	-	front slope of breakwater
	$1:x_r$	xr	-	rear slope of breakwater
	n_v	nv	-	armour layer porosity
	D_n	d_nom	m	nominal diameter of armour units
Sediments	$t_{s,0}$	ts_0	m/year	annual siltation thickness without secondary breakwater
	$t_{s,max}$	ts_max	m/year	annual siltation thickness with breakwater gap >= 1000m
	$t_{s,min}$	ts_min	m/year	annual siltation thickness with breakwater gap equal to channel width
	s_{type}	s_type	-	soil type (1 = mud, 2 = sand/clay, 3 = rock/coral)
Dredging	h_f	hf	m	average fill level of terminal above MSL
	$1:x_b$	xb	-	bank slope of approach channel

Table A.2: The design input parameters

B

Sediment transport assessment

B.1. Sedimentation assessment parameters

Parameter	Value	Unit	Description
θ_{ch}	45	^{o}	Channel angle w.r.t. shore-normal
θ_{res}	90	^{o}	Residual current flow angle w.r.t. shore-normal
θ_{ebb}	0	^{o}	Ebb tidal current flow angle w.r.t. shore-normal
θ_{flood}	0	^{o}	Flood tidal current flow angle w.r.t. shore-normal
u_{ebb}	0.8	m/s	Ebb tidal current flow velocity
u_{flood}	0.8	m/s	Flood tidal current flow velocity
u_{res}	0	m/s	Residual current flow velocity
H_s	0	m	Wave height
T_p	7	s	Peak period
d_{50}	2e-4	m	Median grain size
d_{90}	3e-4	m	90th percentile grain size
v	1.0e-6	m^2/s	Viscosity
z_o	0.006	m	Bed roughness
s	2.58	-	Relative density
β	0	^{o}	Angle of channel slope
h_{in}	10	m	Depth of seabed with respect to MSL
d_{ch}	15	m	Depth of channel with respect to MSL

Table B.1: Default parameter values for the channel siltation assessment

Parameter	Value	Unit	Description
H_{s0}	1.5	m	Significant wave height
T_{p0}	8	s	Peak wave period
θ_0	30	^{o}	Incoming wave angle
ρ_s	2650	kg/m^3	Sediment density
ρ_b	1600	kg/m^3	Bulk sediment density
$tan\beta_b$	0.03	-	Beach zone slope
$tan\beta_s$	0.03	-	Surf zone slope
d_{50}	0.0005	m	median grain size
t	5	yr	time period
d	10	m	profile height

Table B.2: Default parameter values used for the accretion calculation assessment

B.2. Van Rijn test case

Parameter	Value	Unit	Description
ρ_s	2650	kg/m^3	Sediment density
ρ_b	1600	kg/m^3	Bulk sediment density
$tan\beta_b$	0.03	-	Beach zone slope
$tan\beta_s$	0.01	-	Surf zone slope
d_{50}	0.0005	m	median grain size
t	5	yr	time period
d	10	m	profile height

Table B.3: Input parameters for the Van Rijn example case (Van Rijn, 2015)

Significant wave height H_s (m)	Peak wave period T_p (s)	Angle of wave vector to north and to coast normal (°)	Number of days	Significant wave height H_s (m)	Peak wave period T_p (s)	Angle of wave vector to north and to coast normal (°)	Number of days
0.75	8.6	352.5; -7.5	3.3	1.75	10.5	352.5; -7.5	2.5
0.75	9.8	7.5; 7.5	9.7	1.75	12.0	7.5; 7.5	48.1
0.75	11.0	22.5; 22.5	22.2	1.75	12.6	22.5; 22.5	48.5
0.75	9.5	37.5; 37.5	1.7	1.75	5.6	37.5; 37.5	2.3
1.25	9.5	352.5; -7.5	8.8	1.75	5.1	52.5; 52.5	3.0
1.25	10.9	7.5; 7.5	76	1.75	4.9	67.5; 67.5	0.4
1.25	11.8	22.5; 22.5	112.2	2.25	12.9	352.5; -7.5	0.3
1.25	6.5	37.5; 37.5	7.2	2.25	12.8	7.5; 7.5	7.6
1.25	4.6	52.5; 52.5	3.0	2.25	12.9	22.5; 22.5	5.7
1.25	4.3	67.5; 67.5	0.9	2.25	5.8	37.5; 37.5	0.6
				2.25	5.5	52.5; 52.5	0.37
				2.75	12.9	7.5; 7.5	0.51
				2.75	13.7	22.5; 22.5	0.04
Total			245 days				120 days

Figure B.1: Wave conditions used in the Van Rijn example case (Van Rijn, 2015)

C

REFRAC wave modelling

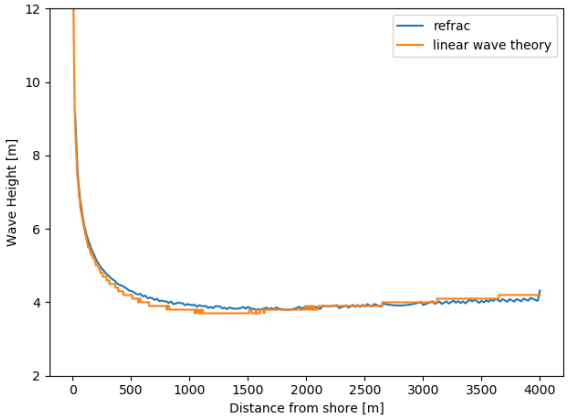

(a) Comparison for incoming wave angle θ = 0^o and incoming wave height of 4 m, between wave development nearshore between REFRAC and linear wave theory (using Chen and Thompson)

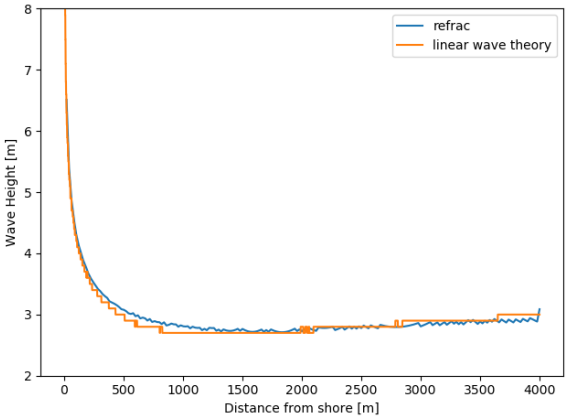

(b) Comparison for incoming wave angle θ = 0^o and incoming wave height of 3 m, between wave development nearshore between REFRAC and linear wave theory (using Chen and Thompson)

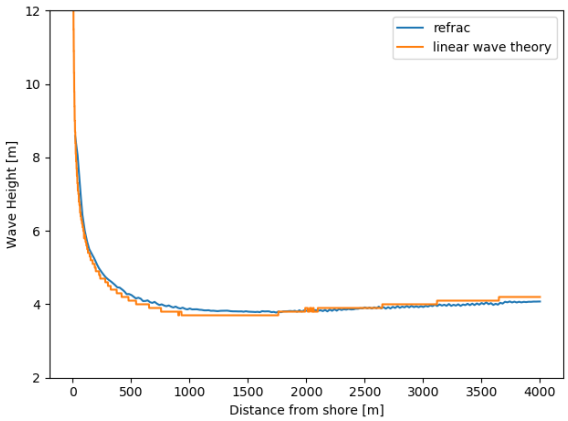

(a) Comparison for incoming wave angle θ = 15^o and incoming wave height of 4 m, between wave development nearshore between REFRAC and linear wave theory (using Chen and Thompson) and AVG = 2 2

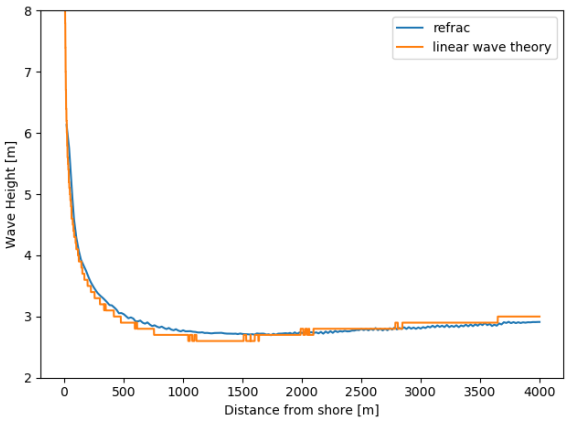

(b) Comparison for incoming wave angle θ = 15^o and incoming wave height of 3 m, between wave development nearshore between REFRAC and linear wave theory (using Chen and Thompson) and AVG = 2 2

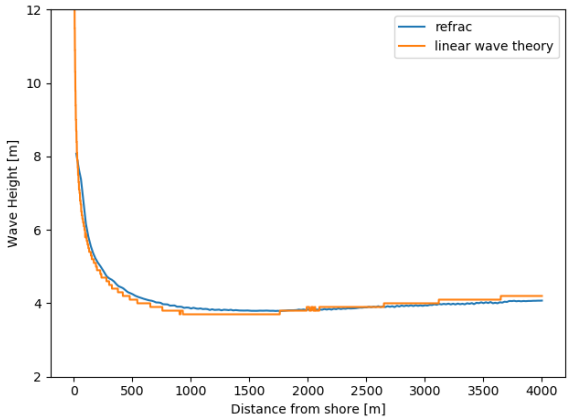

(a) Comparison for incoming wave angle θ = 15^o and incoming wave height of 4 m, between wave development nearshore between REFRAC and linear wave theory (using Chen and Thompson) and AVG = 3 3

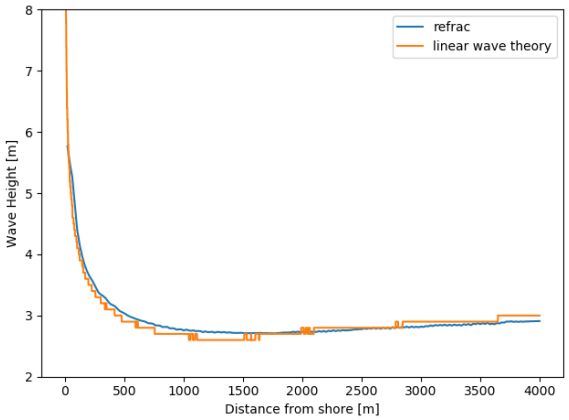

(b) Comparison for incoming wave angle θ = 15^o and incoming wave height of 3 m, between wave development nearshore between REFRAC and linear wave theory (using Chen and Thompson) and AVG = 3 3

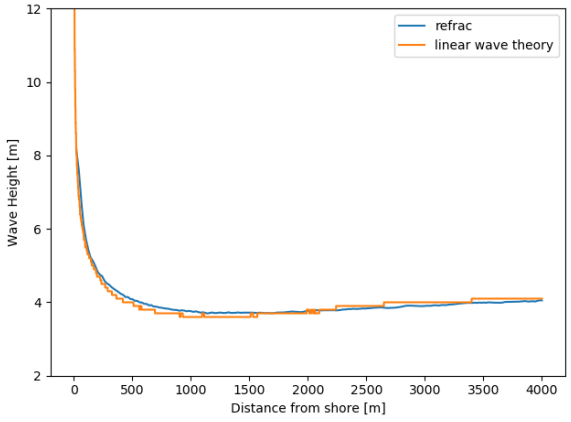

(a) Comparison for incoming wave angle θ = 30^o and incoming wave height of 4 m, between wave development nearshore between REFRAC and linear wave theory (using Chen and Thompson) and AVG = 2 2

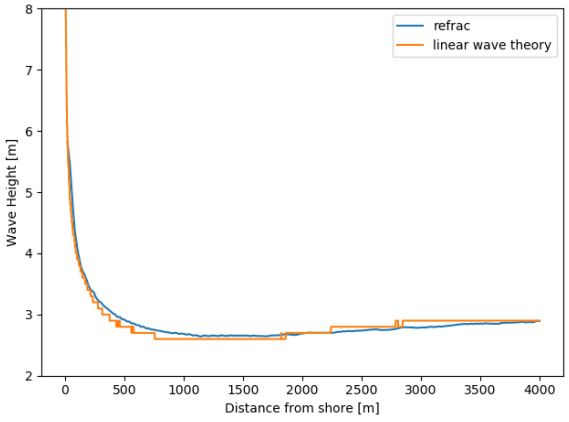

(b) Comparison for incoming wave angle θ = 30^o and incoming wave height of 3 m, between wave development nearshore between REFRAC and linear wave theory (using Chen and Thompson) and AVG = 2 2

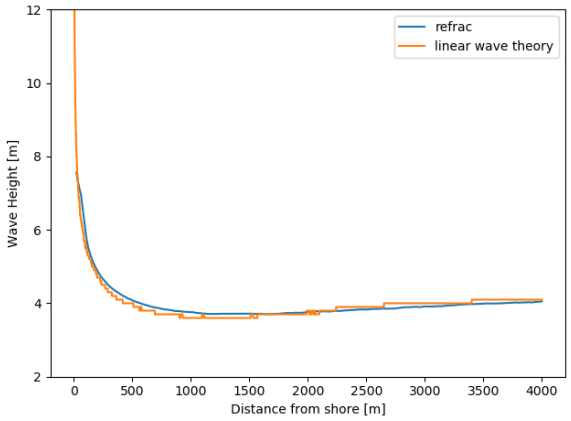

(a) Comparison for incoming wave angle θ = 30^o and incoming wave height of 4 m, between wave development nearshore between REFRAC and linear wave theory (using Chen and Thompson) and AVG = 3 3

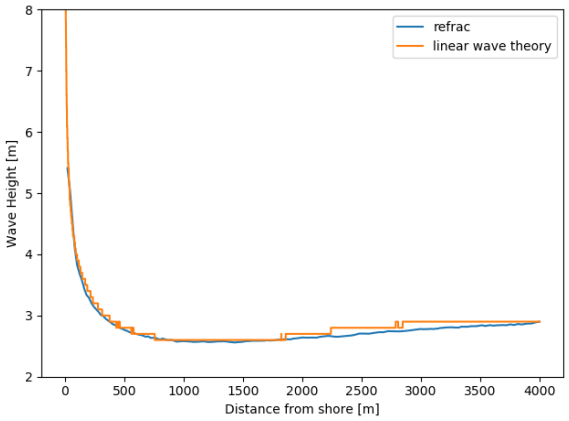

(b) Comparison for incoming wave angle θ = 30^o and incoming wave height of 3 m, between wave development nearshore between REFRAC and linear wave theory (using Chen and Thompson) and AVG = 3 3

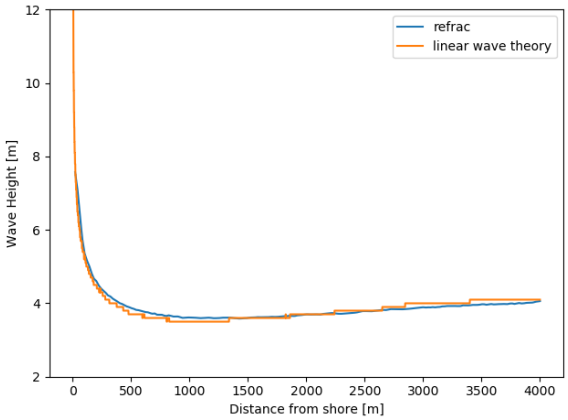

(a) Comparison for incoming wave angle θ = 40^o and incoming wave height of 4 m, between wave development nearshore between REFRAC and linear wave theory (using Chen and Thompson) and AVG = 2 2

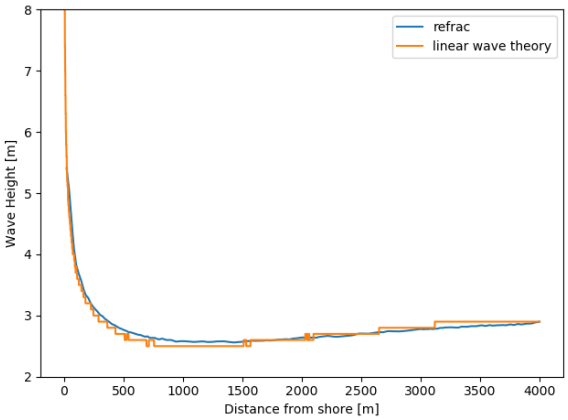

(b) Comparison for incoming wave angle θ = 40^o and incoming wave height of 3 m, between wave development nearshore between REFRAC and linear wave theory (using Chen and Thompson) and AVG = 2 2

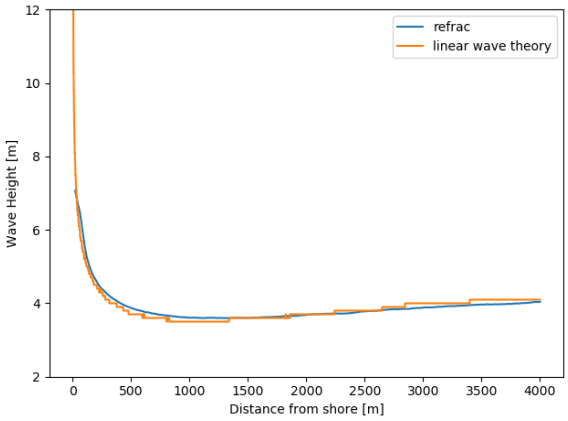

(a) Comparison for incoming wave angle θ = 40^o and incoming wave height of 4 m, between wave development nearshore between REFRAC and linear wave theory (using Chen and Thompson) and AVG = 3 3

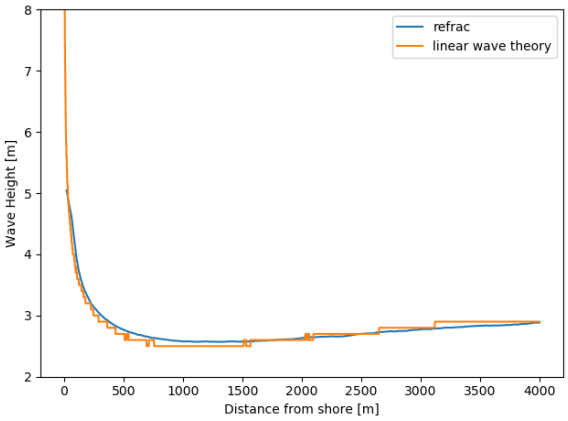

(b) Comparison for incoming wave angle θ = 40^o and incoming wave height of 3 m, between wave development nearshore between REFRAC and linear wave theory (using Chen and Thompson) and AVG = 3 3

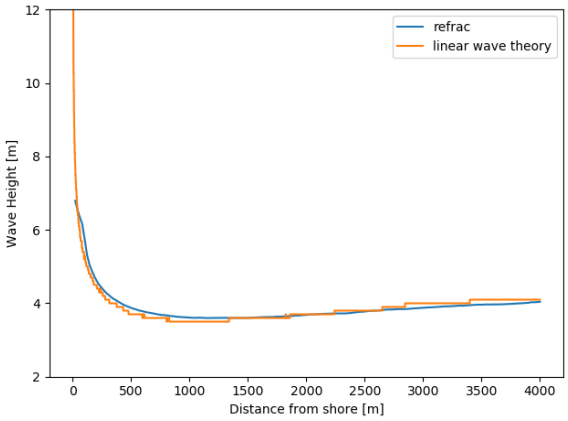

(a) Comparison for incoming wave angle θ = 40^o and incoming wave height of 4 m, between wave development nearshore between REFRAC and linear wave theory (using Chen and Thompson) and AVG = 4 4

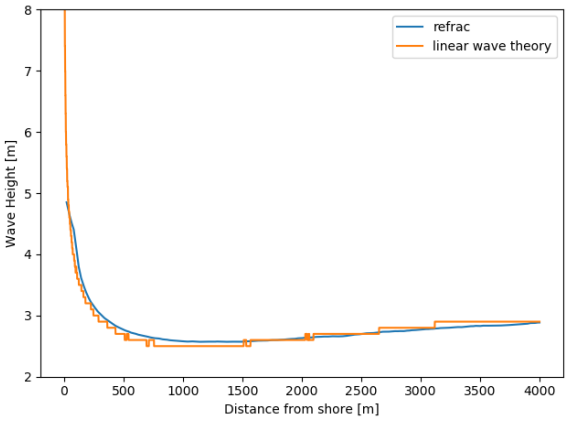

(b) Comparison for incoming wave angle θ = 40^o and incoming wave height of 3 m, between wave development nearshore between REFRAC and linear wave theory (using Chen and Thompson) and AVG = 4 4

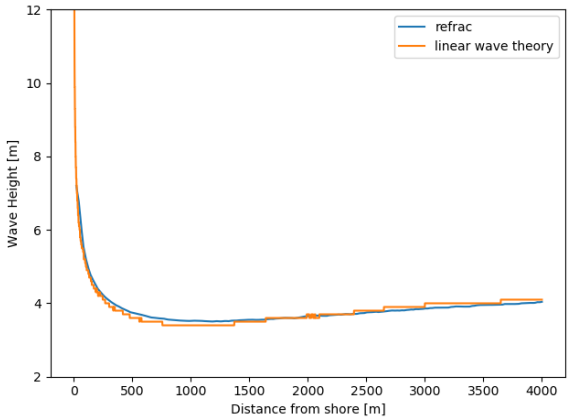

(a) Comparison for incoming wave angle θ = 45^o and incoming wave height of 4 m, between wave development nearshore between REFRAC and linear wave theory (using Chen and Thompson) and AVG = 3 3

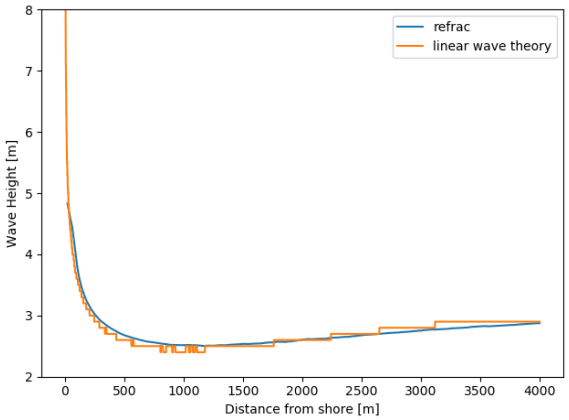

(b) Comparison for incoming wave angle θ = 45^o and incoming wave height of 3 m, between wave development nearshore between REFRAC and linear wave theory (using Chen and Thompson) and AVG = 3 3

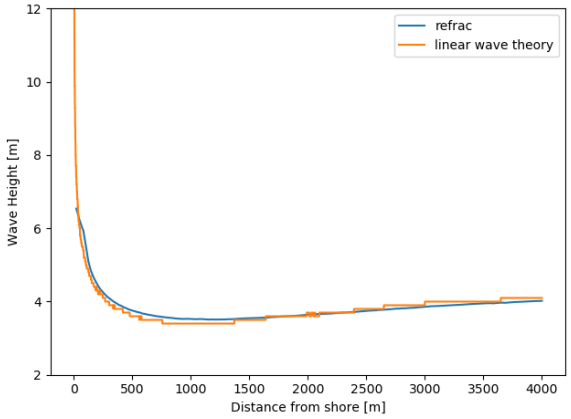

(a) Comparison for incoming wave angle θ = 45^o and incoming wave height of 4 m, between wave development nearshore between REFRAC and linear wave theory (using Chen and Thompson) and AVG = 4 4

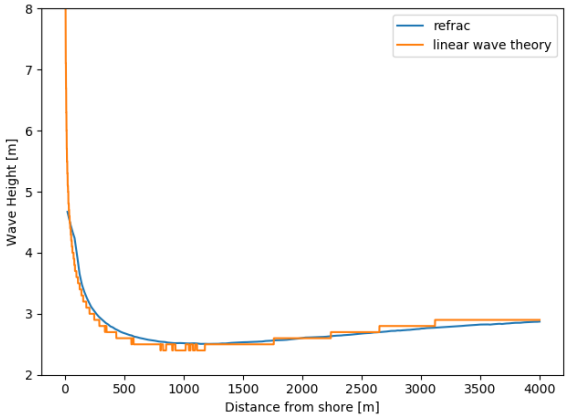

(b) Comparison for incoming wave angle θ = 45^o and incoming wave height of 3 m, between wave development nearshore between REFRAC and linear wave theory (using Chen and Thompson) and AVG = 4 4

Table C.1: REFRAC Model Tuning Results

θ $[^o]$	AVG $[-]$	ΔH_s $[m]$	$Deviation$ [%]
15	2 2	0.209	5.50
15	3 3	0.193	5.10
30	2 2	0.211	5.54
30	3 3	0.222	5.82
40	2 2	0.194	5.55
40	3 3	0.192	5.50
40	4 4	0.196	5.60
45	3 3	0.197	5.62
45	4 4	0.196	5.61

(a) Results of comparison with $H_s = 4\ m$

θ $[^o]$	AVG $[-]$	ΔH_s $[m]$	$Deviation$ [%]
15	2 2	0.162	5.85
15	3 3	0.158	5.74
30	2 2	0.158	5.54
30	3 3	0.167	5.82
40	2 2	0.161	6.04
40	3 3	0.158	5.74
40	4 4	0.160	5.79
45	3 3	0.143	5.63
45	4 4	0.147	5.55

(b) Results of comparison with $H_s = 3\ m$

D

APEX Wave Ray model

The APEX | WAVE RAY model is a one-dimensional wave model that is used to model wave transformation from offshore conditions to a point nearshore. This is done by first defining a input wave field, after which it is possible to model the wave transformation to a user defined point. Both definition of the input wave field as well as wave transformation are executed using operations. The different kind of operations are shown in Figure D.1.

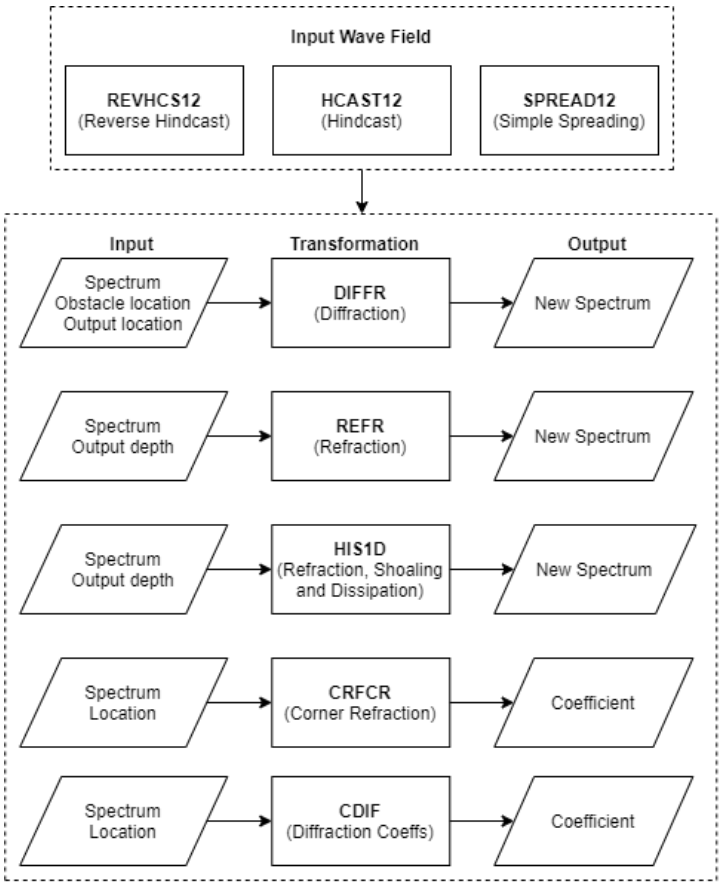

Figure D.1: The main operations of the APEX Wave Ray model

Input Wave Field

First, the input wave field has to be defined. This can be done using one of the following three available operations:

- Reverse Hindcast *(REVHCS12)*
- Hindcast *(HCAST12)*
- Simple Spreading *(SPREAD12)*

Each operation requires specific input. The required input and generated output for each operation is given below. Examples of input files for the operations are given as well.

Reverse Hindcast

When using the Reverse Hindcast operation, the following input is required by the user:

- The integration interval and range for main wave directions (given in degrees w.r.t. shore normal)
- The period factor
- The number of conditions (*nc*), number of wave heights (*nh*), number of wave periods (*nt*), number of wave directions (*nd*)
- input wave heights, input wave periods, input main directions, input spreading index, initial storm durations

The option is available to either give the input in matrix form (referenced to as *MAT*) or as a series (referenced to as *SER*).

When giving input in the matrix format, for each wave height, for each direction, the water level and wind speed have to be defined. Thereafter, the file names for fetches at the data source and the fetches at the output location have to be given, in that specific order (see Figure D.2).

```
REVHCS12
#
# description of source
First test with Smax=10 and gam=1 nfr=100 - no HI  S1D
15-Jun-1994
! Options
!       WIL65 - use growth curves due to Wilson 65 instead of Hurdle and Stive
!               (Good for short fetch lengths in deep water)

# integration interval and range from main wave direction (deg.):
 2.  75.
# period factor
 1.0
# nc,nh,nt,nd
0 15 1 12
# nh input wave heights
    0.10    0.25    0.75    1.25    1.75    2.25    2.75    3.25    3.75
    4.25    4.75    5.25    5.75    6.25    7.25
# nt input wave periods
 3.0  5.0  7.5  10.  12.5  15.0  17.5
# nd input main directions
 -15.  15. 45. 75. 105. 135. 165. 195. 225. 255 285 315
# nd  input spreading index
  12*2.
# nd  init storm dur
  12*12.0
#
```

```
# for each wave height
#     for each direction
#         water level
  12*0.0
  12*0.0
  12*0.0
  12*0.0
  12*0.0
  12*0.0
  12*0.0
  12*0.0
  12*0.0
  12*0.0
  12*0.0
  12*0.0
  12*0.0
  12*0.0
  12*0.0
  12*0.0
  12*0.0
# for each wave height
#     for each direction
#         wind speed
    0.57    0.4    0.57    0.57    0.82    0.57    0.57    0.57    0.57    0.57    0.57    0.57
    1.41    1.01    1.39    1.4    1.96    1.41    1.41    1.41    1.41    1.41    1.41    1.41
       4    3.06    3.92    4.05    5.1       4       4       4       4       4       4       4
    6.31    5.11    6.15    6.49    7.42    6.31    6.31    6.31    6.31    6.31    6.31    6.31
    8.38    7.15    8.15    8.72    9.16    8.38    8.38    8.38    8.38    8.38    8.38    8.38
   10.24    9.16    9.97   10.73   10.57   10.24   10.24   10.24   10.24   10.24   10.24   10.24
   11.92   11.11   11.66   12.51    11.9   11.92   11.92   11.92   11.92   11.92   11.92   11.92
   13.48   12.98   13.28   14.06   13.41   13.48   13.48   13.48   13.48   13.48   13.48   13.48
   14.94   14.78   14.87   15.38   15.26   14.94   14.94   14.94   14.94   14.94   14.94   14.94
   16.33   16.61    16.4   16.59   17.17   16.33   16.33   16.33   16.33   16.33   16.33   16.33
   17.63   18.57   17.85   17.84   18.64   17.63   17.63   17.63   17.63   17.63   17.63   17.63
   18.84   20.78   19.21   19.08   19.17   18.84   18.84   18.84   18.84   18.84   18.84   18.84
   20.01   23.33   20.52   20.19   20.01   20.01   20.01   20.01   20.01   20.01   20.01   20.01
   21.19   26.35   21.79   21.05   21.19   21.19   21.19   21.19   21.19   21.19   21.19   21.19
   23.87   34.18    24.3   21.45   23.87   23.87   23.87   23.87   23.87   23.87   23.87   23.87
# open sea fetch description
# file name for fetches at data source
opensea.ftc
# file name for fetches at output location
local.ftc
```

Figure D.2: Input file for the input wave field using operation REVHCS12 with input given in matrix (MAT) form

When using the series format, the data is given as a series of conditions corresponding to a certain direction. The file name of the file containing the fetches is required thereafter, shown in Figure D.3.

```
REVHCS12
#
# description of source
Reverse hindcast in series format
29 / 3 / 1999
! Options (can define growth curve to be used !)

# integration interval and range from main wave direction (deg.):
 2.  75.
# period factor
 1.0
# nc,nh,nt,nd
12 0 0 0 0
# nh input wave heights
#  DIR    U    dUR  M    Hs_targ      Per   lev
   180.  29.2  5.0  2.0  3.3    12.9  1.0
   180.  33.5  5.0  2.0  3.3    12.9  1.0
   180.  35.0  5.0  2.0  3.3    12.9  1.0
   180.  35.9  5.0  2.0  3.3    12.9  1.0
   240.  32.6  5.0  2.0  3.3    12.9  1.0
   240.  34.6  5.0  2.0  3.3    12.9  1.0
   240.  35.3  5.0  2.0  3.3    12.9  1.0
   240.  35.9  5.0  2.0  3.3    12.9  1.0
   300.0 28.1  5.0  2.0  3.1    12.7  1.0
   300.0 33.3  5.0  2.0  3.1    12.7  1.0
   300.0 34.7  5.0  2.0  3.1    12.7  1.0
   300.0 35.5  5.0  2.0  3.1    12.7  1.0
! name of file with fetches in
example.ftc
```

Figure D.3: Input file for the input wave field using operation REVHCS12 with input given in series (SER) form

Hindcast

When using the Hindcast operation, the input required is comparable to that of the Reverse Hindcast operation. The required input is as follows:

- integration interval and range for main wave directions (given in degrees w.r.t. shore normal)
- period factor
- number of conditions (*nc*), number of wave heights (*nh*), number of wave periods (*nt*), number of wave directions (*nd*)

The option to either use a matrix format or series format is also available. For the matrix format, the following is required (see Figure D.4):

- The water level for each wave height, for each wave direction
- The file name of the file containing fetches at the data source

```
HCAST12
#
# description of source
First test with Smax=10 and gam=1 nfr=100 - no HI  S1D
15-Jun-1994
! Options
! WIL65 - use growth curves due to Wilson 65 instead of Hurdle and Stive
!    (Good for short fetch lengths in deep water)

# integration interval and range from main wave direction (deg.):
 2.  75.
# period factor
 1.0
# nc,nh,nt,nd
0 15 1 12
# nh input wind speeds
    0.5  2.5  5.0 7.5  10.0 12.5 15   17.5
    20   22.5 25  27.5 30  35.0 40.0
# nt input wave periods
  5.0
# nd input main directions
 -15.  15. 45. 75. 105. 135. 165. 195. 225. 255 285 315
# nd  input spreading index
  12*2.
# nd storm dur
  12*12.0
  12*12.0
  12*12.0
  12*12.0
  12*12.0
  12*12.0
  12*12.0
  12*12.0
  12*12.0
  12*12.0
  12*12.0
  12*12.0
  12*12.0
  12*12.0
  12*12.0
# for each wave height
#     for each direction
#         water level
  12*0.0
  12*0.0
  12*0.0
  12*0.0
  12*0.0
  12*0.0
  12*0.0
  12*0.0
  12*0.0
  12*0.0
  12*0.0
  12*0.0
  12*0.0
  12*0.0
  12*0.0
# open sea fetch description
# file name for fetches at data source
opensea.ftc
```

Figure D.4: Input file for the input wave field using operation HCAST12 with input given in matrix (MAT) form

When using the series format, the data should again be given as a series of conditions corresponding to a certain direction, followed by the file name of the data file containing the fetches. An example is given in Figure D.5).

```
HCAST12
#
# description of source
Reverse hindcast in series format
29 / 3 / 1999
! Options (can define growth curve to be used !)

# integration interval and range from main wave direction (deg.):
 2.  75.
# period factor
 1.0
# nc,nh,nt,nd
12 0 0 0 0
# nh input wave heights
#  DIR    U    dUR  M    Per   lev
   180.  29.2  5.0  2.0  12.9  1.0
   180.  33.5  5.0  2.0  12.9  1.0
   180.  35.0  5.0  2.0  12.9  1.0
   180.  35.9  5.0  2.0  12.9  1.0
   240.  32.6  5.0  2.0  12.9  1.0
   240.  34.6  5.0  2.0  12.9  1.0
   240.  35.3  5.0  2.0  12.9  1.0
   240.  35.9  5.0  2.0  12.9  1.0
   300.0 28.1  5.0  2.0  12.7  1.0
   300.0 33.3  5.0  2.0  12.7  1.0
   300.0 34.7  5.0  2.0  12.7  1.0
   300.0 35.5  5.0  2.0  12.7  1.0
! name of file with fetches in
example.ftc
```

Figure D.5: Input file for the input wave field using transformation HCAST12 with input given in series (SER) form

Simple Spreading
The input required for the Simple Spreading operation is as follows:

- The integration interval and range for main wave directions (given in degrees w.r.t. shore normal)
- The period factor
- The number of conditions (*nc*), number of wave heights (*nh*), number of wave periods (*nt*), number of wave directions (*nd*)
- The input wave heights, input wave periods, input main directions, input spreading index, initial storm durations

Just like the input for the Reverse Hindcast and Hindcast operations, the input can then be given in a series format (see Figure D.6), or a matrix format (see Figure D.7).

```
SPREAD12
#
# description of source
Reverse hindcast in series format
29 / 3 / 1999
# Options (can define growth curve to be used !)
#
# integration interval and range from main wave direction (deg.):
 2.  75.
# period factor
# 1.0
# nc,nh,nt,nd
 7 0 0 0
# nc input wave conditions
#         Hs  Per         DIR      M         lev
         4.5  9.5         300.    6.0       1.0
         4.5  9.5         310.    6.0       1.0
         4.5  9.5         320.    6.0       1.0
         4.5  9.5         330.    6.0       1.0
         4.5  9.5         340.    6.0       1.0
         4.5   9.         330.    12.0    5  1.0
         4.5  9.5         330.    2.0       1.0
```

Figure D.6: Input file for the input wave field using transformation SPREAD12 with input given in series (SER) form

```
SPREAD12
#
# description of source
Example spreading matrix
2-Jun-1999
# Options
# WIL65 - use growth curves due to Wilson 65 instead of Hurdle and Stive
#    (Good for short fetch lengths in deep water)
# none
# integration interval and range from main wave direction (deg.):
 2.  75.
# period factor
# 1.0
# nc,nh,nt,nd
0 18 7  12
# nh input wave heights
    0.10    0.25    0.75    1.25    1.75    2.25    2.75    3.25  3.75  4.25  4.75  5.25   5.75    6.25  6.75  7.25
    8.25    8.25
# nt input wave periods
 3.0  5.0  7.5  10.  12.5  15.0  17.5
# nd input main directions
 -15.  15. 45. 75. 105. 135. 165. 195. 225. 255 285 315
# nd  input spreading index
  12*6.
# nd  init storm dur
!  12*12.0
#
# for each wave height
#     for each direction
#         water level
  12*0.0
  12*0.0
  12*0.0
  12*0.0
  12*0.0
  12*0.0
  12*0.0
  12*0.0
  12*0.0
  12*0.0
  12*0.0
  12*0.0
  12*0.0
  12*0.0
  12*0.0
  12*0.0
  12*0.0
  12*0.0
  12*0.0
```

Figure D.7: Input file for the input wave field using transformation SPREAD12 with input given in matrix (MAT) form

Transformations

After the wave input field has been defined, it is possible to model wave transformation towards the shore. The possible operations are:

- Diffraction *(DIFR12)*
- Refraction *(REFR12)*
- Refraction Shoaling and Dissipation *(HIS1D)*
- Corner Refraction *(CRFCR)*
- Diffraction Coefficient *(CDIF)*

Diffraction

For the Diffraction (DIFR12) operation, the required input is a wave spectrum, which is given in the output of the ”Wave Input Field” operations. Next to this spectrum, the following input is required:

- The direction of north with respect to the x-axis, given in degrees
- The coordinate of the output point, given in cartesian coordinates
- The water depth, given in meters
- The coordinate of the head of the breakwater and the orientation (away from the breakwater head)

The generated output is a spectrum on the output location.

```
DIFR12
# title
Diffraction around West headland
1999
# options
 N
# direction of north wrt x
90.
#
# coordinate of output point
 1590   -550.
#  water depth
 20.0
# coordinate of head of breakwater and orientation (away from head)
 690  390  160.0
#
# ------------------------------------------------------------
```

Figure D.8: Input file for wave transformation using operation DIFR12

Refraction
For the Refraction operation, the required input is as follows:

- The direction of north with respect to the x-axis, given in degrees
- The output depth, given in meters
- The offshore depth (given in meters) and representative direction normal to depth contours (given in degrees), for defined wave directions

The output generated is a spectrum on the output location.

```
REFR12
#
#
# titles to describe operation
refraction between open sea and 20 m depth line at St. Maartin
7-3-95
#options
# N  - wave direction and coast normal with respect to north
# RP - compute refraction on basis of input wave period NOT
#      hindcast wave period
#
 N
# direction of north wrt x
 90.
#  output depth
 20.
#number of elements in schemat. array (nr)
11
# nr * ( dir, depth, normal)
 15.0 35.   90.0
 90.0 35.0  90.0
100.0 35.0  145.0
115.0 35.0  170.0
120.0 500.0 190.0
145.0 600   215
180   600   215
215   600   215
345   600   215
360.0   100 150.0
375   35.0  90.0
```

Figure D.9: Input file for wave transformation using operation REFR12

Refraction Shoaling and Dissipation (HIS1D)
When using the HIS1D operation, the following input should be given:

- The direction of north with respect to the x-axis, given in degrees
- The number of sections
- The number of directions
- The input bottom profile for each direction
- The input wave parameters (alfa, gamd, gamma, fw, fc, cfae, rho, dksmin, dksmax)

- The output depth (m)
- The number of elements in schematised array (nr), nr* (direction, depth offshore, normal of contours with resprect to normal)
- The input ratio of max.Hs / depth and wave steepness

The output is a new spectrum at the output location.

```
HIS1D
#
#
# titles to describe operation
wave propagation between deep water and 20 m depth line
at Taiwan  -    Nov - 95
#options
# N  - wave direction and coast normal with respect to north
# RP - compute refraction on basis of input wave period NOT
#      hindcast wave period
#
 N
# direction of north wrt x
 90.
#
# number of sections
1
#
# number of directions
4
# description of bottom profiles
# dir, normal, profile along normal
 240.  270.    'bot240.dat'
 270.  270.    'bot270.dat'
 305.  305.    'bot305.dat'
 340.  305.    'bot340.dat'
#
# wave parameters
# alfa, gamd, gamma
1.0  1.10  0.75
#
# fw, fc, cfae, rho
0.006  0.000  1.12  1020
#
# dksmin,dksmax
0.2  500.
#  output depth
 20.
#number of elements in schemat. array (nr)
7
# nr * ( dir, depth, normal)
 0.0  40.   305.
 90.  40.   305.
 180. 100.   270.
 270. 50.   270.
 305. 50.   305.
 340. 40.   305.
 360. 40.   305.
# ------------------------------------------------------------
#
#  max Hs / depth ratio and wave steepness
#
   0.9    0.05
```

Figure D.10: Input file for wave transformation using operation HIS1D

Corner Refraction
For the input, a wave spectrum is needed.

- The coordinates of the corner where refraction takes place (x- and y-coordinates)
- The orientation of direction away from corner (defined in the same way as for a breakwater / diffraction operation)
- The average depth away from corner, given in meters
- The slope of the corner, given as a ratio
- The global proportionality constant in d_θ / X relation (X is wavelength parameter)
- The local proportionality constant in d_θ / X relation (X is wavelength parameter)
- The available direction is given with respect to North
- The name of corner refraction element

The output is generated by this operation is a new coefficient.

Diffraction Coefficient
This operation needs the same input as the Diffraction operation. However, the generated output are coefficients at the output location.

Coefficient Operations

With coefficients, it is possible to perform the following operations, shown in Figure D.11,

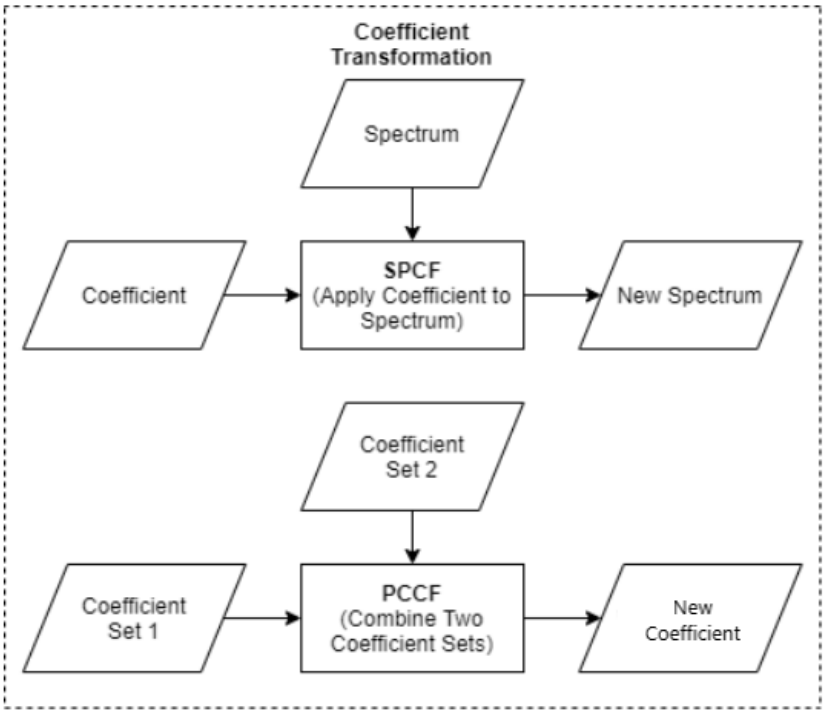

Figure D.11: Operators for coefficient transformation

SPCF
This operation applies a coefficient to a spectrum. The input given is a spectrum and a coefficient. The output is a new spectrum.

PCCF
This operation combines two coefficients. The input required are two coefficients, given in the same form and size. This operation leads to a new coefficient.

E

Sedimentation equations

E.1. Longshore transport equations for the diffraction zone

For the determination of the minimum length of the secondary breakwater, an estimation of the accretion length for a desired period of time has to be determined. This is accomplished using the method described by Van Rijn (2015). In this method, both diffraction as well as circular nearshore currents are taken into account.

Diffraction zone calculations

For estimating the diffraction effects, the Kamphuis method is used (Kamphuis, 2000). First, the diffraction coefficient (denoted by K_d) for a incoming wave is determined in the lee side of a structure (visualised in Figure E.1):

$$K_d = 0.7 - 0.0077\delta \quad \text{for} \quad 0^o \leq \delta \leq 90^o$$
$$K_d = 0.7 - 0.37sin\delta \quad \text{for} \quad 0^o \leq \delta \leq -40^o$$
$$K_d = 0.83 - 0.17sin\delta \quad \text{for} \quad -40^o \leq \delta \leq -90^o$$

in which:

θ = Direction of the incoming wave ray at the breakwater tip [^{o}]
δ = The angle between the incoming wave ray at the tip and the desired location on the breaker line [^{o}]

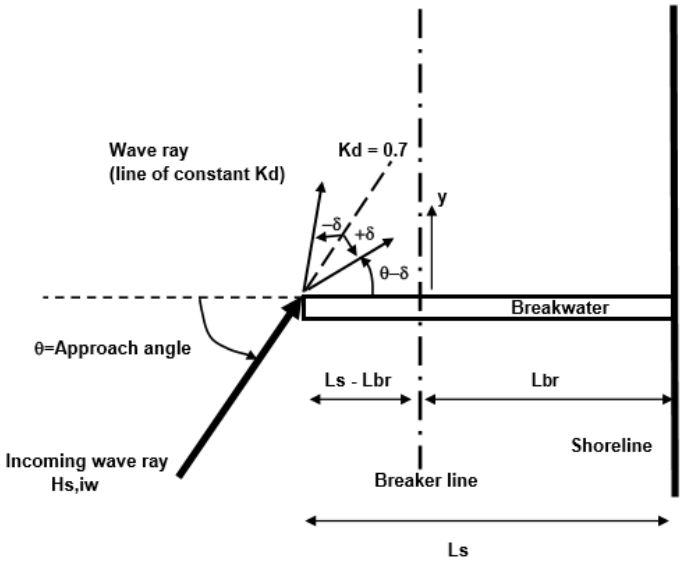

Figure E.1: Visualisation of parameters for the Kamphuis method (Van Rijn, 2015)

Using the diffraction coefficient, it is possible to determine the breaking wave height and the wave angle at the breaker line in the diffraction zone (Van Rijn, 2015). This is determined using Equations E.1 and E.2.

$$H_{br,d} = K_d * H_b \tag{E.1}$$

$$\theta_{br,d} = K_d^{0.38} \theta_b \tag{E.2}$$

in which:

H_b	=	breaking wave height	$[m]$
θ_b	=	wave angle at breaker line	$[^o]$
K_d	=	diffraction coefficient	[-]

Circular Nearshore Current Calculation

The determined wave heights are used for the determination of the circular nearshore current velocity. The circular current velocity is estimated using the difference in wave setup (η) in the diffraction zone (between δ=0 and δ=θ).
To determine the wave setup, Equation E.3 is used.

$$\eta(h) = 0.189 H_b - 0.186 h \tag{E.3}$$

in which:

H_b	=	breaking wave height	$[m]$
h	=	water depth	$[m]$

For the calculation of the circular current velocity, the difference in setup is desired along the breaker line. This means that water depth can be taken out of the equation, giving:

$$\Delta\eta = 0.189 \Delta H_b \tag{E.4}$$

When the setup difference is known, the slope of the wave setup difference is determined. Based on this slope, the circular current velocity is calculated using Equation E.5 (Van Rijn, 2014).

$$V_{circ} = C\sqrt{hi} \tag{E.5}$$

in which:

C	=	Chezy coefficient	$[m^{1/2/s}]$
h	=	water depth	$[m]$
i	=	slope of wave setup	[-]

Sediment Transport Calculation

For the calculation of sediment transport, Van Rijn (2015) presents an equation for the calculation of longshore sediment transport that is linear in velocity (Equation E.6).

$$\mathrm{Q_{t,mass}} = 0.0006 \mathrm{K_{swell}} \rho_\mathrm{s} (\tan\beta)^{0.4} (\mathrm{d_{50}})^{-0.6} (\mathrm{H_{s,br}})^{2.6} \mathrm{V_{longshore}} \tag{E.6}$$

in which:

$Q_{t,mass}$	=	longshore sediment transport	$[kg/s]$
K_{swell}	=	swell coefficient (default = 1)	$[m]$
ρ_s	=	soil density	$[kg/m^3]$
d_{50}	=	median grain size	$[m]$
$tan\beta$	=	slope of beach-surf zone	[-]
$H_{s,br}$	=	wave height at breaker line	$[m]$
$V_{longshore}$	=	longshore current velocity	$[m/s]$

To determine the sediment transport at a location, the longshore current velocity $V_{longshore}$ at that point has to be determined. To determine $V_{longshore}$ for locations inside the diffraction zone, Equation E.7 can be used.

$$V_{longshore} = rV_{\text{wave}} - V_{\text{circ}} \tag{E.7}$$

in which:

$V_{longshore}$	=	longshore current velocity	$[m/s]$
V_{wave}	=	longshore induced current velocity by waves	$[m/s]$
V_{circ}	=	longshore component of circular current velocity	$[m/s]$
r	=	adjustment factor	[-]

Both parameters r and V_{wave} can be calculated using Equations E.8 and E.9.

$$r = y/L_{tip} \qquad (\text{if } y < 0 \text{ then } r = 0, \text{ when } y > y_{null} \text{ then } r = 1) \tag{E.8}$$

$$V_{wave} = 0.3 * (g * H_b)^{0.5} * sin(2\theta_b) \tag{E.9}$$

in which:

y	=	distance from the structure to the location of interest (see Figure E.1)	$[m]$
L_{tip}	=	length of the structure form tip to shoreline	$[m]$
g	=	gravitational acceleration (= 9.81)	$[m^2/s]$
H_b	=	Wave height on the breaker line at the location of interest	$[m]$
θ_b	=	wave angle at the breaker line for location of interest	$[^o]$

Using the equations mentioned above, it is possible to determine sediment transport for each location on the downdrift side of the breakwater.

E.2. Channel siltation equations

The Soulsby-Van Rijn equation is a modification on the Van Rijn equation. This equation is used for determining the channel infill in a comparable study for LNG terminals, conducted by Rustell (Rustell, 2016). It is based around the principle that $q_t = q_{in} - q_{out}$.

The equation for the transport q is as follows:

$$q = A_s\overline{u}\left(\left(\overline{u}^2 + \frac{0.018}{C_D}u_{rms}^2\right)^{0.5} - \overline{u}_{cr}\right)^{2.4}(1 - 1.6\tan\beta) \tag{E.10}$$

in which:

A_s	=	Coefficient for sediment transport	[-]
$\overline{u}$	=	Mean current velocity	$[m/s]$
C_D	=	Drag coefficient due to current	[-]
u_{rms}	=	RMS wave orbital velocity	$[m/s]$
$\overline{u}_{cr}$	=	Treshold current speed	$[m/s]$
$tan\beta$	=	Slope of the channel bank	$[m/s]$

In which $A_s = A_{sb} + A_{ss}$, with A_{sb} and $A_s s$ given by:

$$\mathrm{A_{sb}} = \frac{0.005\mathrm{h_i}\left(\mathrm{d_{50}/h_i}\right)^{1.2}}{\left[(\delta_s - 1)\,\mathrm{gd_{50}}\right]^{1.2}} \tag{E.11}$$

$$A_{ss} = \frac{0.012\mathrm{d_{50}}D*^{-0.6}}{\left[(\delta_s - 1)\,\mathrm{gd_{50}}\right]^{1.2}} \tag{E.12}$$

in which:

h_i	=	Water depth	$[m]$
d_{50}	=	Median grain size	$[m]$
δ_s	=	Relative density of sediment	[-]
g	=	Gravitational acceleration coefficient	$[m/s^2]$
D^*	=	Dimensionless grain size	[-]

The drag coefficient C_D can be calculated as follows:

$$\mathrm{C_D} = \left[\frac{0.4}{\ln(\mathrm{h_i}/z_0) - 1}\right] \tag{E.13}$$

in which:

h_i	=	Water depth	$[m]$
z_o	=	Bed roughness	$[m]$

The root mean squared wave orbital velocity $\overline{u}_{rms}$ is calculated by Soulsby (1997) the following way:

$$\overline{\mathrm{u}}_{\mathrm{rms}} = \frac{\mathrm{H_s}}{4}\sqrt{\frac{\mathrm{g}}{\mathrm{h_i}}}\exp\left(-\frac{3.65}{\mathrm{T_z}}\sqrt{\frac{\mathrm{h_i}}{9}}\right)^{2.1} \tag{E.14}$$

in which:

H_s	=	Significant wave height	$[m]$
g	=	Gravitational acceleration coefficient	$[m/s^2]$
h_i	=	Water depth	$[m]$
T_z	=	Mean zero up-crossing period	$[s]$

The critical current velocity $\overline{u}_{cr}$ can be determined with the following equations, depending on the median grain size diameter:

$$\overline{\mathrm{u}}_{\mathrm{cr}} = \begin{cases} 0.19\,(\mathrm{d_{50}})^{0.1}\log_{10}\left(\frac{4\mathrm{h_i}}{\mathrm{d_{90}}}\right) & : 0.1 \leqslant \mathrm{d_{50}} \leqslant 0.5\mathrm{mm} \\ 8.5\,(\mathrm{d_{50}})^{0.1}\log_{10}\left(\frac{4\mathrm{h_i}}{\mathrm{d_{90}}}\right) & : 0.5 \leqslant \mathrm{d_{50}} \leqslant 2\mathrm{mm} \end{cases} \tag{E.15}$$

in which:

d_{50}	=	Median grain size	$[m]$
d_{90}	=	90th percentile grain size	$[m]$

The last parameter to determine is the dimensionless grain size $D*$, which can be determined using the following equation:

$$\mathrm{D*} = \left(\frac{\mathrm{g}\,(\delta_s - 1)}{v^2}\right)^{1/3}\mathrm{d_{50}} \tag{E.16}$$

in which:

δ_s	=	Relative density of sediment	[-]
g	=	Gravitational acceleration coefficient	$[m/s^2]$
d_{50}	=	Median grain size	$[m]$
v	=	Kinematic viscosity	$[m^2/s]$

When both q_{in} and q_{out} have been determined, it is possible to determine the mean infill rate ψ, which is given in mm/s. This can be determined using:

$$\psi = \frac{\mathrm{q_t}}{W(1-\varepsilon)} \tag{E.17}$$

in which:

ψ	=	Mean infill rate	$[m/s]$
q_t	=	Total sediment transport per unit length	$[m^2/s]$
W	=	Width of the channel section	$[m]$
ϵ	=	Coefficient of settlement (= 0.4)	[-]

F Anaklia case parameters

F.1. Input parameters

Category	Symbol	.py symbol	Default	Unit	Input	Description
Constraints	x_{max}	x_max	4000	m	4000	outermost point for primary breakwater on x-axis
	y_{max}	y_max	3000	m	3000	outermost point for primary breakwater on y-axis
	L_{max}	l_max	4000	m	3000	outermost distance for secondary breakwater in x-direction
Navigation	H_c	h_ch	1,5	m	1,5	limiting wave height in sheltered channel
	H_{berth}	h_berth	0,5	m	0,5	limiting wave height at berth
	$v_{s,min}$	v_smin	2	m/s	2	minimum vessel speed
	t_{tug}	t_tug	10	min	8	tugging time
	$u_{cw,n}$	u_cwn	18	m/s	18	limiting cross-wind speed for navigation
	$u_{lw,n}$	u_lwn	18	m/s	18	limiting longitudinal wind speed for navigation
	$u_{w,o}$	u_wo	20	m/s	20	limiting wind speed for operations
	$u_{cc,n}$	u_ccn	0,5	m/s	0,5	limiting cross-current speed for navigation
	$u_{lc,n}$	u_lcn	2	m/s	2	limiting longitudinal current speed for navigation
Vessel	L_s	ls	300	m	300	length over all of design vessel
	B_s	bs	32	m	48	beam of design vessel
	D_s	ds	12	m	15	draught of design vessel
	v_s	vs	3	m/s	3	entrance speed of a vessel
Costs	C_{core}	c_core	30	€/m^3	74	unit price for breakwater core material
	C_{under}	c_under	25	€/m^3	74	unit price for breakwater underlayer material
	C_{armour}	c_armour	400	€/unit	400	unit price for breakwater armour layer material
	C_{dd}	c_dd	5	€/m^3	5	dredging-dumping costs of sediment
	C_{df}	c_df	4	€/m^3	4	dredging-filling costs of sediment
	C_{TEU}	c_teu	60	€/TEU	60	(un)loading unit rate per twenty-foot equivalent unit
	C_{land}	c_land	2000	€/m	2000	land cost per running meter of coastline stretch

	$\Phi_{bw,m}$	psi_bwm	0,02	-	0,02	ratio of annual breakwater maintenance costs w.r.t. construction
	r	r	0,05	-	0,05	discount rate for present-day value
	T_L	t_life	50	yr	60	design lifetime of breakwater
Terminal	n_b	n_b	-	-	7	number of berths second phase
	n_{bf}	n_bf	-	-	7	number of berths in future
	y_f	yf	-	m	10	fill-up distance in y-direction
	m_b	mb	0,6	-	0,65	berth occupancy factor
	P_b	pb	35	MPH	55	hourly production per berth
	f_{TEU}	f_teu	1,5	-	1,5	TEU-factor
Bathymetry	z_0	z0	-	m	0	ground level above MSL at y = 0
	1 : αb	alpha_b	-	-	100	slope of the sea bed
Coast	θ_s	theta_s	-	°	-135	orientation of offshore-directed normal to coastline w.r.t. North
Environment	s_{max}	smax	10	-	10	maximum directional spreading parameter
Water levels	HAT	hat	-	m	0,2	high astronomical tide level above MSL
	LAT	lat	-	m	0,2	low astronomical tide level below MSL
Breakwater	h_l	h_l	3	m	3	level of leeward armour layer below MSL
	h_c	h_c	0,5	m	1,5	core height above HAT
	t_u	t_u	1	m	1,3	thickness of underlayer
	t_a	t_a	3	m	1,85	thickness of armour layer
	B_{crest}	b_crest	10	m	10	breakwater crest width
	1 : x_f	xf	1,5	-	1,5	front slope of breakwater
	1 : x_r	xr	1,5	-	1,5	rear slope of breakwater
	n_v	nv	0,5	-	0,5	armour layer porosity
	D_n	d_nom	1,5	m	2	nominal diameter of armour units
Sediments	$t_{s,0}$	ts_0	0,4	m/year	0,3	annual siltation thickness without secondary breakwater
	$t_{s,max}$	ts_max	0,3	m/year	0,2	annual siltation thickness with breakwater gap >= 1000m
	$t_{s,min}$	ts_min	0,25	m/year	0,1	annual siltation thickness with breakwater gap equal to channel width
	s_{type}	s_type	2	-	2	soil type (1 = mud, 2 = sand/clay , 3 = rock/coral)
Dredging	h_f	hf	-	m	2,5	average fill level of terminal above MSL
	1 : x_b	xb	4	-	5,5	bank slope of approach channel
Grid	ΔxΔy	delta_xy	10	m	10	step size for grid
	Layout	lay_dir	l	-	l	r = rightward direction, l = leftward direction, np = no preference

Table F.1: Input parameters for the Anaklia case study

H_{0s}	T_{0p}	θ_0	u_w	θ_w	u_c	θ_c	Pr
3	9	270	10	292,5	0,4	315	0,01
4	10	270	16	90	0,4	315	0,001
3	9	248	8	247,5	0,4	315	0,0015
2	8	225	14	270	0,4	315	0,004
0,5	4	281	4	90	0,4	135	0,54
1	6	281	4	67,5	0,4	315	0,19
2	8	281	4	315	0,4	315	0,045
0,5	4	203	10	67,5	0,4	315	0,0125
0,5	4	180	10	90	0,4	315	0,01
0,5	4	248	6	112,5	0,4	315	0,095
0,5	4	248	4	135	0,4	315	0,09

Table F.2: Environmental conditions for the Anaklia case study

Parameter	Value	Unit	Description
u_{ebb}	0	m/s	Ebb tidal current flow velocity
u_{flood}	0	m/s	Flood tidal current flow velocity
u_{res}	0.4	m/s	Residual current flow velocity
θ_{res}	90	^{o}	Flood tidal current flow angle w.r.t. shore-normal
d_{50}	2.5e-4	m	Median grain size
d_{90}	5.0e-4	m	90th percentile grain size
v	1.14e-6	m^2/s	Viscosity
z_o	0.006	m	Bed roughness
s	2.65	-	Relative density
$tan\beta_s$	0.008	-	Surf zone slope
$tan\beta_b$	0.008	-	Beach zone slope
ρ_s	2650	kg/m^3	Sediment density
ρ_{bulk}	1600	kg/m^3	Bulk sediment density
d	-	m	profile depth

Table F.3: Anaklia parameter values for sedimentation calculations

F.2. Downtime estimation results

	Navigation	Berth 1	Berth 2	Berth 3	Berth 4	Berth 5	Berth 6	Berth 7
Downtime [%]	0	1	1	2	7	1	0	0

Table F.4: Downtime percentages corresponding to the optimal layout

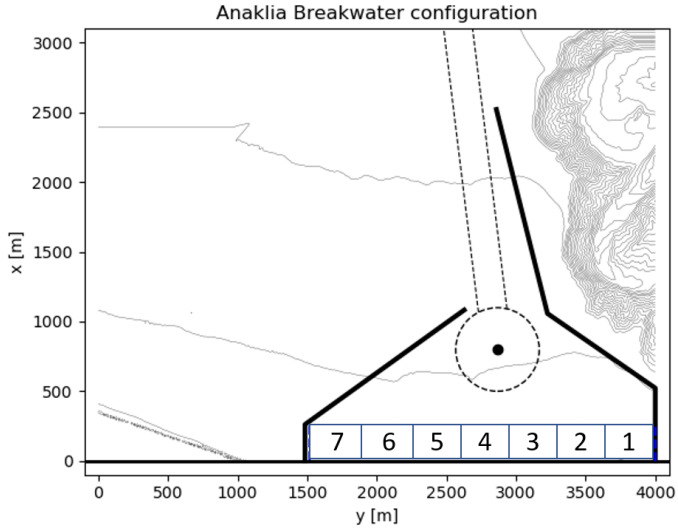

Figure F.1: Berth locations of the optimal layout

F.3. Channel sedimentation volume estimation

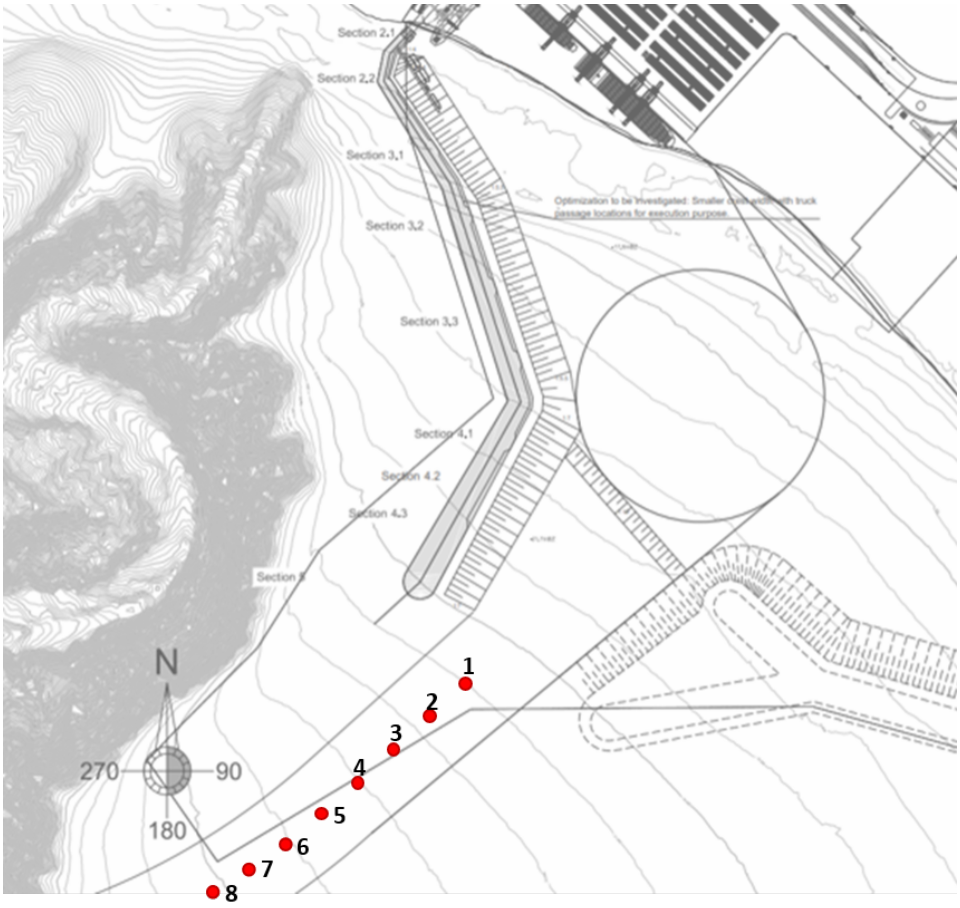

Figure F.2: Visualisation of data points for the channel sedimentation assessment

Point	Filling rate [m/yr]
1	0.21
2	0.25
3	0.19
4	0.14
5	0.08
6	0.05
7	0.02
8	0.009

Table F.5: Determined filling rates for each data point